TEXAS A&M UNIVERSITY
DEPARTMENT OF GEOLOGY & GEOPHYSICS
COLLEGE STATION, TEXAS 77843-3115

Dr. Hongbin Zhan, Endowed Dudley J. Hughes Chair in Geology and Geophysics
Tele: (979) 862-7961 Fax (979) 845-6162
Email:zhan@geos.tamu.edu
http://geoweb.tamu.edu/zhan

May 14, 2020

Memorandum

To: Dr. Philippe Ackerer, Editor of HESS

Subject: Revision of Paper # hess-2019-699

Dear Editor:

Upon the recommendation, we have carefully revised Paper # hess-2019-699 entitled "New Model of Reactive Transport in Single-Well Injection-Withdrawal Test with Aquitard Effect" after considering all the comments made by the reviewers. The following is the point-point response to all the comments.

Response to Reviewer #1:

General comments

1. This is an impressive mathematical work that involves several injection phases, adsorption (linear) and first-order degradation, the presence of aquitards, and the separation between mobile/immobile domains. The solution is fully analytical, just expressed in Laplace space (thus the need for inversion at the end). If the solution is analytical, what is the point to test it? The only reason is that some simplifications are involved. This is tested for example in Figure 2, showing limitations.

Reply: Implemented. See Lines 291-296.

2. Assumptions are quite strong: - Homogeneity – it might also be valid for mild heterogeneity - The well extends all the thickness of the aquifer - Reactions: actually you only include linear sorption (K_d values) and first-order degradation (nmu values). This is a very small subset of reactions.

Reply: Implemented. See Lines 95-99.

3. At the end there is a validation effort with real data. According to the authors, the new model performs better. Yes, it also has many more parameters, and so in a real case some model selection criteria should be performed to discriminate the "best" model. More, the authors provide just a single set of parameters, without any study of uncertainty in the parameters, or even the reason why these numbers were chosen and how they represent real physical quantities.

Reply: Implemented. The real physical quantities and the uncertainty of the estimated parameters have been discussed. See Lines 405-413.

4. The mathematical work is really impressive, and I praise the authors for it, but in my opinion the resulting

work can be hardly used with real data, and the problem would be better solved using a numerical model that can provide best fit, but also some uncertainty evaluation.

Reply: Implemented. See Lines 83-91.

Response to Reviewer #2:

General comments

1. The present work presents a novel analytical treatment of single-well injection withdrawal (SWIW) tests, whereas the impact of mixing in the well and the presence of confining aquitards are considered. I applaud the Authors for the efforts in the derivation of the solution (math not checked) and the commitment to introduce more flexibility in the conceptual model. Yet, I am not sure about its usefulness to other researchers, it is very complicated! Maybe, if the Authors made available a script for the calibration against data it could be beneficial to the usage among practitioners. Regarding the quality of the paper, I see many unclear points or unclear parts. I listed below a series of comments which I hope will make the paper more clear. Moreover, I have some criticisms about the employed sensitivity analysis, which it seems to be a weak one in my personal opinion.

Reply: Thanks. We have carefully revised the manuscript after considering all the comments.

Specific comments

1. line 15: why put emphasis on the use of Green' function for the extraction phase in the abstract? This leads to think 'what about the other phases?'. I would remove this comment.

Reply: Implemented. We have removed it. See Line 14.

2. line 17: I would replace 'tested by' with 'tested against results grounded on numerical simulations', or something similar, i.e., the numerical simulations results serve as reference values to be matched and do not verify the validity of the assumptions directly.

Reply: Implemented. "tested by a numerical solution" has been changed into "against results grounded on numerical simulations". See Lines 18-19.

3. lines 17-19 'The sensitivity analysis demonstrates that the influence of vertical flow velocity and porosity in the aquitards, and radial dispersion of the aquifer is more sensitive to the SWIW test than other parameters.'. Which sensitivity analysis? The fact that the latter has been conducted is not specify earlier in the text. Moreover, specify which kind of sensitivity analysis you are using. Furthermore, the sentence is rather confusing: it says that the influence of three-parameter is more sensitive to the SWIW test, than other. What is the difference between influence and sensitivity? Is it the influence that varies as a function of the SWIW test? … I was thinking that are the results of the SWIW (i.e., model output) to be largely sensitive (i.e., influenced by) to the three mentioned parameters (i.e., model inputs), but maybe I am biased by my previous experiences with sensitivity analysis. Please clarify.

Reply: Implemented. See Lines 19-20.

4. line 23 ‘The new model of this study performs better than previous studies excluding the aquitard effect for interpreting data of the field SWIW test’ too general. Please specify which field test you are referring to, since the quality of the novel solution can be worse than previous ones in case the system do not have an aquitard, for example.

Reply: Implemented. See Lines 24-25, and Lines 277-283.

5. lines 49-50 ‘Another assumption included in many previous models of radial dispersion is that the concentration of the mixing water with the injected tracer is equal to the injected tracer concentration during the injection phase’ the sentence is not very clear. What is the mixing water? ‘is equal to the injected tracer concentration’ of what? Please revise the sentence. Moreover, lines 53-55 ‘This assumption implies that the mixing effect in the wellbore is not considered, where the mixing effect refers to the mixture between the original (or native) water and the injected tracer in the well.’ ow there is the native water which is not mentioned earlier. … I can grasp the general idea that there is a difference between the concentration of tracer between the resident water, injected water and water within the well where mixing occurs, but not in a standalone manner from these lines (i.e., I need to think about them and deduce that this the implied message). Please clarify, maybe with an additional figure.

Reply: Implemented. See Lines 51-62.

6. line 61 ‘mostly because ADE could not adequately interpret anomalous reactive transport,’ this true when the ADE is used to capture the whole behavior of the system, i.e., as an effective model for all the system behavior to be characterized by a single representative value of advection, dispersion and reaction. Instead, if ADE is finely discretized (i.e., the system heterogeneity is properly detailed) and then (numerically) solved it can fairly well capture anomalous behaviors. Please clarify this point. This is in line with the mentioned superior capacity of effective transport models mentioned afterward (e.g., MMT,CTRW, fADE, MIM) to have a superior capacity in rendering anomalous behaviors of heterogeneous system when viewed as a whole (e.g., spatially integrated BTCs).

Reply: Implemented. See Lines 63-79.

7. line 74 ‘anonymous’ I suppose anomalous.

Reply: Implemented. “anonymous” has been changed into “anomalous”. See Line 76.

8. line 86 ‘Some examples of weak heterogeneity include the Borden Site of Canada (Sudicky, 1988)’ this is just one example, either add others or modify the sentence.

Reply: Implemented. The Borden Site of Canada (Sudicky, 1988) is one example of weak aquifer heterogeneity. See Lines 104-105.

9. lines 89-96 ‘Second, for moderate or even strong heterogeneous media such as Cape Code site (Hess, 1989) or MADE site (Bohling et al., 2012), the analytical model developed under the homogeneity assumption is also valuable, but in a statistical sense, as long as the media heterogeneity can be regarded

as spatially stationary, meaning that the statistical structure of the media heterogeneity does not vary in space. In this setting, the analytical model developed under the homogeneity assumption is used to describe the (ensemble) average characteristics of an ensemble of heterogeneous media which are statistically identical but individually different. In another word, such an analytical model will provide a statistically average description of many realizations (an ensemble) which are similar to the heterogeneous media of concern, but it cannot provide an exact description for the particular heterogeneous media under investigation' .… this made me think that the validation strategy based on the direct numerical simulations is not valid: those simulations are considering directly an homogenous media (with deterministic properties) and NOT the statistical average of the SWIW results across a set of Monte Carlo realizations of the conductivity fields, characterized by either small, middle or large variance. Please clarify this point.

Reply: Implemented. See Lines 95-99.

The description of 'Second, for moderate or even strong heterogeneous…" in the original manuscript has been deleted.

Such assumptions might be oversimplified for cases in reality, while they are inevitable for the derivation of the analytical solution, especially for the aquifer homogeneity. For a heterogeneity aquifer, the solution presented here may be regarded as an ensemble-averaged approximation if the heterogeneity is spatially stationary. If the heterogeneity is spatially non-stationary, then one can apply non-stationary stochastic approach and/or Monte Carlo simulations to deal with the issue, which is out of the scope of this investigation.

10. line 99 'A schematic diagram of the model investigated by this study is similar to Figure 1 of Wang and Zhan (2013)' please add this figure and incorporate what mentioned above in comment 5.

Reply: Implemented. A new figure has been added, See Figure 1.

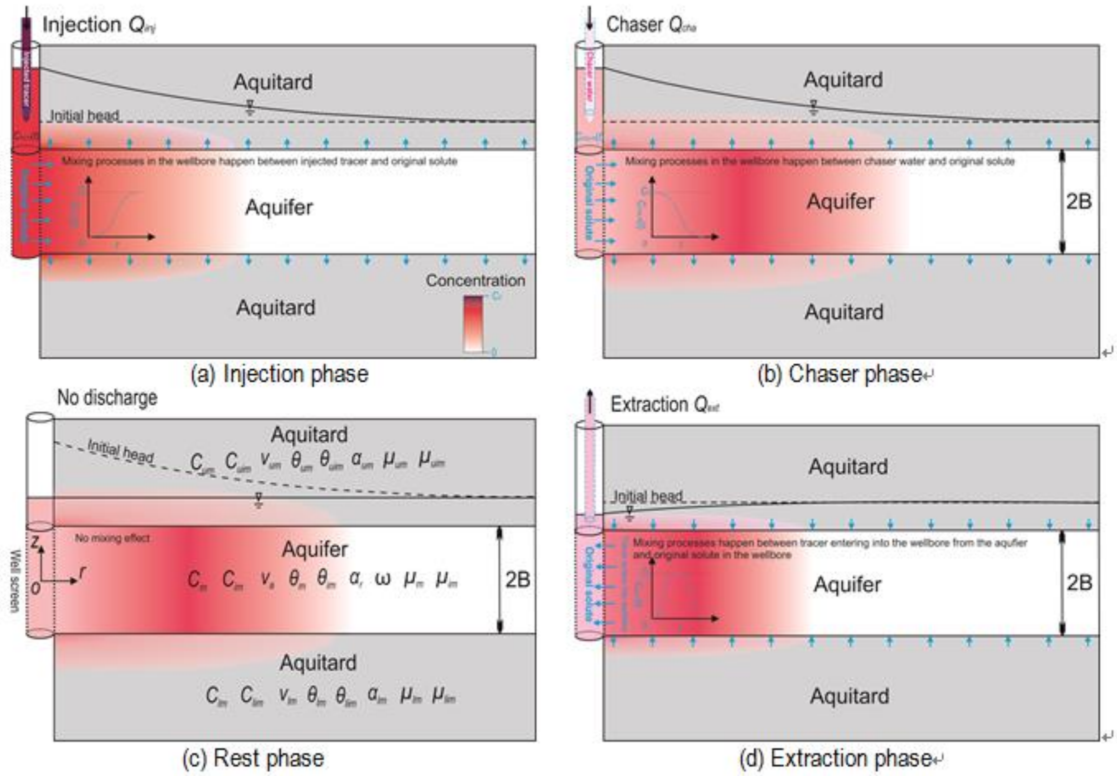

Figure 1: The schematic diagram of the SWPP test.

11. Eq.s (1)-(3) I didn't quite understand the + notation: I would say that the fact that the velocity component is pointing towards the well or in the opposite direction is in the value of (for example) va considering (1), similar for the others velocity components in (2) and (3). I would say that the value of va (and others advective velocities) varies as a function of the SWIW phase. If not va should be the module of the advective component, no? Maybe I am wrong.

<u>Reply:</u> Implemented. Eqs. (1) - (3) have been revised.

12. Eq. (12a) what's C0? (12d) there is a without subscript, what's that?

<u>Reply:</u> Implemented. See Lines 159-161.

$$\xi = 2\pi r_w \theta_m 2B, \tag{12d}$$

where $h_{w,inj}$ is the wellbore water depth [L] in the injection phase, C_0 is concentration [ML^{-3}] of prepared tracer.

13. Eq.s (8)-(11) Highlight that in the imposition of the continuity of flux across the well and the formation only the mobile fractions are considered, for who are not familiar with the MIM model?

<u>Reply:</u> Implemented. See Lines 152-154.

Eqs. (8) - (11) indicate that the flux continuity across the interface between well and the formation is only considered for the mobile continuum (or mobile domain).

14. 'For instance, if the characteristic length of SWIW test is l and the aquifer hydraulic diffusivity is D=Ka/Sa, where Ka are Sa are the radial hydraulic conductivity and specific storage, then the typical characteristic time of unsteady state flow is around tc = lˆ2/2D. For instance, for a typical lc=10 m, Ka=10 m/day and Sa=10-5 (m-1) (which are representative of an aquifer consisting of medium sands), the value of tc is found to be 5x10ˆ-5 day.' How do the authors determine the characteristic length lc? In my experience this length is typically a function of the aquifer diffusivity, e.g., for tidal fluctuations is idealized coastal aquifer (e.g., homogeneous, infinite lateral extension) there is a proportionality of the kind lc = sqrt(K/S) (see e.g., Guarracino et al., 2012). Moreover, the proposed estimate of 10 m disagree with the results presented in figures 2-3 where the solute travels up to 100 m, suggesting that the influence of the SWIW test is at least reaching that distance. I am not entirely convinced about the fact that push-pull tests can be seen as steady state tests and with the justification provided by the Authors, I leave to the Editor the judgment here. Nevertheless, I agree on the need to simplify the (already complex) analysis choosing the steady state!

Reply: Implemented. See Lines 178-190.

In the comment by reviewer: "In my experience this length is typically a function of the aquifer diffusivity, e.g., for tidal fluctuations is idealized coastal aquifer (e.g., homogeneous, infinite lateral extension) there is a proportionality of the kind lc = sqrt(K/S) (see e.g., Guarracino et al., 2012)", the formula of computing the characteristic length lc may be not right, since the dimension of sqrt(K/S) is L/sqrt(T), while the dimension of lc is L. By checking Guarracino et al. (2012), we found that authors employed "sqrt(K/(ωS))" to calculate the characteristic dampening distance, where ω is tidal angular velocity (T^{-1}).

This approximation is generally acceptable given the very limited spatial range of influence of most SWPP tests. For instance, if the characteristic length of SWPP test is l and the aquifer hydraulic diffusivity is $D=K_a/S_a$, where K_a are S_a are respectively the radial hydraulic conductivity and specific storage, then the typical characteristic time of unsteady-state flow is around $t_c \approx \frac{l^2}{2D}$. The typical characteristic time refers to the time of the flow changing from transient state to quasi-steady state, where the spatial distribution of flow velocity does not change while the drawdown varies with time. This model is similar to the model used to calculate the typical characteristic length of the tide-induced head fluctuation in a coastal aquifer system (Guarracino et al., 2012). For K_a=1m/day, S_a=10^{-5}m^{-1} and l=10m (which are representative of an aquifer consisting of medium sands), one has $t_c \approx \frac{l^2}{2D} = 5.0 \times 10^{-3}$ day, which is a very small value. To test the model in computing t_c, the numerical simulation has been conducted, where the other parameters used in the model are the same as ones used in Figures 2 and 3. Figure S2 shows the flow is in quasi-steady state when time is greater than t_c, since two curves of t =5.0×10^{-3} day and t =10.0×10^{-3} day overlap. As for the typical characteristic length, if the values of K_a, S_a, and B have been estimated by the pumping tests before the SWPP test, it could be calculated by numerical modelling exercises using different simulation times.

15. line 289, in the comparison against the numerical solution the porosity of the immobile region of the aquifer is zero, why? There is also a general ω =0, to which mass transfer makes it reference? Why zero? Aren't these choices limiting the testing of the proposed solution?

Reply: Implemented. We have revised it: θ_{im}=0.05, and ω=0.01d^{-1}. See Line 308.

16. lines 309-310 'As mentioned in Section 3.1, the new model is a generalization of many previous models, and the conceptual model is more close to reality.' Again, too general. This novel solution could or not be closer to reality depending on the specific case.

Reply: Implemented. See Lines 24-25, and Lines 277-283.

17. line 323 'To prioritize the sensitivity of parameters involved the new model' an in is missing (i.e., 'in the new model'). Moreover, the sensitivity is not a property of the parameters (or model inputs), but it is of the output with respect to the parameters. You want to quantify/evaluate the sensitivity of predictions with respect to the diverse parameters. Sensitivity cannot be prioritized, it is what it is and it is dictated by the way a model builds relationship between input(s) and output(s). Then you can prioritize the estimate of those parameters that influence the most the output.

Reply: Implemented.

"in" has been added. See Line 339.

To prioritize the sensitivity of predictions with respect to the diverse parameters involved in the new model, a sensitivity analysis is conducted in Section 5.2. See Lines 354-372.

18. Eq. (29), the definition and explanation is quite obscure. The only clar thing is that it sensitivity is grounded here on the concept of derivative. Then, what is ci? Moreover, the subscript i does not vary at all, what is it? Why there is Ij before the derivative?. Furthermore, this equation implies (i) that only variation of a single parameter at time are considered and (ii) it seems that the index associated with a parameter is evaluated around only one value of that parameter. These features prevent the identification of non-linearities and parameters interactions, which are quite likely to occur for the present model. The proposed method is a quite restricted characterization of sensitivity to me, if the model is not expensive I would suggest using a global sensitivity method: Sobol' indices (see Sobol, 2001) or DELSA (see Rakovec et al., 2014). On this point I leave the final decision to the Editor.

Reply: Implemented. See Lines 355-372.

The model of Eq. (29) in the original manuscript is for the local sensitivity analysis, and it has been deleted. Instead, a global sensitivity analysis is conducted using the model of Morris (1991) to investigate the importance of the input parameters on the output concentration.

19. lines 389-390 'The new model is most sensitive to the aquitard porosity and aquifer radial dispersivity' the model results are… 'after a comprehensive sensitivity analysis' you discover the previous thing after performing the sensitivity analysis, and it is not the latter that implies the former results; the sensitivity analysis is just a way to quantify the former aspect. Moreover, I would avoid comprehensive, see comment 18.

Reply: Implemented. See Lines 354-372.

A global sensitivity analysis is conducted using the model of Morris (1991). The description of the sensitivity is also revised.

If you have any further questions about this revision, please contact me.

Sincerely Yours,

Hongbin Zhan, PhD, PG.

Hongbin Zhan

Professor and

Holder of Endowed Dudley J. Hughes Chair in Geology and Geophysics

New Model of Reactive Transport in Single-Well Push-Pull Test with Aquitard Effect and Wellbore Storage

Quanrong Wang[1]*, Junxia Wang[2], and Hongbin Zhan[3]*, Wenguang Shi[1]

[1]School of Environmental Studies, China University of Geosciences, Wuhan, Hubei, 430074, P. R. China
[2]School of Mathematics and Physics, China University of Geosciences, Wuhan, Hubei, 430074, P. R. China
[3]Department of Geology and Geophysics, Texas A& M University, College Station, TX 77843-3115, USA

Correspondence to: Quanrong Wang (wangqr@cug.edu.cn), and Hongbin Zhan (zhan@geos.tamu.edu)

Abstract.

The model of single-well push-pull (SWPP) test has been widely used to investigate reactive radial dispersion in remediation or parameter estimation of the *in situ* aquifers. Previous analytical solutions only focused on a completely isolated aquifer for the SWPP test, excluding any influence of aquitards bounding the tested aquifer, and ignored the wellbore storage of the chaser and rest phases in the SWPP test. Such simplification might be questionable in field applications when test durations are relatively long, because solute transport in or out of the bounding aquitards is inevitable due to molecular diffusion and cross-formational advective transport. Here, a new SWPP model is developed in an aquifer-aquitard system with wellbore storage, and the analytical solution in the Laplace domain is derived. Four phases of the test are included: the injection phase, the chaser phase, the rest phase and the extraction phase.~~ The Green's function method is employed for the solution in the extraction phase.~~ As the permeability of aquitard is much smaller than the permeability of the aquifer, the flow is assumed to be perpendicular to the aquitard, thus only vertical dispersive and advective transports are considered for aquitard. The validity of this treatment is tested against results grounded on numerical simulations~~tested by a numerical solution~~. The global sensitivity analysis indicates that the results of the SWPP test are largely sensitive (i.e., influenced by) to the parameters of ~~sensitivity analysis demonstrates that the influence of~~ porosity and radial dispersion of the aquifer, ~~and~~ where the influence of aquitard on results could not be ignored.~~ is more sensitive to the SWIW test than other parameters~~ In the injection phase, the larger radial dispersivity of the aquifer could result in the smaller values of breakthrough curves (BTCs), while greater BTC values in the chaser and rest phases. In the extraction phase, it could lead to the smaller peak values of BTCs. The new model of this study is a generalization of several previous studies, and it performs better than previous studies ignoring the aquitard effect and wellbore storage for interpreting data of the field SWPP test reported by Yang et al. (2014).

Keywords: Aquifer-aquitard system; Radial dispersion; Parameter estimation; Push-pull test

1 Introduction

A single-well push-pull (SWPP) test could be applied for investigating aquifer properties related to reactive transport in subsurface instead of the inter-well tracer test, due to its advantages of efficiency, low cost, and easy implementation. The SWPP test is sometimes called the single-well injection-withdrawal test, or single-well huff-puff test, or single-well injection-backflow test (Jung and Pruess, 2012). A complete SWPP test includes the injection, the chaser, the rest, and the extraction phase. The second and third phases are generally ignored in the analytical solutions, but recommended in the field applications, since they could increase the reaction time for the injected chemicals with the porous media (Phanikumar and McGuire, 2010;Wang and Zhan, 2019).

Similar to other aquifer tests, the SWPP test is a forced-gradient groundwater tracer test, and analytical solutions are often preferred to determine the *in situ* aquifer properties, due to the computational efficiency. Currently, many analytical models were available for various scenarios of the SWPP tests (Gelhar and Collins, 1971; Huang et al., 2010; Chen et al., 2017; Schroth and Istok, 2005; Wang et al., 2018). However, these studies were based on a common underlying assumption, that the studied aquifer was isolated from adjacent aquitards. In another word, the aquitards bounding the aquifer are taken as two completely impermeable barriers for solute transport. To date, numerous studies demonstrated that such an assumption might cause errors for groundwater flow (Zlotnik and Zhan, 2005;Hantush, 1967), and for reactive transport (Zhan et al., 2009; Chowdhury et al., 2017; Li et al., 2019). This is because even without any flow in the aquitards, molecular diffusion is inevitable to occur when solute injected to the aquifer is close to the aquitard-aquifer interface. This is particularly true when a fully penetrating well is used for injection, thus a portion of injected solute is very close to the aquitard-aquifer interface and the SWPP test duration is relatively long so the effect of molecular diffusion can be materialized. Another important point to note is that the materials of aquitard are usually clay and silt which have strong absorbing capability for chemicals and great mass storage capacities (Chowdhury et al., 2017). To date, the influence of aquitard on reactive transport in aquifers has attracted attentions for several decades. As for radial dispersion, Chen (1985), Wang and Zhan (2013) and Zhou et al. (2017) presented analytical solutions for radial dispersion around an injection well in an aquifer-aquitard system. However, these models only focus on the first phase of the SWPP test (injection).

Another assumption included in many previous models of radial dispersion is that the wellbore storage is ignored for the solute transport. In the injection phase of the SWPP test, the wellbore storage refers to the mixing processes between the prepared tracer injected into the wellbore and original (or native) water in the wellbore. As a result of the wellbore storage, the concentration inside the wellbore varies with time until reaching the same value as the injected concentration, as shown in Figure 1(a). When ignoring it, the concentration inside the wellbore is constant during the entire inject phase, which is certainly not true. Similarly, the wellbore storage in the chaser, rest and extraction phases refers to the concentration variation caused by mixing processes between the original solute in the wellbore and the tracer moving in or out the wellbore. The examples of ignoring wellbore storage include Gelhar and Collins (1971), Chen (1985, 1987), Moench (1989), Chen et al. (2007, 2012), Schroth et al. (2001), Tang and Babu (1979), Chen et al. (2017), Huang et al. (2010), Chen et al. (2012), and Zhou et al. (2017). ~~This assumption implies that the mixing effect in the wellbore is not considered, where the mixing effect refers to the mixture between the original (or native) water and the injected tracer in the well. Such effect is excluded in almost all previous studies except~~Recently, Wang et al. (2018) developed a two-phase (injection and extraction) model for the SWPP test with specific considerations of the wellbore storage. In many field applications, the chaser and rest phases are generally involved and the mixing effect also happens in these two phases in the SWPP test, which ~~is~~ will be investigated in this study.

Besides above-mentioned issues in previous studies, another issue is that the advection-dispersion equation (ADE) was used to govern the reactive transport of SWPP tests (Gelhar and Collins,1971; Wang et al.; 2018; Jung and Pruess, 2012). The validity of ADE was challenged by numerous laboratory and field experimental studies before, when using a single representative value of advection, dispersion and reaction to characterize the whole system. In a hypothetical case, if great details of heterogeneity are known, one may employ a sufficiently fine mesh to discretize the porous media of concern and use ADE to capture anomalous transport characteristics fairly well (e.g. the early arrivals and/or heavy late-time tails of the breakthrough curves (BTCs)). However, such a hypothetical case is rarely been materialized in real applications, especially for field-scale problems. To remedy the situation (at least in some degrees), the multi-rate mass transfer (MMT) model was proposed as an alternative to interpret the data of SWPP test (Huang et al., 2010; Chen et al., 2017). In the MMT model, the porous media is divided into many overlapping continuums (Haggerty et al., 2000;Haggerty and Gorelick, 1995). A subset of MMT is the two overlapping continuums or the mobile-immobile model (MIM) in which the mass transfer between two domains (mobile and immobile) becomes a single parameter instead of a function. The MIM model can grasp most characteristics of MMT and is mathematically simpler than MMT. Besides the MMT model, the continuous time random walk (CTRW) model and the fractional advection-dispersion equation (FADE) model were also applied for anomalous reactive transport in SWPP tests (Hansen et al., 2017; Chen et al., 2017). Due to the complexity of the mathematic models of CTRW and FADE, it is very difficult, or even not possible to derive analytical solutions for those two models, although both methods perform well in a numerical framework.

In this study, a new model of ~~SWIW~~SWPP tests will be established by including both wellbore storage and the aquitard effect under the MIM framework. The reason to choose MIM as the working framework is to capture the possible anomalous ~~anonymous~~ transport characteristics that cannot be described by ADE but at the same time to make the analytical treatment of the problem possible. Four stages of a ~~SWIW~~SWPP test will be considered. The model of the wellbore storage will be developed using a mass balance principle in the chaser and rest phases. It seems not difficult to solve this model of this study using the numerical packages, like MODFLOW-MT3DMS, TOUGH and TOUGHREACT, FEFLOW, and so on. However, the numerical solutions may cause errors in treating the wellbore storage, since the volume of ~~the~~ water in the wellbore was assumed to be constant (Wang et al., 2018), while in reality it changes with time and well discharge. Meanwhile, the numerical errors (like numerical dispersion and numerical oscillation) have to be considered in solving the ADE equation, especially for advection-dominated transport. In this study, analytical solution will be derived to facilitate the data interpretation. Due to the format of analytical solutions, it is much easier to couple such solutions with a proper optimization algorithm (like genetic algorithm). The analytical solution could serve as a benchmark to test the numerical solutions as well. ~~Analytical solution will be derived to facilitate the data interpretation for SWIW tests. The newly developed model will be checked against numerical solutions and field experimental data.~~

2 Model statement of the ~~SWIW~~SWPP test

A single test well is assumed to fully penetrate an aquifer with uniform thickness. Both the aquifer and aquitards are homogeneous and extend laterally to infinity. Linear sorption and first-order degradation are included in the mathematic model of the SWPP test. Such assumptions might be oversimplified for cases in reality, while they are inevitable for the derivation of the analytical solution, especially for the aquifer homogeneity. For a heterogeneity aquifer, the solution presented here may be regarded as an ensemble-averaged approximation if the heterogeneity is spatially stationary. If the heterogeneity is spatially non-stationary, then one can apply non-stationary stochastic approach and/or Monte Carlo simulations to deal with the issue, which is out of the scope of this investigation.

The concept of homogeneity here deserves ~~some~~ clarification. ~~First, d~~Despite the fact that the homogeneity assumption is commonly used in developing analytical and numerical models of subsurface flow and transport, one should be aware that a rigorous sense of homogeneity probably never exists in a real-world setting (unless the media are composed of idealized glass balls as in some laboratory experiments). Therefore, the homogeneity concept here should be envisaged as a media whose hydraulic parameters vary within relatively narrow ranges, or the so-called weak heterogeneity. The Borden site of Canada (Sudicky, 1988) is one example of weak aquifer heterogeneity. Wang et al. (2018) employed a stochastic ~~modeling~~modelling technique to test the assumption of homogeneity associated with the ~~SWIW~~SWPP test, and found that such an assumption could be used to approximate a heterogeneous aquifer when the variance of spatial hydraulic conductivity was small. ~~Second, for moderate or even strong heterogeneous media such as Cape Code site (Hess, 1989) or MADE site (Bohling et al., 2012), the analytical model developed under the homogeneity assumption is also valuable, but in a statistical sense, as long as the media heterogeneity can be regarded as spatially stationary, meaning that the statistical structure of the media heterogeneity does not vary in space. In this setting, the analytical model developed under the homogeneity assumption is used to describe the (ensemble) average characteristics of an ensemble of heterogeneous media which are statistically identical but individually different. In another word, such an analytical model will provide a statistically average description of many realizations (an ensemble) which are similar to the heterogeneous media of concern, but it cannot provide an exact description for the particular heterogeneous media under investigation.~~

A cylindrical coordinate system is employed in this study, and the origin is located at the well ~~center~~centre, as shown in Figure 1(c). The z-axis and the r-axis are vertical and horizontal, respectively. Figure 1 is a schematic diagram of the model investigated by this study~~similar to Figure 1 of Wang and Zhan (2013)~~.

2.1 Reactive transport model

Considering advective effect, dispersive effect and first-order chemical reaction in describing solute transport under the MIM framework, the governing equations the ~~SWIW~~SWPP test are:

$$\theta_m R_m \frac{\partial C_m}{\partial t} = \frac{\theta_m}{r}\frac{\partial}{\partial r}\left(rD_r\frac{\partial C_m}{\partial r}\right) - \theta_m v_a \frac{\partial C_m}{\partial r} - \omega_a(C_m - C_{im}) - \theta_m \mu_m C_m$$
$$-\left(\frac{\theta_{um}v_{um}}{2B}C_{um} - \frac{\theta_{um}D_u}{2B}\frac{\partial C_{um}}{\partial z}\right)\Big|_{z=B} + \left(-\frac{\theta_{lm}v_{lm}}{2B}C_{lm} - \frac{\theta_{lm}D_l}{2B}\frac{\partial C_{lm}}{\partial z}\right)\Big|_{z=-B}, r \geq r_w, \tag{1a}$$

$$\theta_{im} R_{im} \frac{\partial C_{im}}{\partial t} = \omega_a(C_m - C_{im}) - \theta_{im}\mu_{im}C_{im}, r \geq r_w, \tag{1b}$$

$$\theta_{um} R_{um} \frac{\partial C_{um}}{\partial t} = \theta_{um} D_u \frac{\partial^2 C_{um}}{\partial z^2} - \theta_{um} v_{um} \frac{\partial C_{um}}{\partial z} - \omega_u(C_{um} - C_{uim}) - \theta_{um}\mu_{um}C_{um}, z \geq B, \tag{2a}$$

$$\theta_{uim} R_{uim} \frac{\partial C_{uim}}{\partial t} = \omega_u(C_{um} - C_{uim}) - \theta_{uim}\mu_{uim}C_{uim}, z \geq B, \tag{2b}$$

$$\theta_{lm} R_{lm} \frac{\partial C_{lm}}{\partial t} = \theta_{lm} D_l \frac{\partial^2 C_{lm}}{\partial z^2} - \theta_{lm} v_{lm} \frac{\partial C_{lm}}{\partial z} - \omega_l(C_{lm} - C_{lim}) - \theta_{lm}\mu_{lm}C_{lm}, z \leq -B, \tag{3a}$$

$$\theta_{lim} R_{lim} \frac{\partial C_{lim}}{\partial t} = \omega_l(C_{lm} - C_{lim}) - \theta_{lim}\mu_{lim}C_{lim}, z \leq -B, \tag{3b}$$

where subscripts ''u'' and ''l'' refer~~s~~ to parameters in the upper and lower aquitards, respectively; ~~subscript "l" refers to parameters in the lower aquitard;~~ subscripts ''m'' and "im" refer~~s~~ to parameters in the mobile ~~domain; subscript "im" refers to parameters in the~~and immobile domains, respectively~~;~~; C_m and C_{im} are the concentrations [ML^{-3}] of the aquifer; C_{um} ~~and~~, C_{uim} ~~are concentrations [ML^{-3}] of the upper aquitard;~~, C_{lm} and C_{lim} are concentrations [ML^{-3}] of the ~~lower~~ aquitards; t is the time [T]; B is half of the aquifer thickness [L]; r is the radial distance [L]; z represents the vertical distance [L]; r_w is the well radius [L]; D_r is aquifer dispersion coefficient [L^{2}T^{-1}]; D_u and D_l are vertical dispersion coefficients [L^{2}T^{-1}] of the upper aquitard and lower aquitard, respectively; v_a ~~is~~ represents the average velocity [LT^{-1}] in the aquifer and $v_a = \frac{u_a}{\theta_m}$; u_a is Darcian velocity [LT^{-1}]; v_{um} and v_{lm} are vertical velocities [LT^{-1}] in the aquitards; μ_m, μ_{im}, μ_{um}, μ_{uim}, μ_{lm} and μ_{lim} are reaction rates; θ_m, θ_{im}, θ_{um}, θ_{uim}, θ_{lm} and θ_{lim} are the porosities [dimensionless]; $R_m = 1 + \frac{\rho_b K_d}{\theta_m}$, $R_{im} = 1 + \frac{\rho_b K_d}{\theta_{im}}$, $R_{um} = 1 + \frac{\rho_b K_d}{\theta_{um}}$, $R_{uim} = 1 + \frac{\rho_b K_d}{\theta_{uim}}$, $R_{lm} = 1 + \frac{\rho_b K_d}{\theta_{lm}}$ and $R_{lim} = 1 + \frac{\rho_b K_d}{\theta_{lim}}$ are the retardation factors [dimensionless]; K_d is the equilibrium distribution coefficient [M^{-1}L^3]; ρ_b is the bulk density [ML^{-3}]; ω_a, ω_u and ω_l are the first-order mass transfer coefficients [T^{-1}].

The symbol of the advection term is positive in the extraction phase in above equations, while it is negative before that. The dispersions are assumed to be linearly changing with the flow velocity, and one has:

$$D_r = \alpha_r|v_r| + D_r^*, \tag{4a}$$

$$D_u = \alpha_u|v_u| + D_u^*, \tag{4b}$$

$$D_l = \alpha_l|v_l| + D_l^*, \tag{4c}$$

where α_r, α_u and α_l are dispersivities -[L] of the aquifer, upper aquitard, and lower aquitard, respectively; D_r^*, D_u^* and D_l^* are the diffusion coefficients [L^2T^{-1}].

Initial conditions are:

$$C_m(r,t)|_{t=0} = C_{im}(r,t)|_{t=0} = C_{um}(r,z,t)|_{t=0} = C_{uim}(r,z,t)|_{t=0} = C_{lm}(r,z,t)|_{t=0} = C_{lim}(r,z,t)|_{t=0} = 0, r \geq r_w, \tag{5}$$

The boundary conditions at infinity are:

$$C_m(r,t)|_{r\to\infty} = C_{im}(r,t)|_{r\to\infty} = C_{um}(r,z,t)|_{z\to\infty} = C_{uim}(r,z,t)|_{z\to\infty} = C_{lm}(r,z,t)|_{z\to-\infty} = C_{lim}(r,z,t)|_{z\to-\infty},$$

$$= 0, r \geq r_w, \tag{6}$$

Due to the concentration continuity at the aquifer-aquitard interface, one has:

$$C_m(r,t) = C_{um}(r, z = B, t), \tag{7a}$$

$$C_m(r,t) = C_{lm}(r, z = -B, t). \tag{7b}$$

The flux concentration continuity (FCC) is applied on the surface of wellbore, and one has:

$$\left[v_a C_m(r,t) - \alpha_r |v_a| \frac{\partial C_m(r,t)}{\partial r}\right]\Big|_{r=r_w} = \left[v_a C_{inj,m}(t)\right]\Big|_{r=r_w}, 0 < t \leq t_{inj}, \tag{8}$$

$$\left[v_a C_m(r,t) - \alpha_r |v_a| \frac{\partial C_m(r,t)}{\partial r}\right]\Big|_{r=r_w} = \left[v_a C_{cha,m}(t)\right]\Big|_{r=r_w}, t_{inj} < t \leq t_{cha}, \tag{9}$$

$$[C_m(r,t)]|_{r=r_w} = C_{res,m}(r_w,t), t_{cha} < t \leq t_{res}, \tag{10}$$

$$\left[v_a C_m(r,t) - \alpha_r |v_a| \frac{\partial C_m(r,t)}{\partial r}\right]\Big|_{r=r_w} = \left[v_a C_{ext,m}(t)\right]\Big|_{r=r_w}, t_{res} < t \leq t_{ext}, \tag{11}$$

where t_{inj}, t_{cha}, t_{res} and t_{ext} are the end moments [T] of the injection phase, the chaser phase, the rest phase and the extraction phase, respectively; $C_{inj,m}(t)$, $C_{cha,m}(t)$, $C_{res,m}(t)$ and $C_{ext,m}(t)$ represent the wellbore concentrations [ML^{-3}] of tracer in the injection phase, the chaser phase, the rest phase and the extraction phase, respectively. Eqs. (8) - (11) indicate that the flux continuity across the interface between well and the formation is only considered for the mobile continuum (or mobile domain).

The variation of the concentration with mixing effect in the injection phase could be described by (Wang et al., 2018):

$$V_{w,inj} \frac{dC_{inj,m}}{dt} = -\xi v_a(r_w)\left[C_{inj,m}(t) - C_0\right], 0 < t \leq t_{inj}, \tag{12a}$$

$$C_{inj,m}(t)\big|_{t=0} = 0, 0 < t \leq t_{inj}, \tag{12b}$$

$$V_{w,inj} = \pi r_w^2 h_{w,inj}, \tag{12c}$$

$$\xi = 2\pi r_w \theta_m 2B, \tag{12d}$$

where $h_{w,inj}$ is the wellbore water depth [L] in the injection phase, C_0 is concentration [ML^{-3}] of prepared tracer.~~.~~

As for the chaser phase, the models describing the concentration variation in the wellbore could be obtained using mass balance principle:

$$V_{w,cha} \frac{dC_{cha,m}}{dt} = -\xi v_a(r_w)\left[C_{cha,m}(t)\right], t_{inj} < t \le t_{cha}, \tag{13a}$$

$$C_{cha,m}(t)\big|_{t=t_{inj}} = C_{inj,m}(t)\big|_{t=t_{inj}}, t_{inj} < t \le t_{cha}, \tag{13b}$$

$$V_{w,cha} = \pi r_w^2 h_{w,cha}, \tag{13c}$$

where $h_{w,cha}$ is the wellbore water depth [L] in the chaser phase.

In the extraction phase, the boundary condition is (Wang et al., 2018):

$$V_{w,ext} \frac{dC_{ext,m}}{dt}\Big|_{r=r_w} = -\xi \alpha_r v_a(r_w) \frac{dC_{ext,m}}{dt}\Big|_{r=r_w}, t_{res} < \mathrm{t} \le t_{ext}, \tag{14a}$$

$$C_{ext,m}(t)\big|_{t=t_{res}} = C_{res,m}(t)\big|_{t=t_{res}}, t_{res} < t \le t_{ext}, \tag{14b}$$

$$V_{w,ext} = \pi r_w^2 h_{w,ext}, \tag{14c}$$

where $h_{w,ext}$ is the wellbore water depth [L] in the extraction phase.

2.2 Flow field model

The flow problem must be solved first before investigating the transport problem of the ~~SWIW~~SWPP test. The velocity involved in the advection and dispersion terms of the governing equations (1a) and (1b) is:

$$v_a(r_w) = \frac{Q}{4\pi r_w B \theta_m}, r \ge r_w, \tag{15}$$

where Q is the pumping rate [L^{3}T^{-1}], and it is negative for injection and positive for pumping. The use of Eq. (15) implies that quasi-steady state flow can be established very quickly near the injection/pumping well, thus the flow velocity becomes independent of time. This approximation is generally acceptable given the very limited spatial range of influence of most ~~SWIW~~SWPP tests. For instance, if the characteristic length of ~~SWIW~~SWPP test is l and the aquifer hydraulic diffusivity is $D=K_a/S_a$, where K_a are S_a are respectively the radial hydraulic conductivity and specific storage, then the typical characteristic time of unsteady-state flow is around $t_c \approx \frac{l^2}{2D}$. The typical characteristic time refers to the time of the flow changing from transient state to quasi-steady state, where the spatial distribution of flow velocity does not change while the drawdown varies with time. This model is similar to the model used to calculate the typical characteristic length of the tide-induced head fluctuation in a coastal aquifer system (Guarracino et al., 2012). For K_a=1m/day, S_a=10^{-5}m^{-1} and l=10m (which are representative of an aquifer consisting of medium sands), one has $t_c \approx \frac{l^2}{2D} = 5.0 \times 10^{-3}$ day, which is a very small value. To test the model in computing t_c, the numerical simulation has been conducted, where the other parameters used in the model are the same as ones used in Figures 2 and 3. Figure S2 shows the flow is in quasi-steady state when time is greater than t_c, since two curves of t =5.0×10^{-3} day and t =10.0×10^{-3} day overlap. As for the typical characteristic length, if the values of ~~the~~ K_a, S_a, and B have been estimated by the pumping tests before the SWPP test, it could be calculated by numerical modelling exercises using different simulation times.

The water levels in the wellbore in Eqs. (12) - (14) could be calculated by the models of Moench (1985):

$$h_w = \lim_{t\to\infty}\{\mathcal{L}^{-1}[\bar{h}_w(p)]\}, \tag{16}$$

where p is Laplace transform variable; $\mathcal{L}^{-1}$ represents the inverse Laplace transform; the over bar represents the Laplace-domain variable, and

$$\bar{h}_w(p) = h_0 - \frac{Q}{8\pi KB}\frac{2[K_0(x)+xS_wK_1(x)]}{p\{pW_D[K_0(x)+xS_wK_1(x)]+xK_1(x)\}}, \tag{17}$$

$$W_D = \frac{1}{4BS_a}, \tag{18}$$

$$x = \frac{(p+\bar{q})}{2}, \tag{19}$$

$$\bar{q} = (\gamma')^2 m' \coth(m') + (\gamma'')^2 m'' \coth(m''), \tag{20}$$

$$m' = \frac{\left(\frac{S_u B_u p}{S_a B}\right)^{1/2}}{\gamma'}, \tag{21}$$

$$m'' = \frac{\left(\frac{S_l B_l p}{S_a B}\right)^{1/2}}{\gamma''}, \tag{22}$$

$$\gamma' = r_w\left(\frac{K_u}{2K_a B B_u}\right)^{1/2}, \tag{23}$$

$$\gamma'' = r_w\left(\frac{K_l}{2K_a B B_l}\right)^{1/2}, \tag{24}$$

where K_u and K_l are hydraulic conductivities [LT^{-1}]; S_u and S_l are specific storages [L^{-1}]; S_w is the wellbore skin factor [dimensionless]; B_u and B_l are thicknesses [L]; $K_0(\cdot)$ and $K_1(\cdot)$ are the modified Bessel functions.

3 New solution of reactive transport in the SWPP test

In this study, the Laplace transform and Green's function methods will be employed to derive the analytical solution of the new SWPP test models described in Section 2. The dimensionless parameters are defined as follows: $C_{mD} = \frac{C_m}{C_0}$, $C_{imD} = \frac{C_{im}}{C_0}$, $C_{inj,mD} = \frac{C_{inj,m}}{C_0}$, $C_{inj,imD} = \frac{C_{inj,im}}{C_0}$, $C_{cha,mD} = \frac{C_{cha,m}}{C_0}$, $C_{cha,imD} = \frac{C_{cha,im}}{C_0}$, $C_{res,mD} = \frac{C_{res,m}}{C_0}$, $C_{res,imD} = \frac{C_{res,im}}{C_0}$, $C_{ext,mD} = \frac{C_{ext,m}}{C_0}$, $C_{ext,imD} = \frac{C_{ext,im}}{C_0}$, $C_{umD} = \frac{C_{um}}{C_0}$, $C_{uimD} = \frac{C_{uim}}{C_0}$, $C_{lmD} = \frac{C_{lm}}{C_0}$, $C_{limD} = \frac{C_{lim}}{C_0}$, $t_D = \frac{|A|}{\alpha_r^2 R_m} t$, $r_D = \frac{r}{\alpha_r}$, $r_{wD} = \frac{r_w}{\alpha_r}$, $z_D = \frac{z}{B}$, $\mu_{mD} = \frac{\alpha_r^2 \mu_m}{A}$, $\mu_{imD} = \frac{\alpha_r^2 R_m \mu_{im}}{R_{im} A}$, $\mu_{umD} = \frac{\alpha_r^2 \mu_{um}}{A}$, $\mu_{uimD} = \frac{\alpha_r^2 R_m \mu_{uim}}{R_{im} A}$, $\mu_{lmD} = \frac{\alpha_r^2 \mu_{lm}}{A}$, $\mu_{limD} = \frac{\alpha_r^2 R_m \mu_{lim}}{R_{im} A}$ and $A = \frac{Q}{4\pi B \theta_m}$. The detailed derivation of the new solution is listed in Section S1 of ***Supplementary Materials***.

3.1 Solutions in Laplace domain

As for the injection phase of the SWPP test, the solutions in Laplace domain are:

$$\bar{C}_{mD}(r_D, s) = \phi_1 \exp\left(\frac{y_{inj}}{2}\right) A_i\left(E^{1/3} y_{inj}\right), r_D \geq r_{wD}, \tag{25a}$$

$$\bar{C}_{imD} = \frac{\varepsilon_{im}}{(s+\mu_{imD}+\varepsilon_{im})} \bar{C}_{mD}, r_D \geq r_{wD}, \tag{25b}$$

$$\bar{C}_{umD} = \bar{C}_{mD} exp(a_2 z_D - a_2), z_D \geq 1, \tag{25c}$$

$$\bar{C}_{uimD} = \frac{\varepsilon_{uim}}{s+\varepsilon_{uim}+\mu_{uimD}} \bar{C}_{umD}, z_D \geq 1, \tag{25d}$$

$$\bar{C}_{lmD} = \bar{C}_{mD} exp(b_1 z_D + b_1), z_D \leq -1, \tag{25e}$$

$$\bar{C}_{limD} = \frac{\varepsilon_{lim}}{s+\varepsilon_{lim}+\mu_{limD}} \bar{C}_{lmD}, z_D \leq -1, \tag{25f}$$

where *s* represents the Laplace transform parameter for t_D (which is proportional to *p*); $A_i(\cdot)$ is the Airy function $A_i'(\cdot)$ is the derivative of the Airy function; the expressions for a_2, b_1, E, y_{inj}, $y_{inj,w}$, ε_m, ε_{im}, ε_{um}, ε_{uim}, ε_{lm}, ε_{lim}, β_{inj} and ϕ_1 are listed in Table 1.

In the chaser phase, the solutions of the SWPP test in Laplace domain are:

$$\bar{C}_{mD} = \Psi(r_D) + \delta_1 + \delta_2 r_D, r_D \geq r_{wD}, \tag{26a}$$

$$\bar{C}_{imD} = \frac{\varepsilon_{im}}{(s+\mu_{imD}+\varepsilon_{im})} \bar{C}_{mD} + \frac{C_{imD}(r_D, t_{inj,D})}{(s+\mu_{imD}+\varepsilon_{im})}, r_D \geq r_{wD}, \tag{26b}$$

$$\Psi(r_D, E_a; \eta) = \int_{r_{wD}}^{\infty} g(r_D, E_a; \eta)\, \varphi(\eta) d\eta, r_D \geq r_{wD}, \tag{26c}$$

$$\bar{C}_{umD} = \int_1^{\infty} g_u(z_D, E_u; \eta_u)\, f_u(\eta_u) d\eta_u + \frac{z_D - z_{eD}}{1 - z_{eD}} \bar{C}_{mD}(r_D, s), z_D \geq 1, \tag{26d}$$

$$\bar{C}_{uimD} = \frac{\varepsilon_{uim}}{s+\varepsilon_{uim}+\mu_{uimD}}\bar{C}_{umD} + \frac{C_{uimD}(r_D,z_D,t_{inj,D})}{s+\varepsilon_{uim}+\mu_{uimD}}, z_D \geq 1, \tag{26e}$$

$$\bar{C}_{lmD} = \int_{-1}^{-\infty} g_l(z_D,E_l;\eta_l)\, f_l(\eta_l) d\eta_l + \frac{z_{eD}+z_D}{z_{eD}-1}\bar{C}_{mD}(r_D,z_D,s), z_D \leq -1, \tag{26f}$$

$$\bar{C}_{limD} = \frac{\varepsilon_{lim}}{s+\varepsilon_{lim}+\mu_{limD}}\bar{C}_{lmD} + \frac{C_{limD}(r_D,z_D,t_{inj,D})}{s+\varepsilon_{lim}+\mu_{limD}}, z_D \leq -1, \tag{26g}$$

where η varies between r_{wD} and ∞, e.g. $r_{wD} \leq \eta \leq \infty$; η_u varies between 1 and ∞; η_l varies between -1 and $-\infty$; $C_{mD}(r_D, t_{inj,D})$ and $C_{imD}(r_D, t_{inj,D})$ are the concentrations [ML^{-3}] of the aquifer at the end of injection stage, which could be calculated by Eq. (25a) and Eq. (25b) after applying the inverse Laplace transform, $C_{umD}(r_D, z_D, t_{inj,D})$ and $C_{uimD}(r_D, z_D, t_{cha,D})$ represent the concentrations [ML^{-3}] of the upper aquitard at the end of the injection phase, which could be calculated by Eq. (25c) and Eq. (25d) after applying the inverse Laplace transform, $C_{lmD}(r_D, z_D, t_{inj,D})$ and $C_{limD}(r_D, z_D, t_{inj,D})$ are the concentrations [ML^{-3}] of the lower aquitard at the end of the injection phase, which could be calculated by Eq. (25e) and Eq. (25f) after applying the inverse Laplace transform, $g(r_D, E_a; \eta)$, $g_u(z_D, E_u; \eta_u)$ and $g_l(z_D, E_l; \eta_l)$ are the Green's functions; the expressions for $g(r_D, E_a; \eta)$, $g_u(z_D, E_u; \eta_u)$, $g_l(z_D, E_l; \eta_l)$, δ_1, δ_2, $\mathcal{S}_1$, $\mathcal{S}_2$, E_a, E_u, E_l, y_{cha}, $y_{cha,w}$, F, $\varphi(r_D)$, $f_u(\eta_u)$, X, M_1, M_2, M_3, M_4, N_1, N_2, N_3, N_4, $\mathcal{T}_1$, $\mathcal{T}_2$, $\mathcal{T}_3$, $\mathcal{T}_4$ and $\beta_{cha,D}$ are listed in Table 2.

For the rest phase, the solutions of the SWPP test in Laplace domain are:

$$\bar{C}_{mD} = \frac{C_{mD}(r_D,t_{cha,D}) + \frac{\varepsilon_m C_{imD}(r_D,t_{cha,D})}{(s+\mu_{imD}+\varepsilon_{im})}}{\left(s+\varepsilon_m+\mu_{mD}-\frac{\varepsilon_m \varepsilon_{im}}{s+\mu_{imD}+\varepsilon_{im}}\right)}, r_D \geq r_{wD}, \tag{27a}$$

$$\bar{C}_{imD} = \frac{C_{imD}(r_D,t_{cha,D})}{(s+\mu_{imD}+\varepsilon_{im})} + \frac{\varepsilon_{im}\bar{C}_{mD}}{(s+\mu_{imD}+\varepsilon_{im})}, r_D \geq r_{wD}, \tag{27b}$$

$$\bar{C}_{umD} = \frac{C_{umD}(r_D,z_D,t_{cha,D}) + \frac{\varepsilon_{um} C_{uimD}(r_D,z_D,t_{cha,D})}{s+\varepsilon_{uim}+\mu_{uimD}}}{\left(s+\varepsilon_{um}+\mu_{umD}-\frac{\varepsilon_{um}\varepsilon_{uim}}{s+\varepsilon_{uim}+\mu_{uimD}}\right)}, z_D \geq 1, \tag{27c}$$

$$\bar{C}_{uimD} = \frac{\varepsilon_{uim}}{s+\varepsilon_{uim}+\mu_{umD}}\bar{C}_{umD} + \frac{C_{uimD}(r_D,z_D,t_{cha,D})}{s+\varepsilon_{uim}+\mu_{umD}}, z_D \geq 1, \tag{27d}$$

$$\bar{C}_{lmD} = \frac{C_{lmD}(r_D,z_D,t_{cha,D}) + \frac{\varepsilon_{lm} C_{limD}(r_D,z_D,t_{cha,D})}{s+\varepsilon_{lim}+\mu_{limD}}}{\left(s+\varepsilon_{lm}+\mu_{lmD}-\frac{\varepsilon_{lm}\varepsilon_{lim}}{s+\varepsilon_{lim}+\mu_{limD}}\right)}, z_D \leq -1, \tag{27e}$$

$$\bar{C}_{limD} = \frac{\varepsilon_{lim}}{s+\varepsilon_{lim}+\mu_{lmD}}\bar{C}_{lmD} + \frac{C_{limD}(r_D,z_D,t_{cha,D})}{s+\varepsilon_{lim}+\mu_{lmD}}, z_D \leq -1, \tag{27f}$$

where $C_{mD}(r_D, t_{cha,D})$ and $C_{imD}(r_D, t_{cha,D})$ are the concentrations [ML^{-3}] of the aquifer at the end of the chaser phase, which could be calculated by Eq. (26a) and Eq. (26b) after applying the inverse Laplace transform, $C_{umD}(r_D, z_D, t_{cha,D})$ and

$C_{uimD}(r_D, z_D, t_{cha,D})$ are the concentrations [ML^{-3}] of the upper aquitard at the end of the chaser phase, which could be computed by Eq. (26d) and Eq. (26e) after applying the inverse Laplace transform, $C_{lmD}(r_D, z_D, t_{cha,D})$ and $C_{limD}(r_D, z_D, t_{cha,D})$ are the concentrations [ML^{-3}] of the lower aquitard at the end of the chaser phase, which could be calculated by Eq. (26f) and Eq. (26g) after applying the inverse Laplace transform.

As for the extraction phase of the SWPP test, the solutions in Laplace domain are:

$$\bar{C}_{mD}(r_D, s) = exp(-r_D/2)[U(r_D, \zeta; \varepsilon) + \sigma_1 + \sigma_2 r_D], r_D \geq r_{wD}, \tag{28a}$$

$$\bar{C}_{imD} = \frac{\varepsilon_{im}}{(s+\mu_{imD}+\varepsilon_{im})}\bar{C}_{mD} + \frac{C_{imD}(r_D, res)}{s+\mu_{imD}+\varepsilon_{im}}, r_D \geq r_{wD}, \tag{28b}$$

$$U(r_D, \zeta; \varepsilon) = \int_{r_{wD}}^{\infty} g(r_D, \zeta; \varepsilon) f(\varepsilon) d\varepsilon, \tag{28c}$$

$$\bar{C}_{umD} = \int_1^{\infty} g_u(z_D, E_u; b_u) f_u(b_u) db_u + \frac{z_D - z_{eD}}{1 - z_{eD}} \bar{C}_{mD}(r_D, s), z_D \geq 1, \tag{28d}$$

$$\bar{C}_{uimD} = \frac{\varepsilon_{uim}\bar{C}_{um}}{s+\varepsilon_{uim}+\mu_{uimD}} + \frac{C_{uimD}(r_D, z_D, t_{res,D})}{s+\varepsilon_{uim}+\mu_{uimD}}, z_D \geq 1, \tag{28e}$$

$$\bar{C}_{lmD} = \int_{-1}^{-\infty} g_l(z_D, E_l; b_l) f_l(b_l) db_l + \frac{z_D + z_{eD}}{z_{eD} - 1} \bar{C}_{mD}(r_D, s), z_D \leq -1, \tag{28f}$$

$$\bar{C}_{limD} = \frac{\varepsilon_{lim}\bar{C}_{lmD}}{s+\varepsilon_{lim}+\mu_{limD}} + \frac{C_{limD}(r_D, z_D, t_{res,D})}{s+\varepsilon_{lim}+\mu_{limD}}, z_D \leq -1, \tag{28g}$$

where $C_{mD}(r_D, t_{res,D})$ and $C_{imD}(r_D, t_{res,D})$ are the concentrations [ML^{-3}] of the aquifer at the end of the rest phase, which could be calculated by Eq. (27a) and Eq. (27b) after applying the inverse Laplace transform, $C_{umD}(r_D, z_D, t_{res,D})$ and $C_{uimD}(r_D, z_D, t_{res,D})$ are the concentrations [ML^{-3}] of the upper aquitard at the end of the rest phase, which could be calculated by Eq. (27c) and Eq. (27d) after applying the inverse Laplace transform, $C_{lmD}(r_D, z_D, t_{res,D})$ and $C_{limD}(r_D, z_D, t_{res,D})$ are the concentrations [ML^{-3}] of the lower aquitard at the end of the rest phase, which could be calculated by Eq. (27e) and Eq. (27f) after applying the inverse Laplace transform; b_u varies between 1 and ∞; b_l varies between -1 and $-\infty$; ε varies between r_{wD} and ∞ (e.g. $r_{wD} \leq \varepsilon \leq \infty$); $g(r_D, \zeta; \varepsilon)$, $g_u(z_D, E_u; b_u)$ and $g_l(z_D, E_l; b_l)$ are the Green's functions; the expressions for $g(r_D, \zeta; \varepsilon)$, $g_u(z_D, E_u; b_u)$, $g_l(z_D, E_l; b_l)$, σ_1, σ_2, Λ, ζ, $f(\varepsilon)$, $f_u(b_u)$, $f_l(b_l)$, $H_1 \sim H_4$, $I_1 \sim I_4$, $m_1 \sim m_2$, $n_1 \sim n_2$, $P_1 \sim P_4$, W, y_{ext}, $y_{ext,w}$ and $\beta_{ext,D}$ are listed in Table 3.

3.2 Solutions from Laplace domain to real-time domain

Because the analytical solutions in Laplace domain are too complex, it seems impossible to transform it into the real time domain analytically. Alternatively, a numerical method will be introduced for the invers Laplace transform. Currently, several methods are available, like the Stehfest model, Zakian model, Fourier series model, de Hoog model, and Schapery model (Wang and Zhan, 2015). Here, the de Hoog method will be applied to conduct the inverse Laplace transform, since it performed well for radial-dispersion problems (Wang et al., 2018;Wang and Zhan, 2013).

3.3 Assumptions included in the new SWPP test model

The new SWPP test model is a generalization of several previous studies; for instance, the new solution reduces to the solution of Gelhar and Collins (1971) when $\omega_a = \omega_u = \omega_l = D_u = D_l = v_{um} = v_{lm} = V_{w,inj} = V_{w,cha} = V_{w,ext} = t_{cha} = t_{res} = 0$ and~~-~~, to the solution of Chen et al. (2017) when $\omega_u = \omega_l = D_u = D_l = v_{um} = v_{lm} = V_{w,inj} = V_{w,cha} = V_{w,ext} = 0$, and Wang et al., (2018) when $\omega_a = \omega_u = \omega_l = D_u = D_l = v_{um} = v_{lm} = t_{cha} = t_{res} = 0$. "$t_{cha} = t_{res} = 0$" represents the four-phase SWPP test becomes the two-phase SWPP test, where the chaser and rest phases are excluded. Actually, all values of ω_a, ω_u, ω_l, D_u, D_l, v_{um}, v_{lm}, $V_{w,inj}$, $V_{w,cha}$, and $V_{w,ext}$ are not zero in the reality, which have been considered in the new solutions of this study.

However, three assumptions still remain. First, the flow is in the quasi-steady state flow, e.g. Eq. (15). Second, the groundwater flow is horizontal in the aquifer, and is vertical in the aquitard. This treatment relies on the basis that the permeability of the aquitard is smaller than the permeability of the aquifer (Moench, 1985). Third, the model is simplified for the solute transport. For example, only vertical dispersion and advection effects are considered in the aquitard, and only radial dispersion and advection effects are considered in the aquifer. The validation of these assumptions will be discussed in the Section 4.2.

4 Verification of the new model

In this section, the newly derived analytical solutions will be tested from two aspects. Firstly, the new solution of this study could reduce to previous solutions under special cases, as the model established in this study is an extension of previous ones, and comparisons between them will be shown in Section 4.1. Secondly, although some assumptions included in previous models have been relaxed in the new model, some other processes of the reactive transport in the SWPP test have to be simplified in analytical solutions. Assumptions included in the new model have been discussed and their applicability is elaborated in Section 4.2.

4.1 Test of the new solution with previous solutions

To test the new solutions, the model of Chen et al. (2017) serves as a benchmark, who ignored the aquitard effect and wellbore storage in the ~~SWIW~~SWPP test. Figure 2 shows the comparison of BTCs between them, and ~~the~~ parameters used in such a comparison are: $R_m = R_{im} = R_{um} = R_{uim} = R_{lm} = R_{lim}=1$, $\theta_{um} = \theta_{lm}=0.1$, $\alpha_r = \alpha_u = \alpha_l=0.1$m, $\mu_m = \mu_{im} = \mu_{um} = \mu_{uim} = \mu_{lm} = \mu_{lim}=10^{-6}$d^{-1}, r_w =0.2m, Q_{inj}=2.5 m^3/d, Q_{cha}=2.5 m^3/d, Q_{res}=0 m^3/d, Q_{ext}=-2.5 m^3/d, t_{inj}=100day, t_{cha}=50day, t_{res}=40day, B=5 m, θ_m=0.3, θ_{im}=0.15, $\theta_{uim} = \theta_{lim}$=0.~~–~~1, and ω=0.001 d^{-1}. ~~The p~~Parameters of "$h_{w,inj} =$

$h_{w,cha} = h_{w,res} = h_{w,ext}$ =0" represent $V_{w,inj}$ =0, $V_{w,cha}$ =0 and $V_{w,ext}$ =0, and imply that ~~the~~ wellbore storage is neglected. The values of v_{um}=v_{lm}=0 m/d mean that aquitards are neglected. As shown in Figure ~~1~~2, both solutions agree well for the mobile and immobile domains.

4.2 Test of assumptions involved in the analytical solution

To test ~~the~~ three assumptions outlined in Section 3.3, a numerical model will be established, where general three-dimensional transient flow and solute transport are considered in both aquifer and aquitards. A finite-element method with the help of COMSOL Multiphysics will be used to solve the three-dimensional model. The grid system is shown in Section S2 of ***Supplementary Materials***.

In this study, four sets of aquitard hydraulic conductivities are employed, such as K_u=K_l=0.1K_a, K_u=K_l=0.02K_a, K_u=K_l=0.01K_a, and K_u=K_l=0.001K_a. A point to note is that the extreme case of K_u=K_l=0.1K_a used here is only for the purpose of examining the robustness of comparison, while the real values of K_u and K_l are usually much lower than 0.1K_a. In another word, the rest three cases mentioned above are more likely to occur in real applications.

The initial drawdown and the initial concentration are 0 for aquifer and aquitards. The hydraulic parameters are: K_a=0.1 m/day, S_a= S_u= S_l=10^{-4} m^{-1}, and the other parameters are $R_m = R_{im} = R_{um} = R_{uim} = R_{lm} = R_{lim}$=1, $\theta_{um} = \theta_{lm} = 0.1$, $\alpha_r = 2.5$m, $\alpha_u = \alpha_l = 0.5$m, $\mu_m = \mu_{im} = \mu_{um} = \mu_{uim} = \mu_{lm} = \mu_{lim}$=10^{-7}s^{-1}, r_w =0.5m, Q_{inj}=Q_{cha} =50 m^3/d, Q_{res}=0 m^3/d, Q_{ext}=-50 m^3/d, t_{inj}=250day, t_{cha}=50day, t_{res}=50day, B=10m, θ_m=0.~~3~~25, θ_{im}=0.~~0~~05, and ω=~~0~~0.01 d^{-1}. The comparison of concentration between the analytical and numerical solutions is shown in Figures~~.~~ ~~2~~ 3 and ~~3~~4.

As the first assumption in Section 3.3 has been elaborated in Section 2.2, the following discussion will only focus on the second and third assumptions. Figures~~.~~ ~~2a~~3(a), ~~2b~~ 3(b) and ~~2c~~ 3(c) represent the snapshots of concentration distributions in the aquifer along the r-axis at different times. One may conclude that ~~the~~ curves with smaller K_u and K_l values are closer to the analytical solution. This is because aquitards with smaller K_u and K_l (when K_a ~~K_a~~ remains constant) could make flow closer to the horizontal direction (or parallel with the aquitard-aquifer interface) in the aquifer and closer to the vertical direction (or perpendicular with the aquitard-aquifer interface) in the aquitard, according to the law of refraction (Fetter, 2018). In another word, when the values of K_u/K_a and K_l/K_a ~~are~~ approach 0, the flow direction becomes horizontal in the aquifer and vertical in the aquitard, and then the numerical model reduces to the analytical model. Therefore, from this figure, one may conclude that the above-mentioned second assumption in Section 3.3 works well in the aquifer when K_u/K_a and K_l/K_a are samller then 0.01.

Figure~~.~~ ~~3~~4 shows the comparison of the analytical and numerical solutions for aquitards. Fig~~s.~~ures ~~3~~ 4(a1) - (c1) represent the snapshots of concentration distributions obtained from analytical solution~~s~~ of this study at different times, and Fig~~s.~~ures ~~3~~ 4(a2) - (c2) represent the snapshots of concentration distributions obtained from the numerical solution~~s at the same time~~. One may find that the contour maps obtained from both solutions are almost the same in the aquifer, but very different in the aquitards. Therefore, the above-mentioned third assumption in Section 3.3 is generally unacceptable in describing solute transport in the aquitard in the ~~SWIW~~SWPP test, but works well when the aquifer is of the primary concern.

5 Discussions

5.1 Model applications

As mentioned in Section 3.~~1~~3, the new model is a generalization of many previous models, and the conceptual model is more close to reality.~~-~~ However, there are many parameters involved in this new model that have to be determined first for applying this model. For instance, the involved parameters for the aquitards include dispersivity (α_u and α_l), first-order mass transfer coefficient (ω_u and ω_l), retardation factor (R_{um}, R_{uim}, R_{lm}, and R_{lim}), porosity (θ_{um}, θ_{uim}, θ_{lm} and θ_{lim}), reaction rate (μ_{um}, μ_{uim}, μ_{lm} and μ_{lim}), and velocity (v_{um} and v_{lm}). The involved parameters for the aquifer include α_r, ω_a, R_m, R_{im}, θ_m, θ_{im}, and B. Generally, these parameters could not be measured directly. Otherwise, they ~~could~~ have to be obtained by fitting the experimental data using the forward model.

Parameter estimation is an inverse problem, and it is generally conducted by an optimization model, such as genetic algorithm, simulated annealing, and so on. Due to the ill-posedness of many inverse problems or insufficient observation data, the initial guess values of unknown parameters of interest are critical for finding the best values or real values of those parameters in the optimization model. Here, we recommend using values of parameters from literatures as the initial guesses for similar lithology. Table 4 lists some parameter values for sandy and clay aquifers in previous studies. When result is not sensitive to a particular parameter of concern, the value from previous publications for similar lithology and/or situations could be taken as estimated value of that parameter, if there is no direct measurement of that particular parameter of concern. To prioritize the sensitivity of predictions with respect to the diverse parameters involved in the new model, a global sensitivity analysis is conducted in Section 5.2.

5.2 A global sensitivity analysis

From the analytical solutions of Eqs. (26) - (28), one may find that BTCs are affected by several parameters, like α_u, v_{um}, θ_{um}, ω, α_r, θ_m and V_w. As α_l, v_{lm}, θ_{lm} have the similar effect on the results with α_u, v_{um}, θ_{um}, they have been excluded in the following analysis. In this section, a global sensitivity analysis is conducted using the model of Morris (1991), which is a one-step-at-a-time method. Morris (1991) employed μ_k and σ_k to represent the importance of the input parameters on the output concentration and they could be computed by (Morris, 1991 and Lin et al., 2019):

$$\mu_k = \sum_{l=1}^{M}\left(\left|EE_k^l\right|/M\right), k = 1,2,\cdots N, \tag{29a}$$

$$\sigma_k = \sqrt{\frac{1}{M}\sum_{l=1}^{M}\left(EE_k^l - \mu_k\right)}, k = 1,2,\cdots N, \tag{29b}$$

where M is the total sampling number, assuming that the range of parameter value is divided to M intervals; N is the total parameter number of interest, and it is 7 in this study; k is the k^{th} parameter. In this study, $M = 50$;

$$EE_k^l = \frac{C_{mD}(P_1, P_2, \cdots, P_k + l\Delta, \cdots, P_N) - C_{mD}(P_1, P_2, \cdots, P_k, \cdots, P_N)}{l\Delta}$$

where P_i is the random value of the i^{th} parameter in the range of $(P_{i,0}, P_{i,lim})$; $P_{i,0}$ and $P_{i,lim}$ are the smallest and largest values of P_i, as shown in Table S1; Δ is a small increment defined as $1/(M-1)$.

A larger μ_k means a higher sensitive effect of the k^{th} parameter on the output, and a larger σ_k represents that the k^{th} parameter has a greater interaction effect with others. Figures 5(a) and 5(b) represent the variation of μ_k and σ_k with time in the wellbore, respectively. The values of μ_k are greater for α_r and θ_m than for the others, as shown in Figures 5(a), indicating that the influence of θ_m and α_r on the results is more obvious than others. However, the values of σ_k is large for α_u, θ_{um}, α_r, θ_m and V_w, demonstrating that the interactions of these parameters with others are strong; namely, the influence of them on results also could not be ignored.

5.3 Effect of the aquitard

As shown in Section 4.2, the new analytical solution is a good approximation for the numerical model in the aquifer when K_u/K_a and K_l/K_a are smaller ~~then~~than 0.01. In this section, we try to figure out how the aquitards will affect BTCs of the SWPP tests. Since the porosity is an important factor of concern, three sets of porosity values are used for the aquitards: $\theta_{um} = \theta_{lm}$ =0, 0.1, and 0.25. The other parameters are from the case in Figure 4.

Figure 6 shows the difference between the models with and without aquitards for different flow velocities in the aquitard. The case of $\theta_{um} = \theta_{lm} = 0$ represents the model without the aquitard. The difference is not obvious at the beginning of the extraction phase, while such a difference is obvious at the late time. Meanwhile, the smaller aquitard porosity makes the value of BTCs in the aquifer greater at a given time. When the aquitard is ignored, the values of BTCs are the greatest. Therefore, the aquitard effect on transport in the aquifer is quite obvious and should not be ignored in general.

5.4 Effect of the aquifer radial dispersion

Another important parameter is the radial dispersion in the aquifer. In this section, three sets of the radial dispersivity values will be used to analyse the influence: α_r =1.25m, 2.50m, and 5.00m.

Figure 7 shows BTCs in the well face for different radial dispersivity values. Firstly, the difference is obvious among curves in all phases. Secondly, a larger α_r could decrease BTCs at a given time of the injection phase. This could be explained by the boundary condition of Eq. (8). The solute in the mobile domain of the aquifer is transported by both advection and dispersion, thus a larger α_r could lower the values of C_m in the well face. Thirdly, BTCs increase with increasing α_r values in the chaser and rest phases. Fourthly, the peak values of BTCs decrease with increasing α_r values.

6 Data interpretation: Field SWPP test

To test the performance of the new model, the field data reported in Chen et al. (2017) will be employed. Specifically, the experimental data of S1 conducted in the borehole TW3 will be analysed. The reason choosing this dataset is because this borehole penetrated several layers, and it had been interpreted by Chen et al. (2017) before (using a model without considering the aquitard effect and the wellbore storage). The physical parameters of the SWPP test are r_w =0.1m, Q_{inj}=Q_{cha} =7.78L/min, Q_{res}=0 L/min, Q_{ext}=12 L/min, t_{inj}=180min, t_{cha}=26.74min, t_{res}=10080min, B=4m. The other ~~Detailed~~ information of experimental data could be seen in the references of Assayag et al. (2009) and Yang et al. (2014).

Fig~~.~~ure 8(~~7~~a) shows the fitness of the computed and observed BTCs. The estimated parameters are: θ_{um}=0.05, θ_{lm}=0.0, θ_m=0.1, θ_{im}=0.068, $\alpha_r = 0.5$m, $\alpha_u = 0.35$m, α_l=0.0m, $R_m = R_{im} = R_{um} = R_{uim} = R_{lm} = R_{lim}$=1, $\mu_m = \mu_{im} = \mu_{um} = \mu_{uim} = \mu_{lm} = \mu_{lim}$=$10^{-7}$$s^{-1}$, and ω=0.001d^{-1}, and $h_{w,inj} = h_{w,cha}$ =32m, $h_{w,res}$=30m, $h_{w,ext}$=28m. Apparently, the fitness by the new solution is better than the model of Chen et al. (2017). As for the error between the observed and computed BTCs, the new solution is also smaller than that of Chen et al. (2017) as well, where the error is defined as

$$Error = \sum_{i=1}^{N}(C_{OBS} - C_{COM})^2, \quad (30)$$

where C_{OBS} and C_{COM} are the observed and computed concentrations, respectively, and N is the number of sampling points.

How accurate these parameters estimated by best fitting the observed data are in representative of the real aquifer will be discussed as following. The values of retardation factor and reaction rate demonstrate that the chemical reaction and sorption are weak for the tracer of KBr in the SWPP test. It is not surprising since KBr is commonly treated as a "conservative" tracer. The porosity of the real aquifer ranges from 0.01 to 0.1, according to the well log analysis (Yang et al., 2014), where the estimated values are located. The estimated porosity represents the average values of the aquifer and aquitards. The estimated dispersivity of the aquifer is 0.7134m by Chen et al. (2017), which is similar with ours. The values of water level in the test could be observed directly; however, these data are not available, and they have to be estimated in this study. To evaluate the uncertainty in the estimated parameters, the sensitivity of the dispersivity on BTCs is analysed, as shown in Figures 8(b). One may conclude that the estimated values of this study seem to be representative of the reality, since $Error$ is smallest for $\alpha_r = 0.5$m.

7 Summary and conclusions

The single-well Push-Pull (SWPP) test could be applied to estimate the dispersivity, porosity, chemical reaction rates of the *in situ* aquifers. However, previous studies mainly focused on an isolated aquifer, excluding all the possible effect of aquitards bounding the aquifer. In another word, the adjacent layers are assumed to be non-permeable, which is not exactly true in reality. In this study, a new analytical model is established and its associate solutions derived to inspect the effect of overlying and underlying aquitards. Meanwhile, four stages are considered in the new model with wellbore storage, including the injection phase, the chaser phase, the rest phase and the extraction phase. The anomalous behaviours of reactive transport in the test were described by a mobile-immobile framework.

To derive the analytical solution of the new model, some assumptions are inevitable. For instance, only vertical advection and dispersion are considered in the aquitard and only horizontal advection and dispersion are considered in the aquifer, and the flow is quasi-steady state. Although these assumptions have been widely used to describe the radial dispersion in previous studies, the influences on reactive transport have not been discussed in a rigorous sense before. In this study, numerical modelling exercises will be introduced to test the above-mentioned assumptions of the new model. Based on this study, the several conclusions could be obtained.

1. A new model of the SWPP test is a generalizing of many previous models by considering the aquitard effect, the wellbore storage, and the mass transfer rate in both aquifer and aquitards. The sub-model of the wellbore storage is developed.

2. Assumption of vertical advection and dispersion on the aquitard and horizontal advection and dispersion in the aquifer is tested by specially designed finite-element numerical models using COMSOL, and the result shows that this assumption is acceptable when the aquifer is of primary concern, provided that the ratios of the aquitard/aquifer permeability are less than 0.01; while such an assumption is generally unacceptable when the aquitards are of concern, regardless of the ratios of the aquitard/aquifer permeability.

3. The new model is ~~most~~ more sensitive to α_r and θ_m after a ~~comprehensive~~ global sensitivity analysis, and the values of σ_k is large for α_u, θ_{um}, α_r, θ_m and V_w, demonstrating that the influence of aquitard on results could not be ignored.

4. The performance of the new model is better than previous models of excluding the aquitard effect and the wellbore storage in terms of best fitting exercises with field data reported in Chen et al. (2017).

Acknowledgments

This research was partially supported by Programs of Natural Science Foundation of China (No.41772252), and Innovative Research Groups of the National Nature Science Foundation of China (No. 41521001).

References

[1] Assayag, N., Matter, J., Ader, M., Goldberg, D., and Agrinier, P.: Water-rock interactions during a CO2 injection field-test: Implications on host rock dissolution and alteration effects, Chem. Geol., 265, 227-235, 10.1016/j.chemgeo.2009.02.007, 2009.

[2] Bohling, G. C., Liu, G. S., Knobbe, S. J., Reboulet, E. C., Hyndman, D. W., Dietrich, P., and Butler, J. J.: Geostatistical analysis of centimeter-scale hydraulic conductivity variations at the MADE site, Water Resources Research, 48, 10.1029/2011wr010791, 2012.

[3] Chen, C. S.: Analytical solutions for radial dispersion with Cauchy boundary at injection well, Water Resources Research, 23, 1217-1224, 10.1029/WR023i007p01217, 1987.

[4] Chen, C. S.: Analytical and approximate solutions to radial dispersion from an injection well to a geological unit with simultaneous diffusion into adjacent strata, Water Resources Research, 21, 1069-1076, 10.1029/WR021i008p01069, 1985.

[5] Chen, J. S., Chen, C. S., and Chen, C. Y.: Analysis of solute transport in a divergent flow tracer test with scale-dependent dispersion, Hydrological Processes, 21, 2526-2536, 10.1002/hyp.6496, 2007.

[6] Chen, K., Zhan, H., and Yang, Q.: Fractional models simulating non-fickian behavior in four-stage single-well injection-withdrawal tests, Water Resources Research, 53, 9528-9545, 10.1002/2017WR021411, 2017.

[7] Chen, Y. J., Yeh, H. D., and Chang, K. J.: A mathematical solution and analysis of contaminant transport in a radial two-zone confined aquifer, Journal of contaminant hydrology, 138-139, 75-82, 10.1016/j.jconhyd.2012.06.006, 2012.

[8] Chowdhury, A. I. A., Gerhard, J. I., Reynolds, D., Sleep, B. E., and O'Carroll, D. M.: Electrokinetic-enhanced permanganate delivery and remediation of contaminated low permeability porous media, Water Research, 113, 215-222, 10.1016/j.watres.2017.02.005, 2017.

[9] Fetter, C. W.: Applied hydrogeology, Waveland Press, 2018.

[10] Gelhar, L. W., and Collins, M. A.: General analysis of longitudinal dispersion in nonuniform flow, Water Resources Research, 7, 1511-1521, 10.1029/WR007i006p01511, 1971.

[11] Guarracino, L., Carrera, J., Vázquez-Suñé, E.: Analytical study of hydraulic and mechanical effects on tide-induced head fluctuation in a coastal aquifer system that extends under the sea, J. Hydrol., 450-451, 150-158, 2012.

[12] Haggerty, R., and Gorelick, S. M.: Multiple-rate mass-transfer for modeling diffusion and surface-reactions in media with pore-scale heterogeneity, Water Resources Research, 31, 2383-2400, doi:10.1029/95WR10583, 1995.

[13] Haggerty, R., McKenna, S. A., and Meigs, L. C.: On the late-time behavior of tracer test breakthrough curves, Water Resources Research, 36, 3467-3479, 10.1029/2000wr900214, 2000.

[14] Hansen, S. K., Berkowitz, B., Vesselinov, V. V., O'Malley, D., and Karra, S.: Push-pull tracer tests: Their information content and use for characterizing non-Fickian, mobile-immobile behavior, Water Resources Research, 52, 9565-9585, 10.1002/2016WR018769, 2016.

[15] Hansen, S. K., Vesselinov, V. V., Reimus, P. W., and Lu, Z.: Inferring subsurface heterogeneity from push-drift tracer tests, Water Resources Research, 53, 6322-6329, 10.1002/2017WR020852, 2017.

[16] Hantush, M. S.: Flow of groundwater in relatively thick leaky aquifers, Water Resour. Res. , 3 583-590, 10.1029/WR003i002p00583, 1967.

[17] Hess, K. M.: Use of a borehole flowmeter to determine spatial heterogeneity of hydraulic conductivity and macro dispersion in a sand and gravel aquifer, Cape Cod, Massachusettes., Proceedings of the Conference on New Field Techneques for Quantifying the Physical and Chemical Properties of Heterogeneous Aquifers,, Dubin, Ohio., 1989.

[18] Huang, J. Q., Christ, J. A., and Goltz, M. N.: Analytical solutions for efficient interpretation of single-well injection-withdrawal tracer tests, Water Resources Research, 46, W08538, 10.1029/2008wr007647, 2010.

[19] Istok, J. D., Humphrey, M. D., Schroth, M. H., Hyman, M. R., and O'Reilly, K. T.: Single-well, "push-pull" test for in situ determination of microbial activities, Groundwater, 35, 619-631, doi:10.1111/j.1745-6584.1997.tb00127.x, 1997.

[20] Jung, Y., and Pruess, K.: A closed-form analytical solution for thermal single-well injection-withdrawal tests, Water Resources Research, 48, 10.1029/2011WR010979, 2012.

[21] Kabala, Z. J.: Sensitivity analysis of a pumping test on a well with wellbore storage and skin, Advances in Water Resources, 24, 483-504, 10.1016/s0309-1708(00)00051-8, 2001.

[22] Li, Z. F., Zhou, Z. F., Dai, Y. F., and Dai, B. B.: Contaminant transport in a largely-deformed aquitard affected by delayed drainage, J. Contam. Hydrol., 221, 118-126, 10.1016/j.jconhyd.2019.02.002, 2019.

[23] Moench, A. F.: Transient flow to a large-diameter well in an aquifer with storative semiconfining layers, Water Resources Research, 21, 1121-1131, 10.1029/WR021i008p01121, 1985.

[24] Moench, A. F.: Convergent radial dispersion: A Laplace transform solution for aquifer tracer testing, Water Resources Research, 25, 439-447, 1989.

[25] Phanikumar, M. S., and McGuire, J. T.: A multi-species reactive transport model to estimate biogeochemical rates based on single-well injection-withdrawal test data, Computers & Geosciences, 36, 997-1004, 10.1016/j.cageo.2010.04.001, 2010.

[26] Schroth, M. H., Istok, J. D., and Haggerty, R.: In situ evaluation of solute retardation using single-well injection-withdrawal tests, Advances in Water Resources, 24, 105-117, 10.1016/S0309-1708(00)00023-3, 2001.

[27] Schroth, M. H., and Istok, J. D.: Approximate solution for solute transport during spherical-flow push-pull tests, Groundwater, 43, 280-284, 10.1111/j.1745-6584.2005.0002.x, 2005.

[28] Sudicky, E. A.: A natural gradient experiment on solute transport in a sand aquifer: Spatial variability of hydraulic conductivity and its role in the dispersion process, Water Resources Research, 24, 1211-1216, 10.1029/WR024i007p01211, 1988.

[29] Tang, D. H., and Babu, D. K.: Analytical solution of a velocity dependent dispersion problem, Water Resources Research, 15, 1471-1478, 10.1029/WR015i006p01471, 1979.

[30] Wang, Q. R., and Zhan, H. B.: Radial reactive solute transport in an aquifer-aquitard system, Advances in Water Resources, 61, 51-61, 10.1016/j.advwatres.2013.08.013, 2013.

[31] Wang, Q. R., and Zhan, H. B.: On different numerical inverse Laplace methods for solute transport problems, Advances in Water Resources, 75, 80-92, 10.1016/j.advwatres.2014.11.001, 2015.

[32] Wang, Q. R., Shi, W., Zhan, H., Gu, H., and Chen, K.: Models of single-well injection-withdrawal test with mixing effect in the wellbore, Water Resources Research, 54, 10155-10171, 10.1029/2018WR023317, 2018.

[33] Wang, Q. R., and Zhan, H. B.: Reactive transport with wellbore storages in a single-well injection-withdrawal test, Hydrol. Earth Syst. Sci., 23, 2207-2223, 10.5194/hess-23-2207-2019, 2019.

[34] Yang, Q., Matter, J., Stute, M., Takahashi, T., O'Mullan, G., Umemoto, K., Clauson, K., Dueker, M. E., Zakharova, N., Goddard, J., and Goldberg, D.: Groundwater hydrogeochemistry in injection experiments simulating CO2 leakage from geological storage reservoir, Int. J. Greenh. Gas Control, 26, 193-203, 10.1016/j.ijggc.2014.04.025, 2014.

[35] Yang, S. Y., and Yeh, H. D.: Radial groundwater flow to a finite diameter well in a leaky confined aquifer with a finite-thickness skin, Hydrological Processes, 23, 3382-3390, 10.1002/hyp.7449, 2009.

[36] Zhan, H. B., Wen, Z., and Gao, G. Y.: An analytical solution of two-dimensional reactive solute transport in an aquifer-aquitard system, Water Resources Research, 45, 10.1029/2008wr007479, 2009.

[37] Zhou, R., Zhan, H., and Chen, K.: Reactive solute transport in a filled single fracture-matrix system under unilateral and radial flows, Advances in Water Resources, 104, 183-194, 10.1016/j.advwatres.2017.03.022, 2017.

[38] Zlotnik, V. A., and Zhan, H. B.: Aquitard effect on drawdown in water table aquifers, Water Resources Research, 41, 10.1029/2004wr003716, 2005.

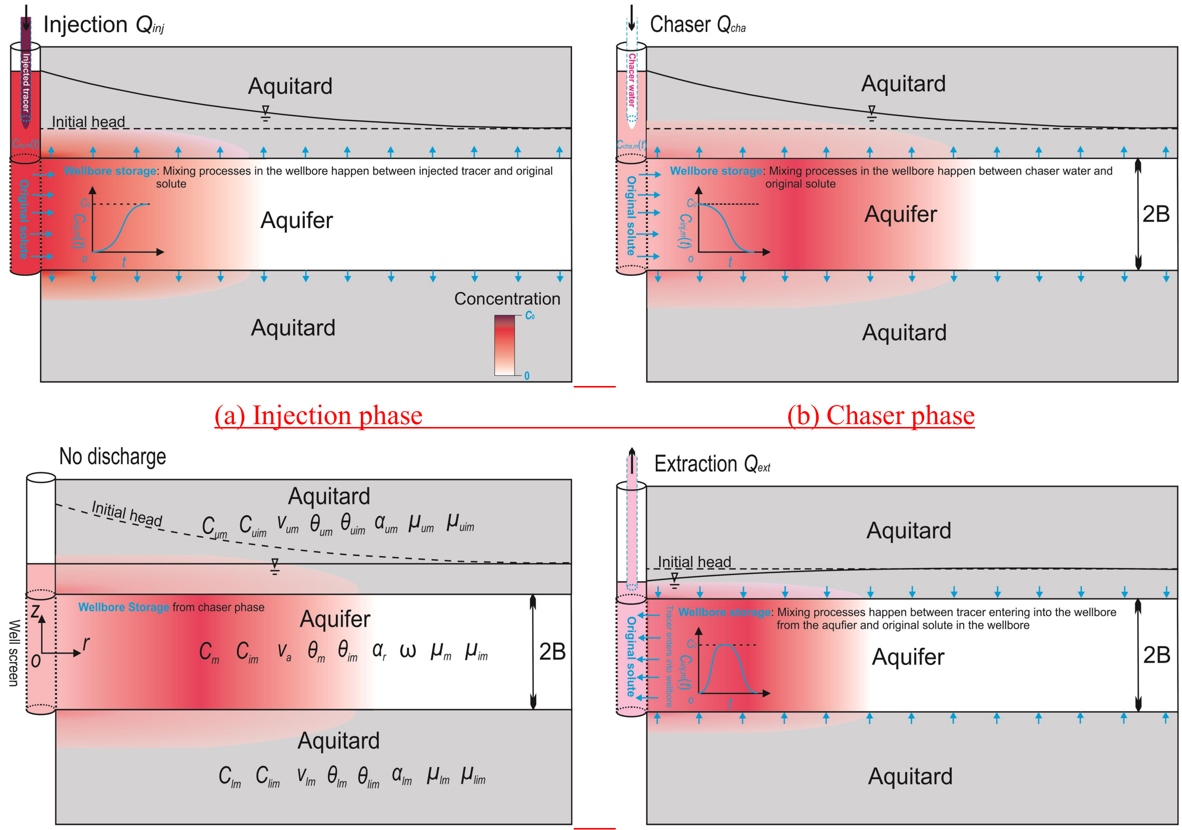

(a) Injection phase (b) Chaser phase

(c) Rest phase (d) Extraction phase

550 **Figure 1: The schematic diagram of the SWPP test.**

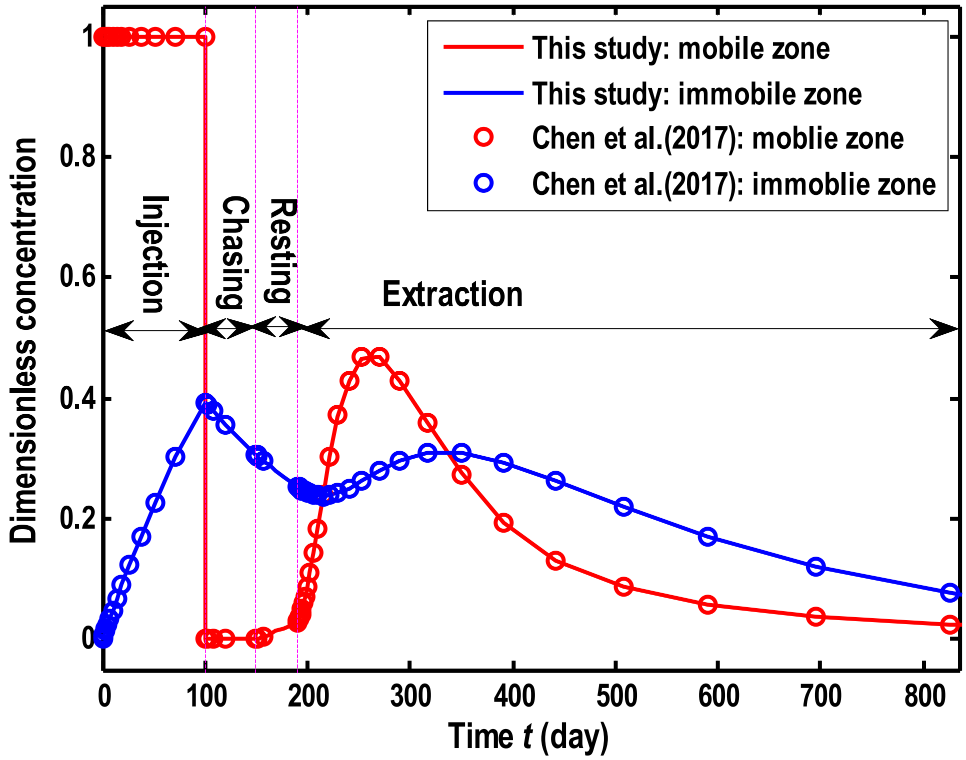

Figure ~~1~~2: Comparison of BTCs at the well screen computed by the solution of this study and Chen et al. (2017).

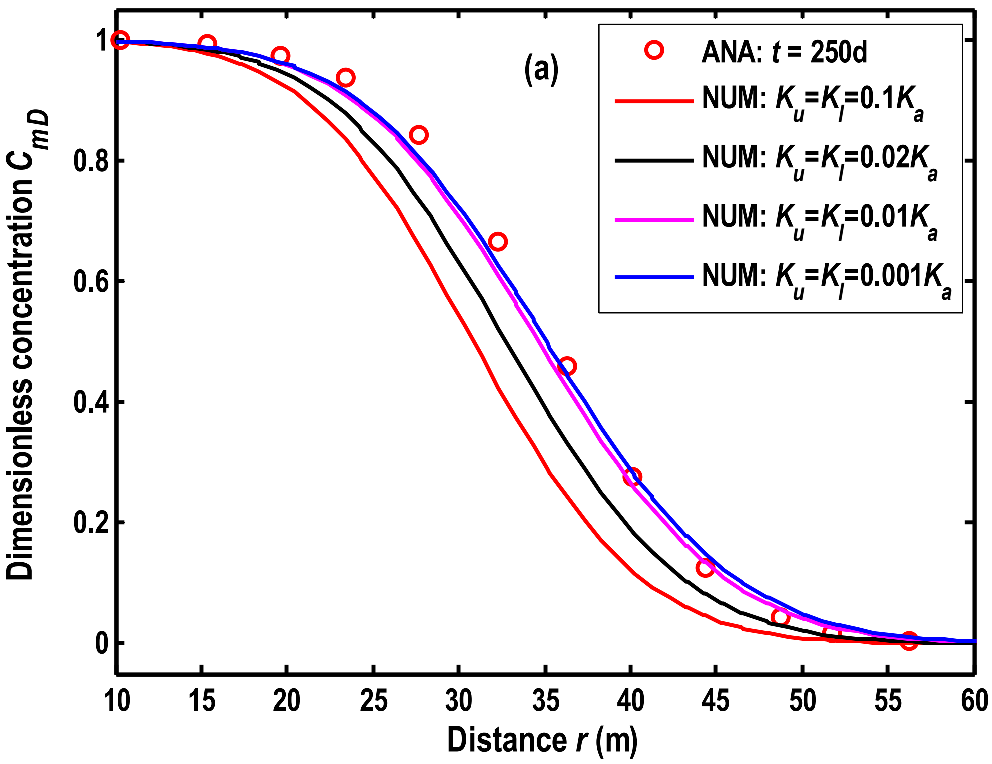

(a) At the end of the injection phase: $t = 250$ day

Figure ~~2~~3: Comparison of the concentration distribution between the analytical and numerical solutions along the r-axis at z=0m. "ANA" and "NUM" represent the analytical and numerical solutions, respectively.

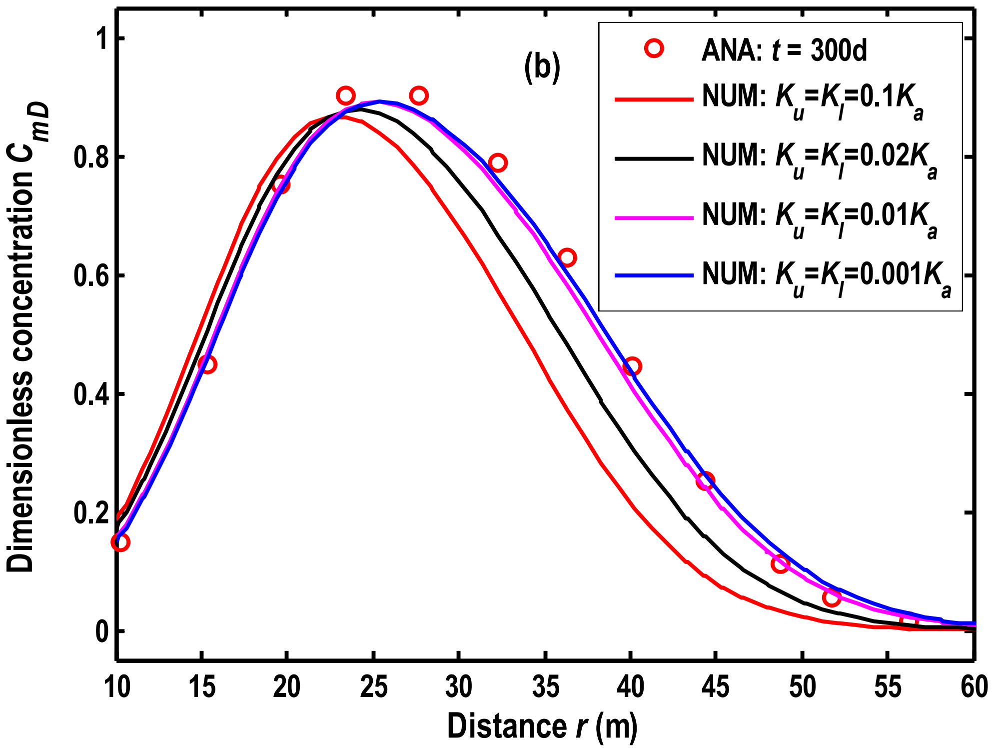

(b) At the end of the chasing phase: t = 300 day

Figure ~~2~~3: Comparison of the concentration distribution between the analytical and numerical solutions along the r-axis at z=0m. "ANA" and "NUM" represent the analytical and numerical solutions, respectively.

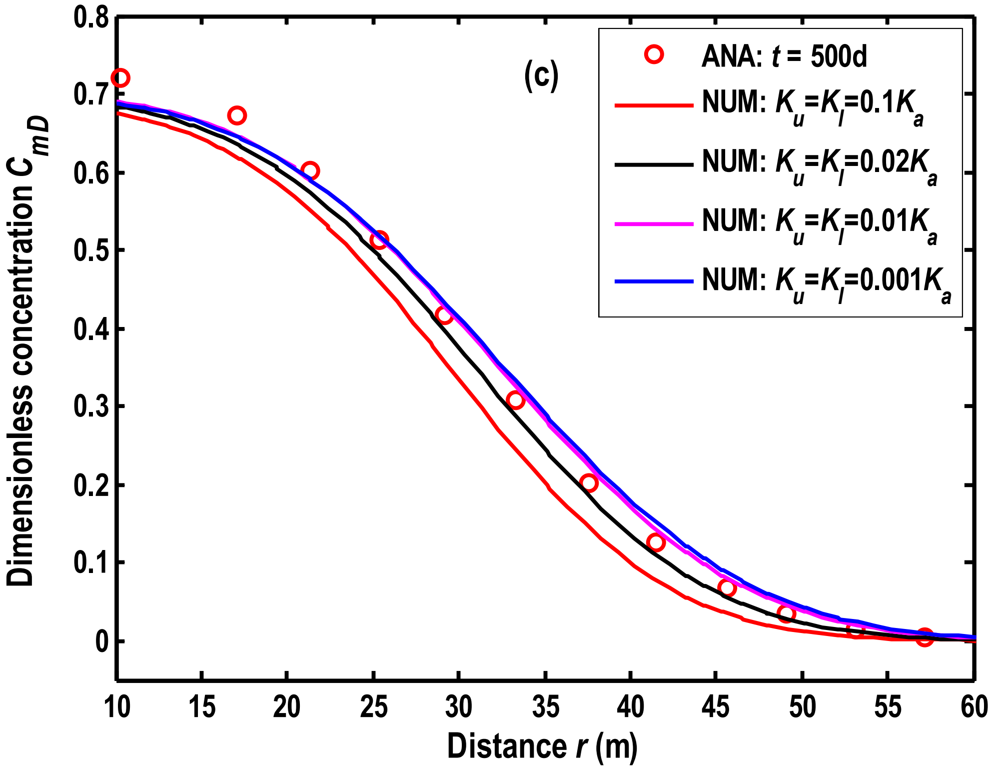

(c) In the extraction phase: t = 500 day

Figure ~~2~~3: Comparison of the concentration distribution between the analytical and numerical solutions along the r-axis at z=0m. "ANA" and "NUM" represent the analytical and numerical solutions, respectively.

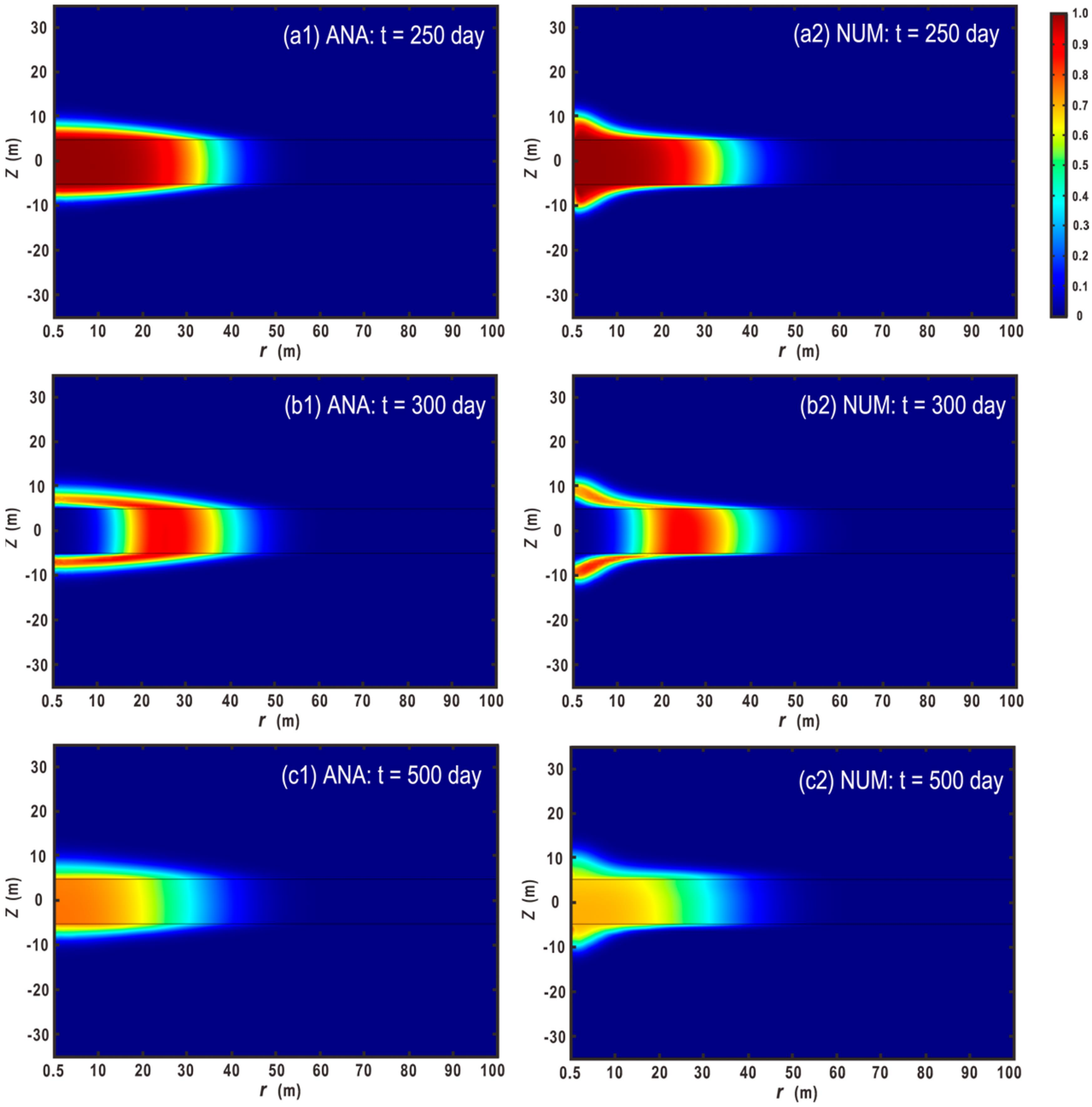

Figure ~~3~~4: The vertical profiles (the *r*-*z* profiles) of the concentrations. (a1) - (c1) represent the analytical solutions at *t*=250, 300 and 500 day, respectively. (a2) - (c2) represent the numerical solutions at *t*=250, 300 and 500 day, respectively.

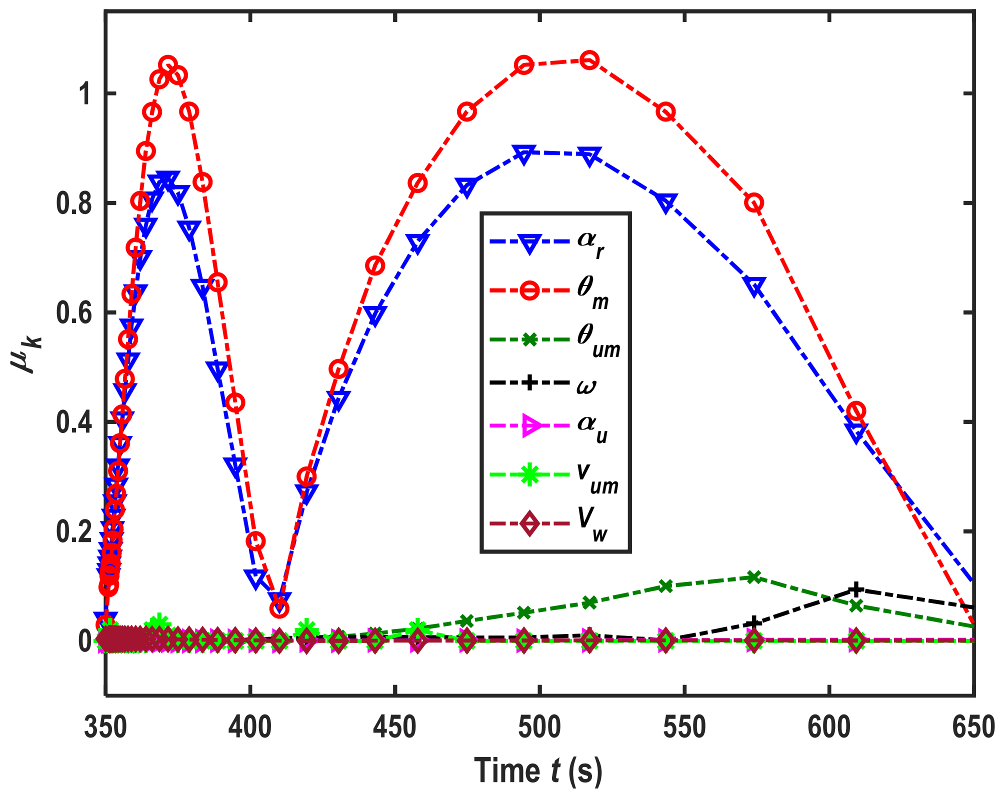

(a) Variation of μ_k with time in the wellbore.

575 **Figure 5: Sensitivity analysis.**

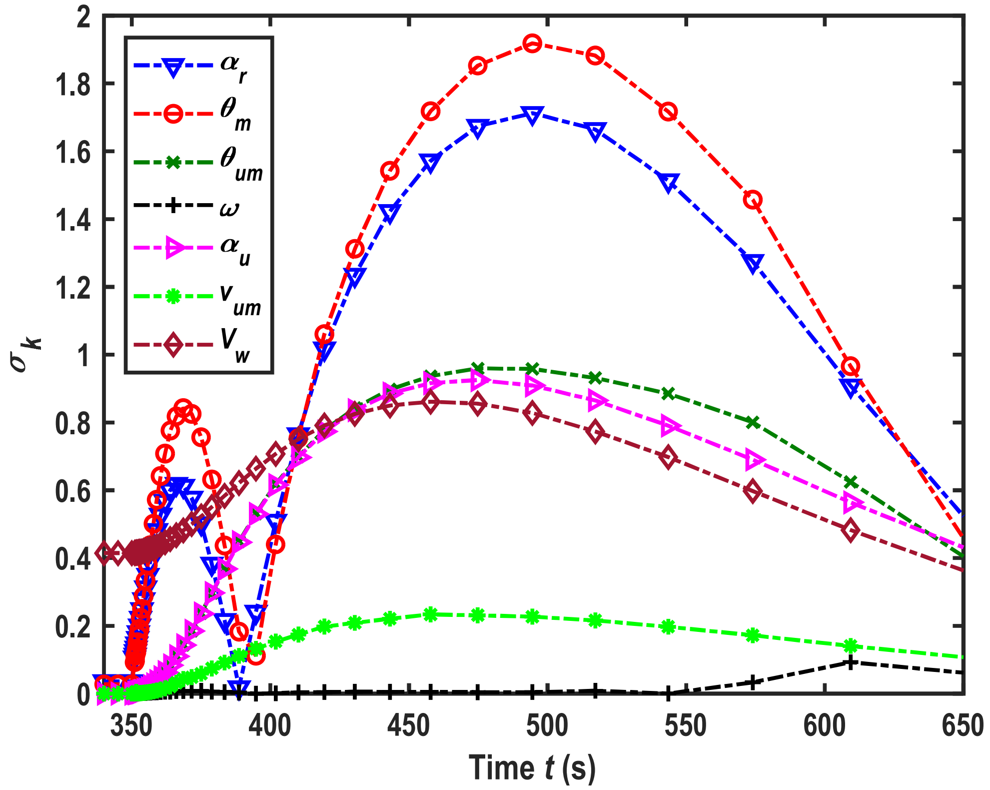

(b) Variation σ_k with time in the wellbore.

Figure 5: Sensitivity analysis.

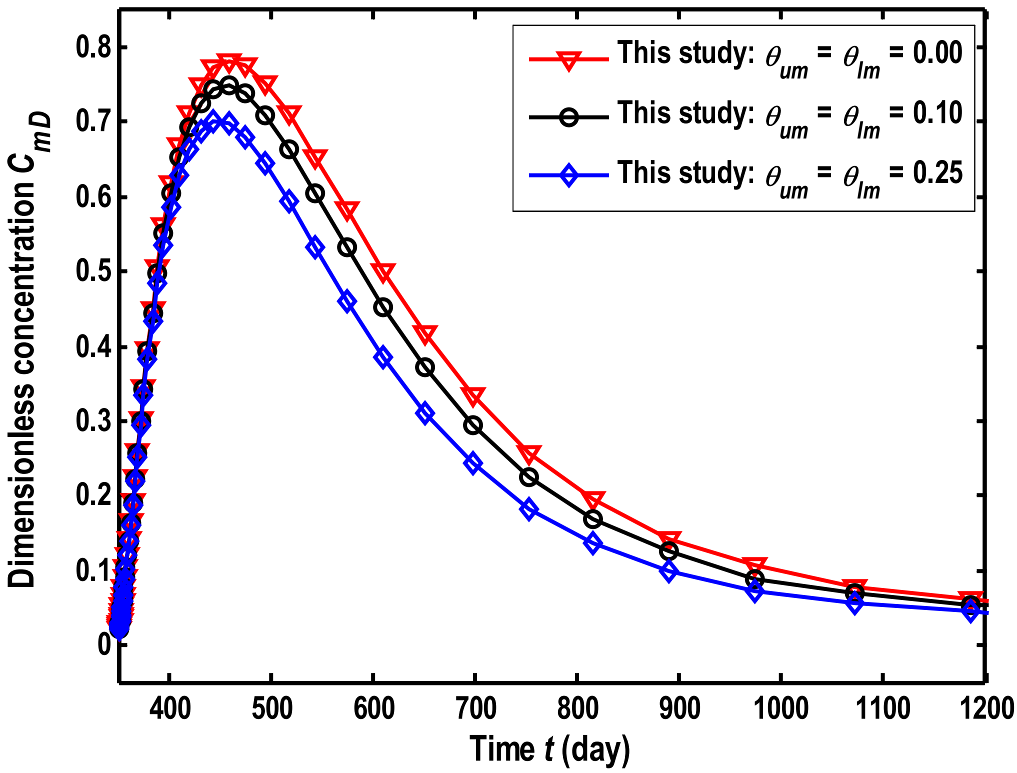

Figure ~~5~~6: Comparison of BTCs between the model with and without aquitards for different porosities.

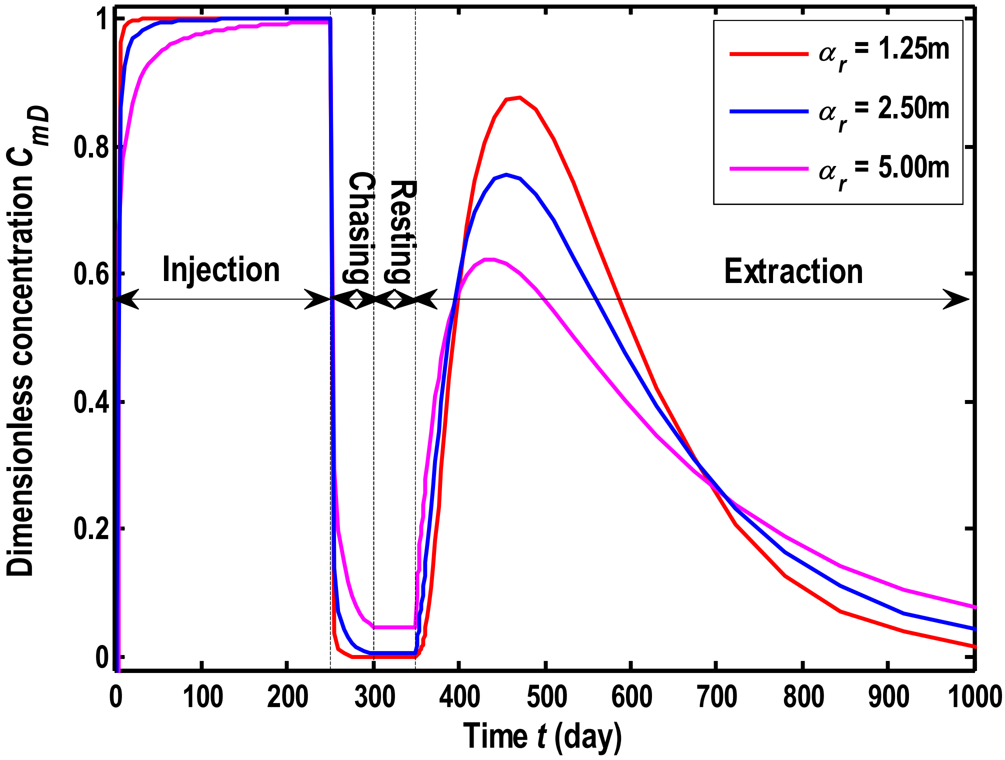

Figure ~~6~~7: BTCs in the wellbore for different α_r.

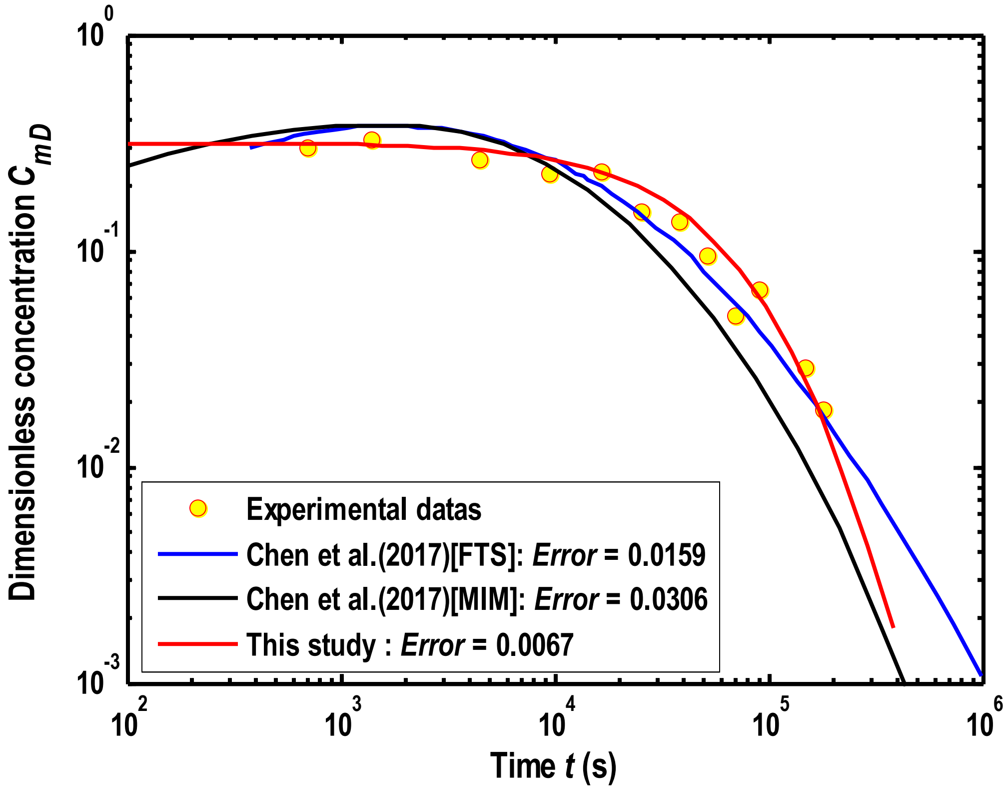

585 (a) Fitness of the observed data by different models.

Figure 8: Fitness of observed BTC.

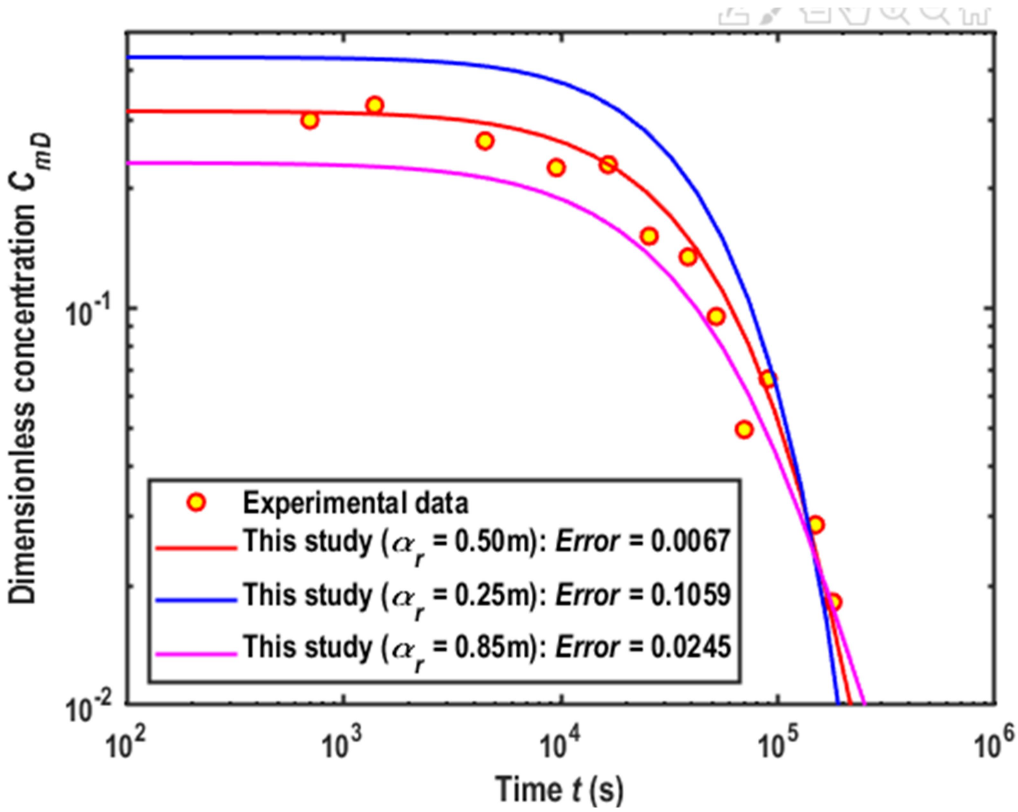

(b) Influence of the dispersivity of the aquifer on BTCs

Figure 8: Fitness of observed BTC.

Table 1. Expressions of the coefficients in the solutions expressed in Eqs.(25a) - (25f).

a_2	$\dfrac{\dfrac{R_m v_{um}\alpha_r^2}{ABR_{um}} - \sqrt{\left(\dfrac{R_m v_{um}\alpha_r^2}{ABR_{um}}\right)^2 + 4\dfrac{R_m\alpha_r^2 D_u}{AB^2R_{um}}\left(s+\varepsilon_{um}+\mu_{umD}-\dfrac{\varepsilon_{um}\varepsilon_{uim}}{s+\mu_{uimD}+\varepsilon_{uim}}\right)}}{2\dfrac{R_m\alpha_r^2 D_u}{AB^2R_{um}}}$
b_1	$\dfrac{-\dfrac{R_m v_{lm}\alpha_r^2}{ABR_{lm}} + \sqrt{\left(\dfrac{R_m v_{lm}\alpha_r^2}{ABR_{lm}}\right)^2 + 4\dfrac{R_m\alpha_r^2 D_l}{AB^2R_{lm}}\left(s+\varepsilon_{lm}+\mu_{lmD}-\dfrac{\varepsilon_{lm}\varepsilon_{lim}}{s+\mu_{limD}+\varepsilon_{lim}}\right)}}{2\dfrac{R_m\alpha_r^2 D_l}{AB^2R_{lm}}}$
E	$s+\varepsilon_m+\mu_{mD}-\dfrac{\varepsilon_m\varepsilon_{im}}{s+\mu_{imD}+\varepsilon_{im}}+\dfrac{\theta_{um}\alpha_r^2 v_{um}}{2A\theta_m B}-\dfrac{\theta_{lm}\alpha_r^2 v_{lm}}{2A\theta_m B}-\dfrac{a_2\theta_{um}\alpha_r^2 D_u}{2A\theta_m B^2}+\dfrac{b_1\theta_{lm}\alpha_r^2 D_l}{2AB^2\theta_m}$
y_{inj}	$r_D+\dfrac{1}{4E}$
$y_{inj,w}$	$r_{wD}+\dfrac{1}{4E}$
ε_m	$\dfrac{\omega_a\alpha_r^2}{A\theta_m}$
ε_{im}	$\dfrac{\omega_a\alpha_r^2}{A\theta_{im}}$
ε_{um}	$\dfrac{\omega_u\alpha_r^2 R_m}{A\theta_{um}R_{um}}$
ε_{uim}	$\dfrac{\omega_l\alpha_r^2 R_m}{A\theta_{um}R_{uim}}$
β_{inj}	$\dfrac{V_{w,inj}r_{wD}}{\xi R_m\alpha_r}$
ξ	$4\pi r_w\theta B$
ϕ_1	$\dfrac{1}{s(s\beta_{inj}+1)}\dfrac{1}{exp\left(\dfrac{y_{inj,w}}{2}\right)\left[\dfrac{A_i(E^{1/3}y_{inj,w})}{2}-E^{1/3}A_i'(E^{1/3}y_{inj})\right]}$

Table 2. Expressions of the coefficients in the solutions expressed in Eqs.(26a) - (26g).

δ_1	$-\dfrac{\beta_{cha,D}}{s\beta_{cha,D}+1}\dfrac{r_D\vert_{r_D\to\infty}}{\left(r_{wD}-r_D\vert_{r_D\to\infty}-1\right)}C_{inj,mD}(r_D,t_D)\Big\vert_{t_D=t_{inj,D}}$
δ_2	$\dfrac{\beta_{cha,D}}{s\beta_{cha,D}+1}\dfrac{1}{\left(r_{wD}-r_D\vert_{r_D\to\infty}-1\right)}C_{inj,mD}(r_D,t_D)\Big\vert_{t_D=t_{inj,D}}$
$\mathscr{s}_1$	$-\mathscr{s}_2 z_{eD}$
$\mathscr{s}_2$	$\dfrac{\bar{C}_{mD}(r_D,s)}{1-z_{eD}}$
$\beta_{cha,D}$	$-\dfrac{V_{w,cha}r_{wD}}{\xi R_m\alpha_r}$
E_a	$s+\varepsilon_m+\mu_{mD}-\dfrac{\varepsilon_m\varepsilon_{im}}{s+\mu_{imD}+\varepsilon_{im}}+\dfrac{\theta_{um}\alpha_r^2 v_{um}}{2A\theta_m B}-\dfrac{\theta_{lm}\alpha_r^2 v_{lm}}{2AB^2\theta_m}$ $-\dfrac{1}{1-z_{eD}}\dfrac{\theta_{um}\alpha_r^2 D_u}{2A\theta_m B^2}+\dfrac{1}{z_{eD}-1}\dfrac{\theta_{lm}\alpha_r^2 D_l}{2AB^2\theta_m}$
E_u	$s+\varepsilon_{um}+\mu_{umD}-\dfrac{\varepsilon_{um}\varepsilon_{uim}}{s+\varepsilon_{uim}+\mu_{uimD}}$
E_l	$s+\varepsilon_{lm}+\mu_{lmD}-\dfrac{\varepsilon_{lm}\varepsilon_{lim}}{s+\varepsilon_{lim}+\mu_{limD}}$
F	$C_{mD}(r_D,t_{inj,D})+\dfrac{\varepsilon_m C_{imD}(r_D,t_{inj})}{s+\mu_{imD}+\varepsilon_{im}}$
$\varphi(\eta)$	$F\eta-[\delta_2+\eta E_a(\delta_1+\delta_2\eta)]$
$f_u(\eta_u)$	$C_{umD}(r_D,\eta_u,t_{inj,D})+\dfrac{\varepsilon_{um}C_{uimD}(r_D,\eta_u,t_{inj,D})}{s+\varepsilon_{uim}+\mu_{uimD}}-\dfrac{R_m v_{um}\alpha_r^2}{ABR_{um}}\mathscr{s}_2$ $-E_u(\mathscr{s}_1+\mathscr{s}_2\eta_u)$
$f_l(\eta_l)$	$C_{lmD}(r_D,\eta_l,t_{inj,D})+\dfrac{\varepsilon_{lm}C_{limD}(r_D,\eta_l,t_{inj,D})}{s+\varepsilon_{lim}+\mu_{limD}}+\dfrac{R_m v_{lm}\alpha_r^2}{ABR_{lm}}\dfrac{\bar{C}_{mD}}{z_{eD}-1}$ $-\bar{C}_{mD}E_l\dfrac{z_{eD}+\eta_l}{z_{eD}-1}$
$g(r_D,E_a;\eta)$	$g_1(r_D,E_a;\eta)=\mathcal{T}_1 exp(\dfrac{y_{cha}}{2})A_i\left(E_a^{\frac{1}{3}}y_{cha}\right)+\mathcal{T}_2\, exp\left(\dfrac{y_{cha}}{2}\right)B_i\left(E_a^{\frac{1}{3}}y_{cha}\right)r_{wD}\le$ $g_2(r_D,E_a;\eta)=\mathcal{T}_3 exp(\dfrac{y_{cha}}{2})A_i\left(E_a^{\frac{1}{3}}y_{cha}\right)+\mathcal{T}_4\, exp\left(\dfrac{y_{cha}}{2}\right)B_i\left(E_a^{\frac{1}{3}}y_{cha}\right)\ \eta\le y$
$g_u(z_D,E_u;\eta_u)$	$g_{u1}(z_D,E_u;\eta_u)=N_1 exp(a_1 z_D)+N_2 exp(a_2 z_D)-\ 1\le z_D<\eta_u$ $g_{u2}(z_D,E_u;\eta_u)=N_3 exp(a_1 z_D)+N_4 exp(a_2 z_D)-\eta_u\le z_D<\infty$

$g_l(z_D, E_l; \eta_l)$	$g_{u1}(z_D, E_l; \eta_l) = M_1 exp(b_1 z_D) + M_2 exp(b_2 z_D) - -1 \leq z_D < \eta_l$ $g_{u2}(z_D, E_l; \eta_l) = M_3 exp(b_1 z_D) + M_4 exp(b_2 z_D) - \eta_l \leq z_D < -\infty$
M_1	$-M_2 exp(b_1 - b_2)$
M_2	$\frac{-AB^2 R_{lm}}{R_m \alpha_r^2 D_l [exp(b_2\eta_l - b_1\eta_l) - b_2 exp(b_2\eta_l)]}$
M_3	$M_2 exp(b_2\eta_l - b_1\eta_l) - M_2 exp(b_1 - b_2)$
M_4	0
N_1	$-N_2 exp(a_2 - a_1)$
N_2	$\frac{-AB^2 R_{um}}{R_m \alpha_r^2 D_u [(a_1 - a_2) exp(a_2 - a_1) exp(a_1 \eta_u)]}$
N_3	0
N_4	$N_2 - N_2 exp(a_2 - a_1) exp(a_1\eta_u - a_2\eta_u)$
X	$\frac{\frac{1}{2} B_i\left({E_a}^{1/3} y_{cha,w}\right) - {E_a}^{1/3} B_i'\left({E_a}^{1/3} y_{cha,w}\right)}{\frac{1}{2} A_i\left({E_a}^{1/3} y_{cha,w}\right) - {E_a}^{1/3} A_i'\left({E_a}^{1/3} y_{cha,w}\right)}$
$\mathcal{T}_1$	$-\frac{\pi A_i\left(y_{ext}\vert_{r_D=\eta^+}\right)}{E^{1/3}} X$
$\mathcal{T}_2$	$\frac{\pi A_i\left(y_{ext}\vert_{r_D=\eta^+}\right)}{{E_a}^{1/3}}$
$\mathcal{T}_3$	$\frac{\pi A_i\left(y_{ext}\vert_{r_D=\eta^+}\right)}{{E_a}^{1/3}} \left[\frac{B_i\left(y_{ext}\vert_{r_D=\eta^+}\right)}{A_i\left(y_{ext}\vert_{r_D=\eta^+}\right)} - X\right]$
$\mathcal{T}_4$	0
y_{cha}	$r_D + \frac{1}{4E_a}$
$y_{cha,w}$	$r_{wD} + \frac{1}{4E_a}$

Table 3. Expressions of the coefficients in the solutions expressed in Eqs.(28a) - (28g).

Λ	$C_{mD}(r_D, t_{res}) + \dfrac{\varepsilon_m C_{imD}(r_D, t_{res})}{s + \mu_{imD} + \varepsilon_{im}}$
$\beta_{ext,D}$	$-\dfrac{V_{w,ext} r_{wD}}{\xi R_m \alpha_r}$
ζ	$s + \varepsilon_m + \mu_{mD} - \dfrac{\varepsilon_{im}\varepsilon_m}{s + \mu_{imD} + \varepsilon_{im}} - \dfrac{\theta_{um}\alpha_r^2 v_{um}}{2A\theta_m B} + \dfrac{\theta_{lm}\alpha_r^2 v_{lm}}{2AB^2\theta_m}$ $- \dfrac{1}{1 - z_{eD}} \dfrac{\theta_{um}\alpha_r^2 D_u}{2A\theta_m b} + \dfrac{1}{z_{eD} - 1} \dfrac{\theta_{lm}\alpha_r^2 D_l}{2Ab^2\theta_m}$
$f(\varepsilon)$	$exp(\varepsilon/2)\varepsilon\Lambda - \left(\varepsilon\zeta + \dfrac{1}{4}\right)(\sigma_1 + \sigma_2\varepsilon)$
$f_u(\mathscr{b}_u)$	$C_{umD}(r_D, \mathscr{b}_u, t_{res,D}) + \dfrac{\varepsilon_{um} C_{uimD}(r_D, \mathscr{b}_u, t_{res,D})}{s + \varepsilon_{uim} + \mu_{uimD}} + \dfrac{R_m v_{um}\alpha_r^2}{ABR_{um}} \dfrac{\bar{C}_{mD}(r_D, s)}{1 - z_{eD}}$ $- \dfrac{\mathscr{b}_u - z_{eD}}{1 - z_{eD}} E_u \bar{C}_{mD}(r_D, s)$
$f_l(\mathscr{b}_l)$	$C_{mD}(r_D, \mathscr{b}_l, t_{res,D}) + \dfrac{\varepsilon_{lm} C_{limD}(r_D, \mathscr{b}_l, t_{res,D})}{s + \varepsilon_{lim} + \mu_{limD}} - \dfrac{R_m v_{lm}\alpha_r^2}{ABR_{lm}} \dfrac{\bar{C}_{mD}(r_D, s)}{z_{eD} - 1}$ $- \dfrac{\mathscr{b}_l + z_{eD}}{z_{eD} - 1} E_l \bar{C}_{mD}(r_D, s)$
$g(r_D, \zeta; \varepsilon)$	$g_1(r_D, \zeta; \varepsilon) = P_1 A_i(y_{ext}) + P_2 B_i(y_{ext})$--- $r_{wD} \le y_{ext} < \varepsilon$ $g_2(r_D, \zeta; \varepsilon) = P_3 A_i(y_{ext}) + P_4 B_i(y_{ext})$------ $\varepsilon \le y_{ext} < \infty$
$g_u(z_D, E_u; \mathscr{b}_u)$	$g_{u1}(z_D, E_u; \mathscr{b}_u) = H_1 exp(m_1 z_D) + H_2 exp(m_2 z_D)$-- $1 \le z_D < \mathscr{b}_u$ $g_{u2}(z_D, E_u; \mathscr{b}_u) = H_3 exp(m_1 z_D) + H_4 exp(m_2 z_D)$- $\mathscr{b}_u \le z_D < \infty$
$g_l(z_D, E_l; \mathscr{b}_l)$	$g_{l1}(z_D, E_l; \mathscr{b}_l) = I_1 exp(n_1 z_D) + I_2 exp(n_2 z_D)$- $-1 \le z_D < \mathscr{b}_l$ $g_{l2}(z_D, E_l; \mathscr{b}_l) = I_3 exp(n_1 z_D) + I_4 exp(n_2 z_D)$- $\mathscr{b}_l \le z_D < -\infty$
H_1	$-H_2 exp(m_2 - m_1)$
H_2	$\dfrac{-AR_{um}B^2}{R_m\alpha_r^2 D_u[(m_1 - m_2)exp(m_2 - m_1)exp(m_1\mathscr{b}_u)]}$
H_3	0
H_4	$H_2 - H_2 exp(m_2 - m_1)exp(m_1\mathscr{b}_u - m_2\mathscr{b}_u)$
I_1	$-I_2 exp(n_1 - n_2)$
I_2	$\dfrac{-AB^2 R_{lm}}{R_m\alpha_r^2 D_l[exp(n_2\mathscr{b}_l - n_1\mathscr{b}_l) - n_2 exp(n_2\mathscr{b}_l)]}$
I_3	$I_2 exp(n_2\mathscr{b}_l - n_1\mathscr{b}_l) - I_2 exp(n_1 - n_2)$

I_4	0
m_1	$\dfrac{-\dfrac{R_m v_{um}\alpha_r^2}{ABR_{um}}+\sqrt{\left(\dfrac{R_m v_{um}\alpha_r^2}{ABR_{um}}\right)^2+4\dfrac{R_m\alpha_r^2 D_u}{AB^2R_{um}}\left(s+\varepsilon_{um}+\mu_{umD}-\dfrac{\varepsilon_{um}\varepsilon_{uim}}{s+\mu_{uimD}+\varepsilon_{uim}}\right)}}{2\dfrac{R_m\alpha_r^2 D_u}{AB^2R_{um}}}$
m_2	$\dfrac{-\dfrac{R_m v_{um}\alpha_r^2}{ABR_{um}}-\sqrt{\left(\dfrac{R_m v_{um}\alpha_r^2}{ABR_{um}}\right)^2+4\dfrac{R_m\alpha_r^2 D_u}{AB^2R_{um}}\left(s+\varepsilon_{um}+\mu_{umD}-\dfrac{\varepsilon_{um}\varepsilon_{uim}}{s+\mu_{uimD}+\varepsilon_{uim}}\right)}}{2\dfrac{R_m\alpha_r^2 D_u}{AB^2R_{um}}}$
n_1	$\dfrac{\dfrac{R_m v_{lm}\alpha_r^2}{ABR_{lm}}+\sqrt{\left(\dfrac{R_m v_{lm}\alpha_r^2}{ABR_{lm}}\right)^2+4\dfrac{R_m\alpha_r^2 D_l}{AB^2R_{lm}}\left(s+\varepsilon_{lm}+\mu_{lmD}-\dfrac{\varepsilon_{lm}\varepsilon_{lim}}{s+\mu_{limD}+\varepsilon_{lim}}\right)}}{2\dfrac{R_m\alpha_r^2 D_l}{AB^2R_{lm}}}$
n_2	$\dfrac{\dfrac{R_m v_{lm}\alpha_r^2}{ABR_{lm}}-\sqrt{\left(\dfrac{R_m v_{lm}\alpha_r^2}{ABR_{lm}}\right)^2+4\dfrac{R_m\alpha_r^2 D_l}{AB^2R_{lm}}\left(s+\varepsilon_{lm}+\mu_{lmD}-\dfrac{\varepsilon_{lm}\varepsilon_{lim}}{s+\mu_{limD}+\varepsilon_{lim}}\right)}}{2\dfrac{R_m\alpha_r^2 D_l}{AB^2R_{lm}}}$
P_1	$-\dfrac{\pi A_i\left(y_{ext}\vert_{r_D=\varepsilon^+}\right)}{\zeta^{1/3}}W$
P_2	$\dfrac{\pi A_i\left(y_{ext}\vert_{r_D=\varepsilon^+}\right)}{\zeta^{1/3}}$
P_3	$\dfrac{\pi A_i\left(y_{ext}\vert_{r_D=\varepsilon^+}\right)}{\zeta^{1/3}}\left[\dfrac{B_i\left(y_{ext}\vert_{r_D=\varepsilon^+}\right)}{A_i\left(y_{ext}\vert_{r_D=\varepsilon^+}\right)}-W\right]$
P_4	0
W	$\dfrac{\left(s\beta_{ext,D}+\dfrac{1}{2}\right)B_i\left(y_{ext,w}\right)-\zeta^{1/3}B_i'\left(y_{ext,w}\right)}{\left(s\beta_{ext,D}+\dfrac{1}{2}\right)A_i\left(y_{ext,w}\right)-\zeta^{1/3}A_i'\left(y_{ext,w}\right)}$
y_{ext}	$\zeta^{1/3}\left(r_D+\dfrac{1}{4\zeta}\right)$
$y_{ext,w}$	$\zeta^{1/3}\left(r_{wD}+\dfrac{1}{4\zeta}\right)$
σ_1	$-\dfrac{\beta_{ext,D}exp(r_{wD}/2)C_{mD}\left(r_{wD},t_{res,D}\right)}{\left(s\beta_{ext,D}+\dfrac{1}{2}\right)r_{wD}-1-\left(s\beta_{ext,D}+\dfrac{1}{2}\right)r_D\vert_{r_D\to\infty}}r_D\vert_{r_D\to\infty}$

σ_2	$\frac{\beta_{ext,D} exp(r_{wD}/2) C_{mD}(r_{wD}, t_{res,D})}{\left(s\beta_{ext,D} + \frac{1}{2}\right) r_{wD} - 1 - \left(s\beta_{ext,D} + \frac{1}{2}\right) r_D\|_{r_D \to \infty}}$

Table 4. A partial list of parameters from literatures.

	Fine sand	Medium sand	Course sand	Clay
Retardation factor [-]	1.20-4.76[a]	11.40-13.24[b]	1.10-7.30[c]	6.98[d]
Dispersivity [cm]	0.15-0.21[e]	0.20-9.00[b]	3.2-38.6[c]	13.80[f]
First-order mass transfer coefficient[1/d]	0.15-0.40[g]	0.50[g]	1.0-4.6[g]	0.05-0.15[g]
Porosity [-]	0.28-0.31[e]	0.36[b]	0.37-0.40[e]	0.40-0.44[f]
Reaction rate[1/d]	6.36-6.84[h]	0.08-2.1[i]	0.55-3.12[j]	0.10-28.80[k]

[a]. Brusseau et al. (1991); [b]. Pickens et al. (1981); [c].Davis et al. (2003); [d].Javadi et al. (2017); [e].Liang et al. (2018); [f].Swami et al. (2016); [g].Kookana et al. (1992); [h].Haggerty et al. (1998); [i].Bouwer and McCarty (1985); [j].Chun et al. (2009); [k].Alvarez et al. (1991). References are shown in Section S3 of ***Supplementary Materials***.

New Model of Reactive Transport in Single-well Push-Pull Test with Aquitard Effect

Quanrong Wang[1]*, Junxia Wang[1], Hongbin Zhan[2]*, Wenguang Shi[1]

[1]School of Environmental Studies, China University of Geosciences, Wuhan, Hubei, 430074, P. R. China

[2]School of Mathematics and Physics, China University of Geosciences, Wuhan, Hubei, 430074, P. R. China

[3]Department of Geology and Geophysics, Texas A& M University, College Station, TX 77843-3115, USA

(*Corresponding author)

Supplementary Materials

S1. Derivation of the analytical solutions for the SWPP test

S2. Numerical solutions

S3. References for Table 4

S4. Parameter range used in sensitivity analysis

Supplementary Materials

S1. Derivation of analytical solutions for the SWPP test

To reduce the complexity in analyzing the influence of input parameters on the output, the dimensionless parameters are introduced as follows: $C_{mD}=\frac{C_m}{C_0}$, $C_{imD}=\frac{C_{im}}{C_0}$, $C_{inj,mD}=\frac{C_{inj,m}}{C_0}$, $C_{inj,imD}=\frac{C_{inj,im}}{C_0}$, $C_{cha,mD}=\frac{C_{cha,m}}{C_0}$, $C_{cha,imD}=\frac{C_{cha,im}}{C_0}$, $C_{res,mD}=\frac{C_{res,m}}{C_0}$, $C_{res,imD}=\frac{C_{res,im}}{C_0}$, $C_{ext,mD}=\frac{C_{ext,m}}{C_0}$, $C_{ext,imD}=\frac{C_{ext,im}}{C_0}$, $C_{umD}=\frac{C_{um}}{C_0}$, $C_{uimD}=\frac{C_{uim}}{C_0}$, $C_{lmD}=\frac{C_{lm}}{C_0}$, $C_{limD}=\frac{C_{lim}}{C_0}$, $t_D=\frac{|A|}{\alpha_r^2R_m}t$, $r_D=\frac{r}{\alpha_r}$, $r_{wD}=\frac{r_w}{\alpha_r}$, $z_D=\frac{z}{B}$, $\mu_{mD}=\frac{\alpha_r^2\mu_m}{A}$, $\mu_{imD}=\frac{\alpha_r^2R_m\mu_{im}}{R_{im}A}$, $\mu_{umD}=\frac{\alpha_r^2\mu_{um}}{A}$, $\mu_{uimD}=\frac{\alpha_r^2R_m\mu_{uim}}{R_{im}A}$, $\mu_{lmD}=\frac{\alpha_r^2\mu_{lm}}{A}$ and $\mu_{limD}=\frac{\alpha_r^2R_m\mu_{lim}}{R_{im}A}$, where the subscript "*D*" represents the dimensionless parameter hereinafter, $A=\frac{Q}{4\pi B\theta_m}$. By substituting these dimensionless parameters into the governing equations, one could obtain the dimensionless model of the SWPP test:

$$\frac{\partial C_{mD}}{\partial t_D}=\frac{1}{r_D}\frac{\partial^2C_{mD}}{\partial r_D^2}-\frac{1}{r_D}\frac{\partial C_{mD}}{\partial r_D}-\varepsilon_m(C_{mD}-C_{imD})-\mu_{mD}C_{mD}-\left(\frac{\theta_{um}\alpha_r^2v_{um}}{2A\theta_mB}C_{umD}-\frac{\theta_{um}\alpha_r^2D_u}{2A\theta_mB^2}\frac{\partial C_{umD}}{\partial z_D}\right)\Big|_{z_D=1}+\left(\frac{\theta_{lm}\alpha_r^2v_{lm}}{2AB\theta_m}C_{lmD}-\frac{\theta_{lm}\alpha_r^2D_l}{2AB^2\theta_m}\frac{\partial C_{lmD}}{\partial z_D}\right)\Big|_{z_D=-1},\ r_D\geq r_{wD}, \tag{S1a}$$

$$\frac{\partial C_{imD}}{\partial t_D}=\varepsilon_{im}(C_{mD}-C_{imD})-\mu_{imD}C_{imD},\ r_D\geq r_{wD}, \tag{S1b}$$

$$\frac{\partial C_{umD}}{\partial t_D}=\frac{R_m\alpha_r^2D_u}{AB^2R_{um}}\frac{\partial^2C_{umD}}{\partial z_D^2}-\frac{R_mv_{um}\alpha_r^2}{ABR_{um}}\frac{\partial C_{umD}}{\partial z_D}-\varepsilon_{um}(C_{umD}-C_{uimD})-\mu_{umD}C_{umD},\ z_D\geq 1, \tag{S2a}$$

$$\frac{\partial C_{uimD}}{\partial t_D}=\varepsilon_{uim}(C_{umD}-C_{uimD})-\mu_{uimD}C_{uimD},\ z_D\geq 1, \tag{S2b}$$

$$\frac{\partial C_{lmD}}{\partial t_D}=\frac{R_m\alpha_r^2D_l}{AB^2R_{lm}}\frac{\partial^2C_{lmD}}{\partial z_D^2}+\frac{R_mv_{lm}\alpha_r^2}{AB\ {}_{lm}}\frac{\partial C_{lmD}}{\partial z_D}-\varepsilon_{lm}(C_{lmD}-C_{limD})-\mu_{lmD}C_{lmD},\ z_D\leq -1, \tag{S3a}$$

$$\frac{\partial C_{limD}}{\partial t_D} = \varepsilon_{lim}(C_{lmD} - C_{limD}) - \mu_{limD}C_{limD}, z_D \leq -1, \tag{S3b}$$

where $\varepsilon_m = \frac{\omega_a \alpha_r^2}{A\theta_m}$, $\varepsilon_{im} = \frac{\omega_a \alpha_r^2 R_m}{A\theta_m R_{im}}$, $\varepsilon_{um} = \frac{\omega_u \alpha_r^2 R_m}{A\theta_{um} R_{um}}$, $\varepsilon_{uim} = \frac{\omega_u \alpha_r^2 R_m}{A\theta_{um} R_{uim}}$, $\varepsilon_{lm} = \frac{\omega_l \alpha_r^2 R_m}{A\theta_{lm} R_{lm}}$, $\varepsilon_{lim} = \frac{\omega_l \alpha_r^2 R_m}{A\theta_{lm} R_{lim}}$.

The analytical solution will be derived using the Laplace transform method and the Green's functions method, and the detailed information could be seen in the following sections.

S1.1 Solutions in the injection phase: Eqs. (25a) and (25f)

Substituting the dimensionless parameters into Eqs. (5) - (6), one could obtain the dimensionless boundary conditions and dimensionless initial conditions for the injection phase:

$$C_{mD}(r_D, t_D)|_{t_D=0} = C_{imD}(r_D, t_D)|_{t_D=0} = C_{umD}(r_D, z_D, t_D)|_{t_D=0} = C_{uimD}(r_D, z_D, t_D)|_{t_D=0} = C_{lmD}(r_D, z_D, t_D)|_{t_D=0} = C_{limD}(r_D, z_D, t_D)|_{t_D=0} = 0, \tag{S4}$$

$$C_{mD}(r_D, t_D)|_{r_D\to\infty} = C_{imD}(r_D, t_D)|_{r_D\to\infty} = C_{umD}(r_D, z_D, t_D)|_{z_D\to\infty} = C_{uimD}(r_D, z_D, t_D)|_{z_D\to\infty} = C_{lmD}(r_D, z_D, t)|_{z_D\to-\infty} = C_{limD}(r_D, z_D, t_D)|_{z_D\to-\infty} = 0, \tag{S5}$$

$$C_{mD}(r_D, t_D) = C_{umD}(r_D, z_D = 1, t_D), \tag{S6a}$$

$$C_{mD}(r_D, t_D) = C_{lmD}(r_D, z_D = -1, t_D). \tag{S6b}$$

Conducting Laplace transform to Eqs. (S2a) - (S2b), one has:

$$s\bar{C}_{umD} = \frac{R_m \alpha_r^2 D_u}{AB^2 R_{um}} \frac{\partial^2 \bar{C}_{umD}}{\partial z_D^2} - \frac{R_m v_{um} \alpha_r^2}{ABR_{um}} \frac{\partial \bar{C}_{umD}}{\partial z_D} - (\varepsilon_{um} + \mu_{umD})\bar{C}_{umD} + \varepsilon_{um}\bar{C}_{uimD}, \quad z_D \geq 1, \tag{S7a}$$

$$s\bar{C}_{uimD} = \varepsilon_{uim}(\bar{C}_{umD} - \bar{C}_{uimD}) - \mu_{uimD}\bar{C}_{uimD}, z_D \geq 1, \tag{S7b}$$

Substituting Eq. (S7b) into Eq. (S7a) will lead to:

$$s\bar{C}_{umD} = \frac{R_m \alpha_r^2 D_u}{AB^2 R_{um}} \frac{\partial^2 \bar{C}_{umD}}{\partial z_D^2} - \frac{R_m v_{um} \alpha_r^2}{AB\ \ _{um}} \frac{\partial \bar{C}_{umD}}{\partial z_D} - \left(\varepsilon_{um} + \mu_{umD} - \frac{\varepsilon_{um}\varepsilon_{uim}}{s+\mu_{uimD}+\varepsilon_{uim}}\right)\bar{C}_{umD},$$

$$z_D \geq 1, \tag{S8}$$

Similarly, Eqs. (S3a) - (S3b) become:

$$s\bar{C}_{lmD} = \frac{R_m \alpha_r^2 D_l}{AB^2 R_{lm}} \frac{\partial^2 \bar{C}_{lmD}}{\partial z_D^2} + \frac{R_m v_{lm} \alpha_r^2}{ABR_{lm}} \frac{\partial \bar{C}_{lmD}}{\partial z_D} - (\varepsilon_{lm} + \mu_{lmD})\bar{C}_{lmD} + \varepsilon_{lm}\bar{C}_{limD},$$

$$z_D \leq -1, \tag{S9a}$$

$$s\bar{C}_{limD} = \varepsilon_{lim}(\bar{C}_{lmD} - \bar{C}_{limD}) - \mu_{limD}\bar{C}_{limD}, z_D \leq -1, \tag{S9b}$$

Substituting Eq. (S9b) into Eq.(S9a) results in:

$$s\bar{C}_{lmD} = \frac{R_m \alpha_r^2 D_l}{AB^2 R_{lm}} \frac{\partial^2 \bar{C}_{lmD}}{\partial z_D^2} + \frac{R_m v_{lm} \alpha_r^2}{ABR_{lm}} \frac{\partial \bar{C}_{lmD}}{\partial z_D} - \left(\varepsilon_{lm} + \mu_{lmD} - \frac{\varepsilon_{lm}\varepsilon_{lim}}{s+\mu_{limD}+\varepsilon_{lim}}\right)\bar{C}_{lmD},$$

$$z_D \leq -1, \tag{S10}$$

where overbar represents the variables in Laplace domain hereinafter; *s* is the Laplace transform parameter in respect to dimensionless time.

Eqs. (S5), (S6a)-(S6b) and (S8) compose a model of the second-order ordinary differential equation (ODE) with boundary conditions, the general solution of Eq. (S8) is:

$$\bar{C}_{umD} = A_1 e^{a_1 z_D} + B_1 e^{a_2 z_D}. \tag{S11a}$$

Similarly, the general solution of Eq. (S10) is:

$$\bar{C}_{lmD} = A_2 e^{b_1 z_D} + B_2 e^{b_2 z_D}. \tag{S11b}$$

where $a_1 = \dfrac{\frac{R_m v_{um}\alpha_r^2}{ABR_{um}} + \sqrt{\left(\frac{R_m v_{um}\alpha_r^2}{ABR_{um}}\right)^2 + 4\frac{R_m\alpha_r^2 D_u}{AB^2 R_{um}}\left(s+\varepsilon_{um}+\mu_{umD}-\frac{\varepsilon_{um}\varepsilon_{uim}}{s+\mu_{uimD}+\varepsilon_{uim}}\right)}}{2\frac{R_m\alpha_r^2 D_u}{AB^2 R_{um}}}$,

$$a_2 = \frac{\frac{R_m v_{um}\alpha_r^2}{ABR_{um}} - \sqrt{\left(\frac{R_m v_{um}\alpha_r^2}{ABR_{um}}\right)^2 + 4\frac{R_m\alpha_r^2 D_u}{AB^2 R_{um}}\left(s+\varepsilon_{um}+\mu_{umD}-\frac{\varepsilon_{um}\varepsilon_{uim}}{s+\mu_{uimD}+\varepsilon_{uim}}\right)}}{2\frac{R_m\alpha_r^2 D_u}{AB^2 R_{um}}},$$

$$b_1 = \frac{-\frac{R_m v_{lm}\alpha_r^2}{ABR_{lm}} + \sqrt{\left(\frac{R_m v_{lm}\alpha_r^2}{AB\quad lm}\right)^2 + 4\frac{R_m\alpha_r^2 D_l}{AB^2 R_{lm}}\left(s+\varepsilon_{lm}+\mu_{lmD}-\frac{\varepsilon_{lm}\varepsilon_{lim}}{s+\mu_{limD}+\varepsilon_{lim}}\right)}}{2\frac{R_m\alpha_r^2 D_l}{AB^2 R_{lm}}} \text{ and}$$

$$b_2 = \frac{-\frac{R_m v_{lm}\alpha_r^2}{ABR_{lm}} - \sqrt{\left(\frac{R_m v_{lm}\alpha_r^2}{ABR_{lm}}\right)^2 + 4\frac{R_m\alpha_r^2 D_l}{AB^2R_{lm}}\left(s+\varepsilon_{lm}+\mu_{lmD}-\frac{\varepsilon_{lm}\varepsilon_{lim}}{s+\mu_{limD}+\varepsilon_{lim}}\right)}}{2\frac{R_m\alpha_r^2 D_l}{AB^2R_{lm}}}.$$

Substituting Eqs. (S11a) - (S11b) into Eqs. (S5)-(S6b) leads to:

$$\bar{C}_{umD} = B_1 e^{a_2 z_D}. \tag{S12a}$$

$$\bar{C}_{lmD} = A_2 e^{b_1 z_D}. \tag{S12b}$$

where $B_1 = \bar{C}_{mD}exp(-a_2)$, $B_2 = 0$, $A_1 = 0$ and $A_2 = \bar{C}_{mD}exp(b_1)$.

Thus, we could obtain the solutions for the aquitards as:

$$\bar{C}_{umD} = \bar{C}_{mD}exp(a_2 z_D - a_2). \tag{S13a}$$

$$\bar{C}_{uimD} = \frac{\varepsilon_{uim}}{s+\varepsilon_{uim}+\mu_{uimD}}\bar{C}_{umD}, \tag{S13b}$$

$$\bar{C}_{lmD} = \bar{C}_{mD}exp(b_1 z_D + b_1). \tag{S14a}$$

$$\bar{C}_{limD} = \frac{\varepsilon_{lim}}{s+\varepsilon_{lim}+\mu_{limD}}\bar{C}_{lmD}, \tag{S14b}$$

In the injection phase, the dimensional boundary conditions Eq. (8) and Eqs. (12a)-(12b) are transformed into their dimensionless forms:

$$\left[C_{mD} - \frac{\partial C_{mD}(r_D,t_D)}{\partial r_D}\right]\Big|_{r=r_{wD}} = C_{inj,mD}(t_D), 0 < t_D \le t_{inj,D} \tag{S15}$$

$$\beta_{inj}\frac{dC_{inj,mD}(t_D)}{dt_D} = 1 - C_{inj,mD}(t_D)\ , 0 < t_D \le t_{inj,D}, \tag{S16a}$$

$$C_{inj,mD}(t_D = 0) = 0, \tag{S16b}$$

where $\beta_{inj} = \frac{V_{w,inj}r_{wD}}{\xi R_m \alpha_r}$.

Conducting Laplace transform to Eqs. (S1a) - (S1b), one has:

$$s\bar{C}_{mD} = \frac{1}{r_D}\frac{\partial^2\bar{C}_{mD}}{\partial r_D^2} - \frac{1}{r_D}\frac{\partial\bar{C}_{mD}}{\partial r_D} - (\varepsilon_m + \mu_{mD})\bar{C}_{mD} + \varepsilon_m\bar{C}_{imD} -$$

$$\left(\frac{\theta_{um}\alpha_r^2 v_{um}}{2A\theta_m B}\bar{C}_{umD} - \frac{\theta_{um}\alpha_r^2 D_u}{2A\theta_m B^2}\frac{\partial\bar{C}_{umD}}{\partial z_D}\right)\Big|_{z_D=1} + \left(\frac{\theta_{lm}\alpha_r^2 v_{lm}}{2A\theta_m B}\bar{C}_{lmD} - \frac{\theta_{lm}\alpha_r^2 D_l}{2AB^2\theta_m}\frac{\partial\bar{C}_{lmD}}{\partial z_D}\right)\Big|_{z_D=-1},$$

$$r_D \geq r_{wD}. \tag{S17a}$$

$$\bar{C}_{imD} = \frac{\varepsilon_{im}}{(s+\mu_{imD}+\varepsilon_{im})}\bar{C}_{mD}, r_D \geq r_{wD}, \tag{S17b}$$

Substituting Eqs. (S13a), (S14a) and (S17b) into Eq. (S17a),one has:

$$\frac{1}{r_D}\frac{\partial^2 \bar{C}_{mD}}{\partial r_D^2} - \frac{1}{r_D}\frac{\partial \bar{C}_{mD}}{\partial r_D} - E\bar{C}_{mD} = 0. \tag{S18}$$

where

$$E = s + \varepsilon_m + \mu_{mD} - \frac{\varepsilon_m \varepsilon_{im}}{s+\mu_{imD}+\varepsilon_{im}} + \frac{\theta_{um}\alpha_r^2 v_{um}}{2A\theta_m B} - \frac{\theta_{lm}\alpha_r^2 v_{lm}}{2AB\theta_m} - \frac{a_2\theta_{um}\alpha_r^2 D_u}{2A\theta_m B^2} + \frac{b_1\theta_{lm}\alpha_r^2 D_l}{2AB^2\theta_m}.$$

The boundary conditions of the wellbore and infinity in the Laplace domain are:

$$\left[\bar{C}_{mD} - \frac{\partial \bar{C}_{mD}(r_D,s)}{\partial r_D}\right]\Bigg|_{r=r_{wD}} = \bar{C}_{inj,mD}(s), \tag{S19a}$$

$$\bar{C}_{mD}(r_D,s)|_{r_D\to\infty} = 0. \tag{S19b}$$

Conducting Laplace transform on Eqs. (S16a)- (S16b), one has:

$$\bar{C}_{inj,mD}(r_w,s) = \frac{1}{s(s\beta_{inj}+1)}, \tag{S20}$$

Eqs. (S18), (S19a)-(S19b), and (S20) compose a model of the second-order ordinary differential equation (ODE) with boundary conditions. The general solution of Eq. (S18) is:

$$\bar{C}_{mD}(r_D,s) = \phi_1\, exp\left(\frac{y_{inj}}{2}\right) A_i\left(E^{1/3}y_{inj}\right) + \phi_2 \exp\left(\frac{y_{inj}}{2}\right) B_i\left(E^{1/3}y_{inj}\right). \tag{S21}$$

where $y_{inj} = r_D + \frac{1}{4E}$, $y_{inj,w} = r_{wD} + \frac{1}{4E}$; ϕ_1 and ϕ_2 are constants which could be determined by the boundary conditions; $A_i(\cdot)$ and $B_i(\cdot)$ are the Airy functions of the first kind and second kind, respectively. As $B_i(r_D)$ diverges when $r_D \to \infty$, ϕ_2 has to be zero.

Substituting Eqs. (S21), (S20) and $\phi_2 = 0$ into Eq. (S19a), the value of ϕ_1 is:

$$\phi_1 = \frac{1}{s(s\beta_{inj}+1)} \frac{1}{exp\left(\frac{y_{inj,w}}{2}\right)\left[\frac{A_i\left(E^{1/3}y_{inj,w}\right)}{2} - E^{1/3}A_i'\left(E^{1/3}y_{inj}\right)\right]}. \tag{S22}$$

where $A_i'(\cdot)$ is the derivative of the Airy function.

Substituting Eq. (S22) and $\phi_2 = 0$ into Eqs. (S21) and (S17b), one could obtain the Laplace-domain analytical solution of solute transport in the injection phase of the SWPP test.

S1.2 Solutions in the chaser phase: Eqs. (26a) - (26g)

For the chaser phase, conducting Laplace transform on Eqs. (S2a)-(S2b), one has:

$$\frac{R_m \alpha_r^2 D_u}{AB^2 R_{um}} \frac{\partial^2 \bar{C}_{umD}}{\partial z_D^2} - \frac{R_m v_{um} \alpha_r^2}{ABR_{um}} \frac{\partial \bar{C}_{umD}}{\partial z_D} - (s + \varepsilon_{um} + \mu_{umD}) \bar{C}_{umD} + \varepsilon_{um} \bar{C}_{uimD} +$$

$$C_{umD}\left(r_D, z_D, t_{inj,D}\right) = 0, \quad z_D \geq 1, \qquad \text{(S23a)}$$

$$s\bar{C}_{uimD} - C_{uimD}\left(r_D, z_D, t_{inj,D}\right) = \varepsilon_{uim}(\bar{C}_{umD} - \bar{C}_{uimD}) - \mu_{uimD} \bar{C}_{uimD}\ , \qquad \text{(S23b)}$$

Eq. (S23b) could be rewritten as:

$$\bar{C}_{uimD} = \frac{\varepsilon_{uim}}{s+\varepsilon_{uim}+\mu_{uimD}} \bar{C}_{umD} + \frac{C_{uimD}\left(r_D, z_D, t_{inj,D}\right)}{s+\varepsilon_{uim}+\mu_{uimD}}, \qquad \text{(S23c)}$$

Substituting Eq. (S23c) into Eq. (S23a), one has:

$$\frac{R_m \alpha_r^2 D_u}{AB^2 R_{um}} \frac{\partial^2 \bar{C}_{umD}}{\partial z_D^2} - \frac{R_m v_{um} \alpha_r^2}{ABR_{um}} \frac{\partial \bar{C}_{umD}}{\partial z_D} - \left(s + \varepsilon_{um} + \mu_{umD} - \frac{\varepsilon_{um}\varepsilon_{uim}}{s+\varepsilon_{uim}+\mu_{uimD}}\right) \bar{C}_{umD} +$$

$$C_{umD}\left(r_D, z_D, t_{inj,D}\right) + \frac{\varepsilon_{um} C_{uimD}\left(r_D, z_D, t_{inj,D}\right)}{s+\varepsilon_{uim}+\mu_{uimD}} = 0.\ z_D \geq 1, \qquad \text{(S24)}$$

Similarly, Eqs. (S3a) - (S3b) become:

$$\frac{R_m \alpha_r^2 D_l}{AB^2 R_{lm}} \frac{\partial^2 \bar{C}_{lmD}}{\partial z_D^2} + \frac{R_m v_{lm} \alpha_r^2}{AB\ _{lm}} \frac{\partial \bar{C}_{lmD}}{\partial z_D} - (s + \varepsilon_{lm} + \mu_{lmD}) \bar{C}_{lmD} + \varepsilon_{lm} \bar{C}_{limD} +$$

$$C_{lmD}\left(r_D, z_D, t_{inj,D}\right) = 0, \quad z_D \leq -1, \qquad \text{(S25a)}$$

$$s\bar{C}_{limD} - C_{limD}\left(r_D, z_D, t_{inj,D}\right) = \varepsilon_{lim}(\bar{C}_{lmD} - \bar{C}_{limD}) - \mu_{limD} C_{limD}\ , \qquad \text{(S25b)}$$

Eq. (S23b) could be rewritten as :

$$\bar{C}_{limD} = \frac{\varepsilon_{lim}}{s+\varepsilon_{lim}+\mu_{limD}} \bar{C}_{lmD} + \frac{C_{limD}\left(r_D, z_D, t_{inj,D}\right)}{s+\varepsilon_{lim}+\mu_{limD}}, \qquad \text{(S25c)}$$

Substituting Eq. (S25c) into Eq. (S25a), one has:

$$\frac{R_m\alpha_r^2 D_l}{AB^2 R_{lm}}\frac{\partial^2 \bar{C}_{lmD}}{\partial z_D^2}+\frac{R_m v_{lm}\alpha_r^2}{ABR_{lm}}\frac{\partial \bar{C}_{lmD}}{\partial z_D}-\left(s+\varepsilon_{lm}+\mu_{lmD}-\frac{\varepsilon_{lm}\varepsilon_{lim}}{s+\varepsilon_{lim}+\mu_{limD}}\right)\bar{C}_{lmD}+$$

$$C_{lmD}\left(r_D,z_D,t_{inj,D}\right)+\frac{\varepsilon_{lm}C_{limD}\left(r_D,z_D,t_{inj,D}\right)}{s+\varepsilon_{lim}+\mu_{limD}}=0.\ z_D\leq -1, \tag{S26}$$

where $C_{umD}\left(r_D,z_D,t_{inj,D}\right)$ and $C_{uimD}\left(r_D,z_D,t_{inj,D}\right)$ are respectively the mobile and immobile concentrations [ML^{-3}] of the upper aquitard at the end of the injection phase, $C_{lmD}\left(r_D,z_D,t_{inj,D}\right)$ and $C_{limD}\left(r_D,z_D,t_{inj,D}\right)$ are respectively the mobile and immobile concentrations [ML^{-3}] of the lower aquitard at the end of the injection phase. In this study, we use the Green's function method to derive the analytical solution of Eqs. (S24) and (S26).

Notice that the boundary condition of Eq. (S6a) is inhomogeneous, thus we need to homogenize it first. Letting $\bar{C}_{umD}=\mathscr{k}(z_D)+\mathscr{s}_1+\mathscr{s}_2 z_D$, and substituting them into Eqs. (S5) and (S6a) yields:

$$[\mathscr{k}(z_D)]|_{z_D\to\infty}=0, \tag{S27a}$$

$$[\mathscr{k}(z_D)]|_{z_D=1}=0, \tag{S27b}$$

where $\mathscr{s}_1=-\mathscr{s}_2 z_{eD}$ and $\mathscr{s}_2=\frac{\bar{C}_{mD}(r_D,s)}{1-z_{eD}}$.

Defining the spatial operator: $L_u=-\left[\frac{R_m\alpha_r^2 D_u}{AB^2R_{um}}\frac{d^2}{dz_D^2}-\frac{R_m v_{um}\alpha_r^2}{ABR_{um}}\frac{d}{dz_D}-E_u\right]$, one has:

$$L_u\bar{C}_{umD}=L_u[\mathscr{k}(z_D)+\mathscr{s}_1]=F_u(z_D), \tag{S28}$$

Let $f_u(z_D)=F_u(z_D)-L_u[\mathscr{s}_1+\mathscr{s}_2 z_D]$, one has:

$$\frac{R_m\alpha_r^2 D_u}{AB^2R_{um}}\frac{d^2\mathscr{k}}{dz_D^2}-\frac{R_m v_{um}\alpha_r^2}{ABR_{um}}\frac{d\mathscr{k}}{dz_D}-E_u\mathscr{k}=-f_u(z_D)\ , \tag{S29}$$

where $E_u=s+\varepsilon_{um}+\mu_{um}\ \ -\frac{\varepsilon_{um}\varepsilon_{uim}}{s+\varepsilon_{uim}+\mu_{uimD}}$,

$F_u(z_D)=C_{umD}\left(r_D,z_D,t_{inj,D}\right)+\frac{\varepsilon_{um}C_{uimD}\left(r_D,z_D,t_{inj,D}\right)}{s+\varepsilon_{uim}+\mu_{uimD}}$ and $f_u(z_D)=C_{umD}\left(r_D,z_D,t_{inj,D}\right)+$ $\frac{\varepsilon_{um}C_{uimD}\left(r_D,z_D,t_{inj,D}\right)}{s+\varepsilon_{uim}+\mu_{uimD}}-\frac{R_m v_{um}\alpha_r^2}{AB\ \ {}_{um}}\mathscr{s}_2-E_u(\mathscr{s}_1+\mathscr{s}_2 z_D)$.

The general solution of Eq. (S24) is:

$$\bar{C}_{umD} = \int_1^\infty g_u(z_D, E_u; \eta_u)\, f_u(\eta_u) d\eta_u + \frac{z_D - z_{eD}}{1 - z_{eD}} \bar{C}_{mD}(r_D, s), z_D \geq 1. \quad \text{(S30)}$$

where $f_u(\eta_u) = C_{umD}\left(r_D, \eta_u, t_{inj,D}\right) + \frac{\varepsilon_{um} C_{uimD}\left(r_D, \eta_u, t_{inj,D}\right)}{s + \varepsilon_{uim} + \mu_{uimD}} - \frac{R_m v_{um} \alpha_r^2}{ABR_{um}} \mathscr{s}_2 - E_u(\mathscr{s}_1 + \mathscr{s}_2 \eta_u)$, η_u is a positive value varying between 1 and ∞ (e.g. $1 \leq \eta_u \leq \infty$); $g_u(z_D, E_u; \eta_u)$ is the Green's function, and could be expressed as :

$$g_u(z_D, E_u; \eta_u) = \begin{cases} g_{u1}(z_D, E_u; \eta_u) = N_1 exp(a_1 z_D) + N_2 exp(a_2 z_D) & 1 \leq z_D < \eta_u \\ g_{u2}(z_D, E_u; \eta_u) = N_3 exp(a_1 z_D) + N_4 exp(a_2 z_D) & \eta_u \leq z_D < \infty \end{cases}, \quad \text{(S31)}$$

where N_1， N_2， N_3 and N_4 are coefficients to be detrmined using the following conditions [*Chen and Woodside* ,1988]:

a) $g_u(z_D, E_u; \eta_u)$ satisfying the model of Eqs. (S29) and (S27a)-(S27b);

b) $g_{u1}(z_D, E_u; \eta_u) = g_{u2}(z_D, E_u; \eta_u)$;

c) $\left.\frac{dg_{u2}}{dz_D}\right|_{z_D = \eta_u^+} - \left.\frac{dg_{u1}}{dz_D}\right|_{z_D = \eta_u^-} = -\frac{AB^2 R_{um}}{R_m \alpha_r^2 D_u}$;

Substituting Eq. (S31) into Eq. (S27a), one has:

$$N_3 = 0, \quad \text{(S32)}$$

Substituting Eq. (S31) into Eq. (S27b), one has:

$$N_1 exp(a_1) + N_2 exp(a_2) = 0, \quad \text{(S33a)}$$

According to Eq. (S33a), one has:

$$N_1 = -N_2 exp(a_2 - a_1), \quad \text{(S33b)}$$

According to above condition of b), one has:

$$N_1 exp(a_1 \eta_u) + N_2 exp(a_2 \eta_u) = N_4 exp(a_2 \eta_u), \quad \text{(S34)}$$

According to above condition of c), one has:

$$N_4 a_2 exp(a_2 \eta_u) - [N_1 a_1 exp(a_1 \eta_u) + N_2 a_2 exp(a_2 \eta_u)] = -\frac{AB^2 R_{um}}{R_m \alpha_r^2 D_u}. \quad \text{(S35)}$$

In the chaser phase, the values of N_1, N_2 , $N_3$and N_4 could be determined by Eqs. (S33a) - (S35), namely:

$N_1 = -N_2 exp(a_2 - a_1)$, $N_2 = \frac{-AB^2 R_{um}}{R_m \alpha_r^2 D_u[(a_1 - a_2)exp(a_2 - a_1)exp(a_1 \eta_u)]}$, $N_3 = 0$ and

$N_4 = N_2 - N_2 exp(a_2 - a_1)exp(a_1 \eta_u - a_2 \eta_u)$.

As for the analytical solution of the lower aquitard, one could use a similar approach as that used for deriving the analytical solution of the upper aquitard to obtain, and the general solution of Eq. (S26) could be described as:

$$\bar{C}_{lmD} = \int_{-1}^{-\infty} g_l(z_D, E_l; \eta_l)\, f_l(\eta_l) d\eta_l + \frac{z_{eD} + z_D}{z_{eD} - 1} \bar{C}_{mD}(r_D, z_D, s),\ z_D \leq -1. \quad \text{(S36a)}$$

$$g_l(z_D, E_l; \eta_l) = \begin{cases} g_{l1}(z_D, E_l; \eta_l) = M_1 exp(b_1 z_D) + M_2 exp(b_2 z_D) & -1 \leq z_D < \eta_l \\ g_{l2}(z_D, E_l; \eta_l) = M_3 exp(b_1 z_D) + M_4 exp(b_2 z_D) & \eta_l \leq z_D < -\infty \end{cases}, \quad \text{(S36b)}$$

$$f_l(\eta_l) = C_{lmD}(r_D, \eta_l, t_{inj,D}) + \frac{\varepsilon_{lm} C_{limD}(r_D, \eta_l, t_{inj,D})}{s + \varepsilon_{lim} + \mu_{limD}} + \frac{R_m v_{lm} \alpha_r^2}{ABR_{lm}} \frac{\bar{C}_{mD}}{z_{eD} - 1} - \bar{C}_{mD} E_l \frac{z_{eD} + \eta_l}{z_{eD} - 1}, \quad \text{(S36c)}$$

where η_l is a negative value varying between -1 and $-\infty$ (e.g.$-1 \leq \eta_l \leq -\infty$); $g_l(z_D, E_l; \eta_l)$ is the Green's function, $E_l = s + \varepsilon_{lm} + \mu_{lmD} - \frac{\varepsilon_{lm}\varepsilon_{lim}}{s + \varepsilon_{lim} + \mu_{limD}}$, and the values of M_1, M_2 , $M_3$and M_4 could be described as: $M_1 = -M_2 exp(b_1 - b_2)$, $M_2 = \frac{-AB^2 R_{lm}}{R_m \alpha_r^2 D_l[exp(b_2 \eta_l - b_1 \eta_l) - b_2 exp(b_2 \eta_l)]}$, $M_3 = M_2 exp(b_2 \eta_l - b_1 \eta_l) - M_2 exp(b_1 - b_2)$, $M_4 = 0$, and the values of a_1, a_2 , b_1 and b_2 are the same as used in the injection phase.

In the chaser phase, the dimensional boundary conditions Eqs. (15a)-(15b) are transformed into dimensionless forms as:

$$\beta_{cha,D} \frac{\partial C_{mD}(r_D, t_D)}{\partial t_D}\bigg|_{r_D = r_{wD}} = C_{mD}(r_D, t_D),\ t_{inj,D} < t_D \leq t_{cha,D}, \quad \text{(S37a)}$$

$$C_{cha,mD}(r_D, t_D)\big|_{t_D = t_{inj,D}} = C_{inj,mD}(r_D, t_D)\big|_{t_D = t_{inj,D}},\ t_{inj,D} < t_D \leq t_{cha,D}. \quad \text{(S37b)}$$

where $\beta_{cha,D} = -\frac{V_{w,cha} r_{wD}}{\xi R_m \alpha_r}$.

Conducting Laplace transform on Eqs. (S1a)-(S1b) in the chaser phase, one has:

$$s\bar{C}_{mD} - C_{mD}\left(r_D, t_{inj,D}\right) = \frac{1}{r_D}\frac{\partial^2 \bar{C}_{mD}}{\partial r_D^2} - \frac{1}{r_D}\frac{\partial \bar{C}_{mD}}{\partial r_D} - (\varepsilon_m + \mu_{mD})\bar{C}_{mD} + \varepsilon_m \bar{C}_{imD} -$$

$$\left(\frac{\theta_{um}\alpha_r^2 v_{um}}{2A\theta_m B}\bar{C}_{umD} - \frac{\theta_{um}\alpha_r^2 D_u}{2A\theta_m B^2}\frac{\partial \bar{C}_{umD}}{\partial z_D}\right)\Bigg|_{z_D=1} + \left(\frac{\theta_{lm}\alpha_r^2 v_{lm}}{2A\theta_m B}\bar{C}_{lmD} - \frac{\theta_{lm}\alpha_r^2 D_l}{2AB^2\theta_m}\frac{\partial \bar{C}_{lmD}}{\partial z_D}\right)\Bigg|_{z_D=-1},$$

$$r_D \geq r_{wD}. \tag{S38a}$$

$$\bar{C}_{imD} = \frac{\varepsilon_{im}}{(s+\mu_{imD}+\varepsilon_{im})}\bar{C}_{mD} + \frac{C_{imD}\left(r_D, t_{inj,D}\right)}{(s+\mu_{imD}+\varepsilon_{im})}, r_D \geq r_{wD}, \tag{S38b}$$

where $C_{mD}\left(r_D, t_{inj,D}\right)$ and $C_{imD}\left(r_D, t_{inj,D}\right)$ are respectively the mobile and immobile concentrations [ML^{-3}] of the aquifer at the end of the injection phase, which could be calculated by Eqs. (S21) and (S17b).

After substituting Eqs. (S30), (S36a)-(S36c) and (S38b) into Eq. (S38a), one has:

$$\frac{1}{r_D}\frac{\partial^2 \bar{C}_{mD}}{\partial r_D^2} - \frac{1}{r_D}\frac{\partial \bar{C}_{mD}}{\partial r_D} - E_a\bar{C}_{mD} + F = 0, r_D \geq r_{wD}, \tag{S39}$$

where $E_a = s + \varepsilon_m + \mu_{mD} - \frac{\varepsilon_m\varepsilon_{im}}{s+\mu_{imD}+\varepsilon_{im}} + \frac{\theta_{um}\alpha_r^2 v_{um}}{2A\theta_m B} - \frac{\theta_{lm}\alpha_r^2 v_{lm}}{2AB^2\theta_m} - \frac{1}{1-z_{eD}}\frac{\theta_{um}\alpha_r^2 D_u}{2A\theta_m B^2} + \frac{1}{z_{eD}-1}\frac{\theta_{lm}\alpha_r^2 D_l}{2AB^2\theta_m}$ and $F = C_{mD}\left(r_D, t_{inj,D}\right) + \frac{\varepsilon_m C_{imD}\left(r_D, t_{inj}\right)}{s+\mu_{imD}+\varepsilon_{im}}$.

The boundary conditions of Eqs. (S37a)-(S37b) in Laplace domain becomes:

$$\bar{C}_{cha,mD}(r_{wD}, s) = \frac{\beta_{cha,D}}{s\beta_{cha,D}+1}C_{inj,mD}(r_D, t_D)\big|_{t_D=t_{inj,D}}. \tag{S40}$$

The boundary conditions of the wellbore and infinity in Laplace domain are:

$$\left[\bar{C}_{mD} - \frac{\partial \bar{C}_{mD}(r_D,s)}{\partial r_D}\right]\Bigg|_{r=r_{wD}} = \frac{\beta_{cha,D}}{s\beta_{cha,D}+1}C_{inj,mD}(r_D, t_D)\big|_{t_D=t_{inj,D}}, \tag{S41a}$$

$$\bar{C}_{cha,mD}(r_{wD}, s)\big|_{r_D\to\infty} = 0, \tag{S41b}$$

Similar to the model of the SWPP test in the injection phase, Eqs. (S39) and (S40)-(S41b) compose a model of the second-order ordinary differential equation (ODE) with boundary conditions, however, the governing equation is an inhomogeneous differential equation. In this study, we use the Green's function method to derive the analytical solution of Eq. (S39).

Notice that the boundary condition of Eq. (S41a) is inhomogeneous, and we need to homogenize it first. Assigning $\bar{C}_{mD} = \Psi(r_D) + \delta_1 + \delta_2 r_D$, and substituting it into Eqs. (S41a) and (S41b) yields:

$$\left[\Psi(r_D, s) - \frac{\partial \Psi(r_D, s)}{\partial r_D}\right]\Big|_{r=r_{wD}} = 0, \tag{S42a}$$

$$\Psi(r_D, s)|_{r_D \to \infty} = 0, \tag{S42b}$$

where $\delta_1 = -\frac{\beta_{cha,D}}{s\beta_{cha,D}+1} \frac{r_D|_{r_D\to\infty}}{(r_{wD} - r_D|_{r_D\to\infty} - 1)} C_{inj,mD}(r_D, t_D)\big|_{t_D = t_{inj,D}}$ and

$$\delta_2 = \frac{\beta_{cha,D}}{s\beta_{cha,D}+1} \frac{1}{(r_{wD} - r_D|_{r_D\to\infty} - 1)} C_{inj,mD}(r_D, t_D)\big|_{t_D = t_{inj,D}}.$$

Defining a spatial operator:$L = -\left[\frac{d^2}{dr_D^2} - \frac{d}{dr_D} - r_D E_a\right]$, one has:

$$L\bar{C}_{mD} = L[\Psi(r_D) + \delta_1 + \delta_2 r_D] = F r_D, \tag{S43}$$

Let $\varphi(r_D) = F r_D - L(\delta_1 + \delta_2 r_D)$, one has:

$$\frac{\partial^2 \Psi}{\partial r_D^2} - \frac{\partial \Psi}{\partial r_D} - r_D E_a \Psi = -\varphi(r_D). \tag{S44}$$

where $\varphi(r_D) = F r_D - [\delta_2 + r_D E_a(\delta_1 + \delta_2 r_D)]$.

The general solution of Eqs. (S42a) - (S44) is:

$$\Psi(r_D, E_a; \eta) = \int_{r_{wD}}^{\infty} g(r_D, E_a; \eta)\, \varphi(\eta) d\eta. \tag{S45}$$

where η is a positive value varying between r_{wD} and ∞ (e.g. $r_{wD} \le \eta \le \infty$); $g(r_D, E_a; \eta)$ is the Green's function, and could be expressed as :

$$g(r_D, E_a; \eta) = \begin{cases} g_1(r_D, E_a; \eta) = \mathcal{T}_1 exp(\frac{y_{cha}}{2}) A_i\left(E_a^{\frac{1}{3}} y_{cha}\right) + \mathcal{T}_2\, exp\left(\frac{y_{cha}}{2}\right) B_i\left(E_a^{\frac{1}{3}} y_{cha}\right) r_{wD} \le y_{cha} \le \eta \\ g_2(r_D, E_a; \eta) = \mathcal{T}_3 exp(\frac{y_{cha}}{2}) A_i\left(E_a^{\frac{1}{3}} y_{cha}\right) + \mathcal{T}_4\, exp\left(\frac{y_{cha}}{2}\right) B_i\left(E_a^{\frac{1}{3}} y_{cha}\right)\ \eta \le y_{cha} \le \infty \end{cases}. \tag{S46}$$

where $\varphi(\eta) = F\eta - [\delta_2 + \eta E_a(\delta_1 + \delta_2\eta)]$, $y_{cha} = r_D + \frac{1}{4E_a}$. As $B_i(r_D)$ diverges when $r_D \to \infty$, $\mathcal{T}_4$ has to be zero. Substituting Eq. (S45) into Eq. (S42a), one has:

$$\left[g_1 - \frac{\partial g_1}{\partial r_D}\right]\Big|_{r_D=r_{wD}} = 0, \tag{S47}$$

According to Eq. (S47), one has:

$$\mathcal{T}_1 = -\mathcal{T}_2 X. \tag{S48}$$

where $X = \frac{\frac{1}{2}B_i({E_a}^{1/3}y_{cha,w}) - {E_a}^{1/3}B_i'({E_a}^{1/3}y_{cha,w})}{\frac{1}{2}A_i({E_a}^{1/3}y_{cha,w}) - {E_a}^{1/3}A_i'({E_a}^{1/3}y_{cha,w})}$ and $y_{cha,w} = r_{wD} + \frac{1}{4E_a}$.

According to above condition of b), one has:

$$\mathcal{T}_1 A_i\left({E_a}^{\frac{1}{3}} y_{cha}|_{r_D=\eta^+}\right) + \mathcal{T}_2 B_i\left({E_a}^{\frac{1}{3}} y_{cha}|_{r_D=\eta^+}\right) = \mathcal{T}_3 A_i\left({E_a}^{1/3} y_{cha}|_{r_D=\eta^-}\right). \tag{S49}$$

According to above condition of c), one has:

$$\left[\frac{1}{2}\mathcal{T}_3\, exp\left(\frac{y_{cha}}{2}\right) A_i\left({E_a}^{\frac{1}{3}} y_{cha}\right) + {E_a}^{\frac{1}{3}}\mathcal{T}_3\, exp\left(\frac{y_{cha}}{2}\right) A_i'\left({E_a}^{\frac{1}{3}} y_{cha}\right)\right]\Big|_{r_D=\eta^-} -$$
$$\left[0.5\mathcal{T}_1\, exp\left(\frac{y_{cha}}{2}\right) A_i\left({E_a}^{\frac{1}{3}} y_{cha}\right) + {E_a}^{\frac{1}{3}}\mathcal{T}_1\, exp\left(\frac{y_{cha}}{2}\right) A_i'\left({E_a}^{\frac{1}{3}} y_{cha}\right)\right]\Big|_{r_D=\eta^+} -$$
$$\left[\frac{1}{2}\mathcal{T}_2\, exp\left(\frac{y_{cha}}{2}\right) B_i\left({E_a}^{\frac{1}{3}} y_{cha}\right) + {E_a}^{\frac{1}{3}}\mathcal{T}_2\, exp\left(\frac{y_{cha}}{2}\right) B_i'\left({E_a}^{\frac{1}{3}} y_{cha}\right)\right]\Big|_{r_D=\eta^+} = -1. \tag{S50}$$

For solution in the chaser phase, the values of $\mathcal{T}_1$, $\mathcal{T}_2$, $\mathcal{T}_3$ and $\mathcal{T}_4$ could be determined by Eqs. (S48) - (S50), namely:

$\mathcal{T}_1 = -\frac{\pi A_i\left(y_{ext}|_{r_D=\eta^+}\right)}{{E_a}^{1/3}} X$, $\mathcal{T}_2 = \frac{\pi A_i\left(y_{ext}|_{r_D=\eta^+}\right)}{{E_a}^{1/3}}$, $\mathcal{T}_3 = \frac{\pi A_i\left(y_{ext}|_{r_D=\eta^+}\right)}{{E_a}^{1/3}}\left[\frac{B_i\left(y_{ext}|_{r_D=\eta^+}\right)}{A_i\left(y_{ext}|_{r_D=\eta^+}\right)} - X\right]$ and $\mathcal{T}_4 = 0$.

S1.3 Solutions in the rest phase: Eqs. (27a) - (27f)

In the rest phase, the flow velocity become zero, and the advection and dispersion terms drop out of the governing equations. After conducting Laplace transform on Eqs. (S2a)-(S2b), the following equations would be obtained:

$$(s+\varepsilon_{um}+\mu_{umD})\bar{C}_{umD}-\varepsilon_{um}\bar{C}_{uimD}-C_{umD}\left(r_D,z_D,t_{cha,D}\right)=0.\ z_D\geq 1. \quad \text{(S51a)}$$

$$\bar{C}_{uimD}=\frac{\varepsilon_{uim}}{s+\varepsilon_{uim}+\mu_{umD}}\bar{C}_{umD}+\frac{C_{uimD}\left(r_D,z_D,t_{cha,D}\right)}{s+\varepsilon_{uim}+\mu_{umD}},\ z_D\geq 1, \quad \text{(S51b)}$$

Substituting Eq. (S51b) into Eq. (S51a), one has:

$$\left(s+\varepsilon_{um}+\mu_{umD}-\frac{\varepsilon_{um}\varepsilon_{uim}}{s+\varepsilon_{uim}+\mu_{uimD}}\right)\bar{C}_{umD}-C_{umD}\left(r_D,z_D,t_{cha,D}\right)-\frac{\varepsilon_{um}C_{uimD}\left(r_D,z_D,t_{cha,D}\right)}{s+\varepsilon_{uim}+\mu_{uimD}}=$$

$$0.\ z_D\geq 1. \quad \text{(S52)}$$

Similarly, Eqs. (S3a) - (S3b) become:

$$(s+\varepsilon_{lm}+\mu_{lmD})\bar{C}_{lmD}-\varepsilon_{lm}\bar{C}_{limD}-C_{lmD}\left(r_D,z_D,t_{cha,D}\right)=0.\ z_D\leq -1. \quad \text{(S53a)}$$

$$\bar{C}_{limD}=\frac{\varepsilon_{lim}}{s+\varepsilon_{lim}+\mu_{lmD}}\bar{C}_{lmD}+\frac{C_{limD}\left(r_D,z_D,t_{cha,D}\right)}{s+\varepsilon_{lim}+\mu_{lmD}},\quad z_D\leq -1, \quad \text{(S53b)}$$

Substituting Eq. (S45b) into Eq. (S45a), one has:

$$\left(s+\varepsilon_{lm}+\mu_{lmD}-\frac{\varepsilon_{lm}\varepsilon_{lim}}{s+\varepsilon_{lim}+\mu_{limD}}\right)\bar{C}_{lmD}-C_{lmD}\left(r_D,z_D,t_{cha,D}\right)-\frac{\varepsilon_{lm}C_{limD}\left(r_D,z_D,t_{cha,D}\right)}{s+\varepsilon_{lim}+\mu_{limD}}=$$

$$0.\ z_D\leq -1. \quad \text{(S54)}$$

According to Eqs. (S52) and (S54), one has:

$$\bar{C}_{umD}=\frac{C_{umD}\left(r_D,z_D,t_{cha,D}\right)+\frac{\varepsilon_{um}C_{uimD}\left(r_D,z_D,t_{cha,D}\right)}{s+\varepsilon_{uim}+\mu_{uimD}}}{\left(s+\varepsilon_{um}+\mu_{umD}-\frac{\varepsilon_{um}\varepsilon_{uim}}{s+\varepsilon_{uim}+\mu_{uimD}}\right)},\ z_D\geq 1, \quad \text{(S55a)}$$

$$\bar{C}_{lmD}=\frac{C_{lmD}\left(r_D,z_D,t_{cha,D}\right)+\frac{\varepsilon_{lm}C_{limD}\left(r_D,z_D,t_{cha,D}\right)}{s+\varepsilon_{lim}+\mu_{limD}}}{\left(s+\varepsilon_{lm}+\mu_{lmD}-\frac{\varepsilon_{lm}\varepsilon_{lim}}{s+\varepsilon_{lim}+\mu_{limD}}\right)},\ z_D\leq -1, \quad \text{(S55b)}$$

where $C_{umD}\left(r_D,z_D,t_{cha,D}\right)$and $C_{uimD}\left(r_D,z_D,t_{cha,D}\right)$ are respectively the mobile and immobile concentrations [ML^{-3}] of the upper aquitard at the end of the chaser phase, $C_{lmD}\left(r_D,z_D,t_{cha,D}\right)$

and $C_{limD}\left(r_D, z_D, t_{cha,D}\right)$ are respectively the mobile and immobile concentrations [ML^{-3}] of the lower aquitard at the end of the chaser phase.

Similarly, the dimensionless governing equation of the mobile zone during the rest phase is:

$$\frac{\partial C_{mD}}{\partial t_D} = -\varepsilon_m(C_{mD} - C_{imD}) - \mu_{mD}C_{mD}, r_D \geq r_{wD}. \tag{S56a}$$

$$\frac{\partial C_{imD}}{\partial t_D} = \varepsilon_{im}(C_{mD} - C_{imD}) - \mu_{imD}C_{imD}, r_D \geq r_{wD}, \tag{S56b}$$

Conducting Laplace transform to Eqs. (S56a) and (S56b) for the rest phase, one has:

$$s\bar{C}_{mD} - C_{mD}(r_D, t_{cha,D}) = -\varepsilon_m(\bar{C}_{mD} - \bar{C}_{imD}) - \mu_{mD}\bar{C}_{mD}, r_D \geq r_{wD}. \tag{S57a}$$

$$s\bar{C}_{imD} - C_{imD}(r_D, t_{cha,D}) = \varepsilon_{im}(\bar{C}_{mD} - \bar{C}_{imD}) - \mu_{imD}\bar{C}_{imD}, r_D \geq r_{wD}, \tag{S57b}$$

According to Eqs. (S57a)-(S57b) , one has:

$$\bar{C}_{mD} = \frac{C_{mD}(r_D, t_{cha,D}) + \frac{\varepsilon_m C_{imD}\left(r_D, t_{cha,D}\right)}{(s+\mu_{imD}+\varepsilon_{im})}}{\left[s+\varepsilon_m+\mu_{mD}-\frac{\varepsilon_m\varepsilon_{im}}{(s+\mu_{imD}+\varepsilon_{im})}\right]}. \tag{S58a}$$

$$\bar{C}_{imD} = \frac{C_{imD}\left(r_D, t_{cha,D}\right)}{(s+\mu_{imD}+\varepsilon_{im})} + \frac{\varepsilon_{im}\bar{C}_{mD}}{(s+\mu_{imD}+\varepsilon_{im})}. \tag{S58b}$$

S1.4 Solutions in the extraction phase: Eqs. (28a) - (28g)

Contrary to the injection and chaser phases, the direction of advective flux is reversed in the extraction stage, Eqs. (S2a) and (S3a) are modified as:

$$\frac{\partial C_{umD}}{\partial t_D} = \frac{R_m\alpha_r^2 D_u}{AB^2 R_{um}}\frac{\partial^2 C_{umD}}{\partial z_D^2} + \frac{R_m v_{um}\alpha_r^2}{ABR_{um}}\frac{\partial C_{umD}}{\partial z_D} - \varepsilon_{um}(C_{umD} - C_{uimD}) - \mu_{umD}C_{umD},$$

$$z_D \geq 1, \tag{S59a}$$

$$\frac{\partial C_{lmD}}{\partial t_D} = \frac{R_m\alpha_r^2 D_l}{AB^2 R_{lm}}\frac{\partial^2 C_{lmD}}{\partial z_D^2} - \frac{R_m v_{lm}\alpha_r^2}{ABR_{lm}}\frac{\partial C_{lmD}}{\partial z_D} - \varepsilon_{lm}(C_{lmD} - C_{limD}) - \mu_{lmD}C_{lmD},$$

$$z_D \leq -1, \tag{S59b}$$

Conducting Laplace transform on Eqs. (S2b) and (S59a), one has:

$$s\bar{C}_{umD} - C_{umD}\left(r_D, z_D, t_{res,D}\right) = \frac{R_m\alpha_r^2 D_u}{AB^2 R_{um}}\frac{\partial^2 \bar{C}_{umD}}{\partial z_D^2} + \frac{R_m v_{um}\alpha_r^2}{ABR_{um}}\frac{\partial \bar{C}_{umD}}{\partial z_D} - \varepsilon_{um}(\bar{C}_{umD} - \bar{C}_{uimD}) -$$

$$\mu_{umD}\bar{C}_{umD},\ z_D \geq 1, \qquad \text{(S60a)}$$

$$\bar{C}_{uimD} = \frac{\varepsilon_{uim}\bar{C}_{umD}}{s+\varepsilon_{uim}+\mu_{uimD}} + \frac{C_{uimD}\left(r_D, z_D, t_{res,D}\right)}{s+\varepsilon_{uim}+\mu_{uimD}},\ z_D \geq 1, \qquad \text{(S60b)}$$

Substituting Eqs. (S60b) into Eq. (S60a) ,one can has:

$$\frac{R_m\alpha_r^2 D_u}{AB^2 R_{um}}\frac{\partial^2 \bar{C}_{umD}}{\partial z_D^2} + \frac{R_m v_{um}\alpha_r^2}{ABR_{um}}\frac{\partial \bar{C}_{umD}}{\partial z_D} - \left(s + \varepsilon_{um} + \mu_{umD} - \frac{\varepsilon_{um}\varepsilon_{uim}}{s+\varepsilon_{uim}+\mu_{uimD}}\right)\bar{C}_{umD} +$$

$$C_{umD}\left(r_D, z_D, t_{res,D}\right) + \frac{\varepsilon_{um}C_{uimD}\left(r_D, z_D, t_{res,D}\right)}{s+\varepsilon_{uim}+\mu_{uimD}} = 0.\ z_D \geq 1, \qquad \text{(S61)}$$

Similarly, conducting Laplace transform on Eqs. (S3b) and (S59b), one has:

$$s\bar{C}_{lmD} - C_{lmD}\left(r_D, z_D, t_{res,D}\right) = \frac{R_m\alpha_r^2 D_l}{AB^2 R_{lm}}\frac{\partial^2 \bar{C}_{lmD}}{\partial z_D^2} - \frac{R_m v_{lm}\alpha_r^2}{AB\ \ _{lm}}\frac{\partial \bar{C}_{lmD}}{\partial z_D} - \varepsilon_{lm}(\bar{C}_{lmD} - \bar{C}_{limD}) -$$

$$\mu_{lmD}\bar{C}_{lmD},\ z_D \leq -1, \qquad \text{(S62a)}$$

$$\bar{C}_{limD} = \frac{\varepsilon_{lim}\bar{C}_{lmD}}{s+\varepsilon_{lim}+\mu_{limD}} + \frac{C_{limD}\left(r_D, z_D, t_{res,D}\right)}{s+\varepsilon_{lim}+\mu_{limD}},\ z_D \leq -1, \qquad \text{(S62b)}$$

Substituting Eqs. (S62b) into Eq.(S62a), one has:

$$\frac{R_m\alpha_r^2 D_l}{AB^2 R_{lm}}\frac{\partial^2 \bar{C}_{lmD}}{\partial z_D^2} - \frac{R_m v_{lm}\alpha_r^2}{ABR_{lm}}\frac{\partial \bar{C}_{lmD}}{\partial z_D} - \left(s + \varepsilon_{lm} + \mu_{lmD} - \frac{\varepsilon_{lm}\varepsilon_{lim}}{s+\varepsilon_{lim}+\mu_{limD}}\right)\bar{C}_{lmD} +$$

$$C_{lmD}\left(r_D, z_D, t_{res,D}\right) + \frac{\varepsilon_{lm}C_{limD}\left(r_D, z_D, t_{res,D}\right)}{s+\varepsilon_{lim}+\mu_{limD}} = 0.\ z_D \leq -1, \qquad \text{(S63)}$$

where $C_{umD}\left(r_D, z_D, t_{res,D}\right)$and $C_{uimD}\left(r_D, z_D, t_{res,D}\right)$ are respectively the mobile and immobile concentrations [ML^{-3}] of the upper aquitard at the end of the rest phase, $C_{lmD}\left(r_D, z_D, t_{res,D}\right)$ and $C_{limD}\left(r_D, z_D, t_{res,D}\right)$ are respectively the mobile and immobile concentrations [ML^{-3}] of the lower aquitard at the end of the rest phase.

One could use a similar approach of obtaining the analytical solution of aquitards in the chaser phase to derive the solution of aquitards in the extraction phase. The general solution of (S61) is:

$$\bar{C}_{umD} = \int_1^{\infty} g_u(z_D, E_u; \mathscr{b}_u)\, f_u(\mathscr{b}_u) d\mathscr{b}_u + \frac{z_D - z_{eD}}{1 - z_{eD}} \bar{C}_{mD}(r_D, s), z_D \geq 1, \quad \text{(S64a)}$$

$$g_u(z_D, E_u; \mathscr{b}_u) = \begin{cases} g_{u1}(z_D, E_u; \mathscr{b}_u) = H_1 exp(m_1 z_D) + H_2 exp(m_2 z_D) & 1 \leq z_D < \mathscr{b}_u \\ g_{u2}(z_D, E_u; \mathscr{b}_u) = H_3 exp(m_1 z_D) + H_4 exp(m_2 z_D) & \mathscr{b}_u \leq z_D < \infty \end{cases}, \quad \text{(S64b)}$$

$f_u(\mathscr{b}_u) =$

$$C_{umD}(r_D, \mathscr{b}_u, t_{res,D}) + \frac{\varepsilon_{um} C_{uimD}(r_D, \mathscr{b}_u, t_{res,D})}{s + \varepsilon_{uim} + \mu_{uimD}} + \frac{R_m v_{um} \alpha_r^2}{ABR_{um}} \frac{\bar{C}_{mD}(r_D, s)}{1 - z_{eD}} - \frac{\mathscr{b}_u - z_{eD}}{1 - z_{eD}} E_u \bar{C}_{mD}(r_D, s),$$

(S64c)

The general solution of Eq. (S63) could be described as:

$$\bar{C}_{lmD} = \int_{-1}^{-\infty} g_l(z_D, E_l; \mathscr{b}_l)\, f_l(\mathscr{b}_l) d\mathscr{b}_l + \frac{z_D + z_{eD}}{z_{eD} - 1} \bar{C}_{mD}(r_D, s), z_D \leq -1, \quad \text{(S65a)}$$

$$g_l(z_D, E_l; \mathscr{b}_l) = \begin{cases} g_{l1}(z_D, E_l; \mathscr{b}_l) = I_1 exp(n_1 z_D) + I_2 exp(n_2 z_D) & -1 \leq z_D < \mathscr{b}_l \\ g_{l2}(z_D, E_l; \mathscr{b}_l) = I_3 exp(n_1 z_D) + I_4 exp(n_2 z_D) & \mathscr{b}_l \leq z_D < -\infty \end{cases}, \quad \text{(S65b)}$$

$f_l(\mathscr{b}_l) =$

$$C_{mD}(r_D, \mathscr{b}_l, t_{res,D}) + \frac{\varepsilon_{lm} C_{limD}(r_D, \mathscr{b}_l, t_{res,D})}{s + \varepsilon_{lim} + \mu_{limD}} - \frac{R_m v_{lm} \alpha_r^2}{ABR_{lm}} \frac{\bar{C}_{mD}(r_D, s)}{z_{eD} - 1} - \frac{\mathscr{b}_l + z_{eD}}{z_{eD} - 1} E_l \bar{C}_{mD}(r_D, s),$$

(S65c)

where $\mathscr{b}_u$ is a positive value varying between 1 and ∞; $\mathscr{b}_l$ is a negative value varying between -1 and $-\infty$; $g_u(z_D, E_u; \mathscr{b}_u)$ and $g_l(z_D, E_l; \mathscr{b}_l)$ are the Green's functions, $H_1 \sim H_4$ and $I_1 \sim I_4$ are contants which could be determined by the boundary conditions and conditions of a)~c), the values of $H_1 \sim H_4$ and $I_1 \sim I_4$ are as follows: $H_1 = -H_2 exp(m_2 - m_1)$,

$$H_2 = \frac{-AR_{um}B^2}{R_m \alpha_r^2 D_u [(m_1 - m_2) exp(m_2 - m_1) exp(m_1 \mathscr{b}_u)]}, H_3 = 0, H_4 = H_2 - H_2 exp(m_2 - m_1) exp(m_1 \mathscr{b}_u - m_2 \mathscr{b}_u),$$

$$I_1 = -I_2 exp(n_1 - n_2), I_2 = \frac{-AB^2 R_{lm}}{R_m \alpha_r^2 D_l [exp(n_2 \mathscr{b}_l - n_1 \mathscr{b}_l) - n_2 exp(n_2 \mathscr{b}_l)]},$$

$$I_3 = I_2 exp(n_2 \mathscr{b}_l - n_1 \mathscr{b}_l) - I_2 exp(n_1 - n_2), I_4 = 0,$$

$$m_1 = \frac{-\frac{R_m v_{um} \alpha_r^2}{AB\ \ um} + \sqrt{\left(\frac{R_m v_{um} \alpha_r^2}{ABR_{um}}\right)^2 + 4 \frac{R_m \alpha_r^2 D_u}{AB^2 R_{um}} \left(s + \varepsilon_{um} + \mu_{umD} - \frac{\varepsilon_{um} \varepsilon_{uim}}{s + \mu_{uimD} + \varepsilon_{uim}}\right)}}{2 \frac{R_m \alpha_r^2 D_u}{AB^2 R_{um}}},$$

$$m_2 = \frac{-\frac{R_m v_{um}\alpha_r^2}{ABR_{um}} - \sqrt{\left(\frac{R_m v_{um}\alpha_r^2}{ABR_{um}}\right)^2 + 4\frac{R_m\alpha_r^2 D_u}{AB^2 R_{um}}\left(s+\varepsilon_{um}+\mu_{umD}-\frac{\varepsilon_{um}\varepsilon_{uim}}{s+\mu_{uimD}+\varepsilon_{uim}}\right)}}{2\frac{R_m\alpha_r^2 D_u}{AB^2 R_{um}}},$$

$$n_1 = \frac{\frac{R_m v_{lm}\alpha_r^2}{ABR_{lm}} + \sqrt{\left(\frac{R_m v_{lm}\alpha_r^2}{ABR_{lm}}\right)^2 + 4\frac{R_m\alpha_r^2 D_l}{AB^2 R_{lm}}\left(s+\varepsilon_{lm}+\mu_{lmD}-\frac{\varepsilon_{lm}\varepsilon_{lim}}{s+\mu_{limD}+\varepsilon_{lim}}\right)}}{2\frac{R_m\alpha_r^2 D_l}{AB^2 R_{lm}}} \text{ and}$$

$$n_2 = \frac{\frac{R_m v_{lm}\alpha_r^2}{ABR_{lm}} - \sqrt{\left(\frac{R_m v_{lm}\alpha_r^2}{ABR_{lm}}\right)^2 + 4\frac{R_m\alpha_r^2 D_l}{AB^2 R_{lm}}\left(s+\varepsilon_{lm}+\mu_{lmD}-\frac{\varepsilon_{lm}\varepsilon_{lim}}{s+\mu_{limD}+\varepsilon_{lim}}\right)}}{2\frac{R_m\alpha_r^2 D_l}{AB^2 R_{lm}}}.$$

Similarly, contrary to the injection and chaser phases, the direction of advective flux is reversed in the extraction stage, and Eq. (S1a) is modified as:

$$\frac{\partial C_{mD}}{\partial t_D} = \frac{1}{r_D}\frac{\partial^2 C_{mD}}{\partial r_D^2} + \frac{1}{r_D}\frac{\partial C_{mD}}{\partial r_D} - \varepsilon_m(C_{mD} - C_{imD}) - \mu_{mD}C_{mD} - \left(-\frac{\theta_{um}\alpha_r^2 v_{um}}{2A\theta_m B}C_{umD} - \frac{\theta_{um}\alpha_r^2 D_u}{2A\theta_m B}\frac{\partial C_{umD}}{\partial z_D}\right)\Big|_{z=1} + \left(-\frac{\theta_{lm}\alpha_r^2 v_{lm}}{2AB^2\theta_m}C_{lmD} - \frac{\theta_{lm}\alpha_r^2 D_l}{2AB^2\theta_m}\frac{\partial C_{lmD}}{\partial z_D}\right)\Big|_{z=-1}, r_D \geq r_{wD}. \tag{S66}$$

In the extraction phase, the dimensional boundary conditions Eqs. (14a)-(14b) are transformed to the dimensionless format:

$$\beta_{ext,D}\frac{\partial C_{mD}(r_D,t_D)}{\partial t_D}\Big|_{r_D=r_{wD}} = \frac{\partial C_{mD}(r_D,t_D)}{\partial r_D}\Big|_{r_D=r_{wD}}, t_{res,D} < t_D \leq t_{ext,D} \tag{S67a}$$

$$C_{mD}(r_D,t_D)|_{t_D=t_{res,D}} = C_{res,mD}(r_D,t_D)\big|_{t_D=t_{res,D}}. \tag{S67b}$$

where $\beta_{ext,D} = -\frac{V_{w,ext}r_{wD}}{\xi R_m\alpha_r}$.

Conducting Laplace transform on Eqs. (S58) and (S1b) in the extraction phase, one has:

$$s\bar{C}_{mD} - C_{mD}(r_D,t_{res}) = \frac{1}{r_D}\frac{\partial^2\bar{C}_{mD}}{\partial r_D^2} + \frac{1}{r_D}\frac{\partial\bar{C}_{mD}}{\partial r_D} - (\varepsilon_m + \mu_{mD})\bar{C}_{mD} + \varepsilon_m\bar{C}_{imD} - \left(-\frac{\theta_{um}\alpha_r^2 v_{um}\bar{C}_{umD}}{2A\theta_m b} - \frac{\theta_{um}\alpha_r^2 D_u}{2A\theta_m b}\frac{\partial\bar{C}_{umD}}{\partial z_D}\right)\Big|_{z_D=1} - \left(\frac{\theta_{lm}\alpha_r^2 v_{lm}\bar{C}_{lmD}}{2Ab^2\theta_m} + \frac{\theta_{lm}\alpha_r^2 D_l}{2Ab^2\theta_m}\frac{\partial\bar{C}_{lmD}}{\partial z_D}\right)\Big|_{z_D=-1},$$

$$r_D \geq r_{wD}. \tag{S68a}$$

$$\bar{C}_{imD} = \frac{\varepsilon_{im}}{(s+\mu_{imD}+\varepsilon_{im})}\bar{C}_{mD} + \frac{C_{imD}(r_D,t_{res})}{s+\mu_{imD}+\varepsilon_{im}}, r_D \geq r_{wD}, \quad \text{(S68b)}$$

After substituting Eqs. (S64a)- (S65c) and Eq. (S68b) into Eq. (S68a), one has

$$\frac{\partial^2 \bar{C}_{mD}}{\partial r_D^2} + \frac{\partial \bar{C}_{mD}}{\partial r_D} - r_D \zeta \bar{C}_{mD} + r_D \Lambda = 0. \quad \text{(S69)}$$

where $\zeta = s + \varepsilon_m + \mu_{mD} - \frac{\varepsilon_{im}\varepsilon_m}{s+\mu_{imD}+\varepsilon_{im}} - \frac{\theta_{um}\alpha_r^2 v_{um}}{2A\theta_m B} + \frac{\theta_{lm}\alpha_r^2 v_{lm}}{2AB^2\theta_m} - \frac{1}{1-z_{eD}}\frac{\theta_{um}\alpha_r^2 D_u}{2A\theta_m b} + \frac{1}{z_{eD}-1}\frac{\theta_{lm}\alpha_r^2 D_l}{2Ab^2\theta_m}$,

$\Lambda = C_{mD}(r_D, t_{res}) + \frac{\varepsilon_m C_{imD}(r_D,t_{res})}{s+\mu_{imD}+\varepsilon_{im}}$; $C_{imD}(r_D, t_{res})$ and $C_{mD}(r_D, t_{res})$ represent the initial concentrations in the immobile and mobile domains of the SWPP test in the rest phase.

The boundary condition of Eqs. (S67a)-(S67b) in Laplace domain becomes:

$$s\beta_{ext,D}\bar{C}_{mD}(r_D, s)|_{r_D=r_{wD}} - \beta_{ext,D}C_{res,m}(r_D, t_D)\big|_{t_D=t_{res,D}} = \left.\frac{\partial \bar{C}_{mD}(r_D,s)}{\partial r_D}\right|_{r_D=r_{wD}}. \quad \text{(S70)}$$

Similar to the model of the SWPP test in the injection phase, Eqs. (S5), (S61) and (S70) compose a model of the second-order ordinary differential equation (ODE) with boundary conditions. However, the governing equation is an inhomogeneous differential equation. In this study, we use the Green's function method to derive the analytical solution of Eq. (S69).

Similar to *Chen and Woodside* [1988], Eq. (S69) could be transferred into a self-adjoint form:

$$\frac{\partial^2 G}{\partial r_D^2} - \left(r_D\zeta + \frac{1}{4}\right)G = -\ell(r_D). \quad \text{(S71)}$$

where $G = exp(r_D/2)\bar{C}_{mD}$ and $\ell(r_D) = exp(r_D/2)r_D\Lambda$.

The boundary conditions of Eqs. (S5) and (S70) could be rewritten as：

$$G(r_D, s)|_{r_D=\infty} = 0, \quad \text{(S72a)}$$

$$\left.\left[\left(s\beta_{ext,D} + \frac{1}{2}\right)G - \frac{\partial G}{\partial r_D}\right]\right|_{r_D=r_{wD}} = \beta_{ext,D}exp(r_{wD}/2)C_{mD}(r_{wD}, t_{res,D}), \quad \text{(S72b)}$$

One could find that the boundary condition of Eq. (S72b) is inhomogeneous, and we need to homogenize it first. Assigning $G = U(r_D) + V(r_D)$ and $V(r_D) = \sigma_1 + \sigma_2 r_D$, and substituting them into Eqs. (S72a) and (S72b) yields:

$$U(r_D, s)|_{r_D=\infty} = 0, \tag{S73a}$$

$$\left[\left(s\beta_{ext,D} + \frac{1}{2}\right) U - \frac{\partial U}{\partial r_D}\right]\Bigg|_{r_D=r_{wD}} = 0, \tag{S73b}$$

where $\sigma_1 = -\frac{\beta_{ext,D} exp(r_{wD}/2) C_{mD}(r_{wD}, t_{res,D})}{\left(s\beta_{ext,D}+\frac{1}{2}\right) r_{wD} - 1 - \left(s\beta_{ext,D}+\frac{1}{2}\right) r_D|_{r_D\to\infty}} r_D|_{r_D\to\infty}$,

$$\sigma_2 = \frac{\beta_{ext,D} exp(r_{wD}/2) C_{mD}(r_{wD}, t_{res,D})}{\left(s\beta_{ext,D}+\frac{1}{2}\right) r_{wD} - 1 - \left(s\beta_{ext,D}+\frac{1}{2}\right) r_D|_{r_D\to\infty}}.$$

After defining a spatial operator:$\mathrm{L} = -\frac{d^2}{dr_D^2} + \left(r_D\zeta + \frac{1}{4}\right)$, one has:

$$LG = LU(r_D) + LV(r_D) = \ell(r_D), \tag{S74}$$

and

$$LU(r_D) = \ell(r_D) - LV(r_D). \tag{S75}$$

Let $f(r_D) = \ell(r_D) - LV(r_D)$, one has:

$$\frac{\partial^2 U}{\partial r_D^2} - \left(r_D\zeta + \frac{1}{4}\right) U = -f(r_D). \tag{S76}$$

where $f(r_D) = exp(r_D/2) r_D \Lambda - \left(r_D\zeta + \frac{1}{4}\right)(\sigma_1 + \sigma_2 r_D)$.

Right now, the model with an inhomogeneous boundary condition becomes a regular Sturm-Louisville problem. The general solution of Eqs. (S73a) - (S73b) and (S76) is:

$$U(r_D, \zeta; \varepsilon) = \int_{r_{wD}}^{\infty} g(r_D, \zeta; \varepsilon) f(\varepsilon) d\varepsilon. \tag{S77}$$

where ε is a positive value varying between r_{wD} and ∞ (e.g. $r_{wD} \le \varepsilon \le \infty$); $g(r_D, \zeta; \varepsilon)$ is the Green's function, and could be expressed as :

$$g(r_D, \zeta; \varepsilon) = \begin{cases} g_1(r_D, \zeta; \varepsilon) = P_1 A_i(y_{ext}) + P_2 B_i(y_{ext}) & r_{wD} \le y_{ext} \le \varepsilon \\ g_2(r_D, \zeta; \varepsilon) = P_3 A_i(y_{ext}) + P_4 B_i(y_{ext}) & \varepsilon \le y_{ext} \le \infty \end{cases}, \tag{S78}$$

where $f(\varepsilon) = exp(\varepsilon/2)\varepsilon\Lambda - \left(\varepsilon\zeta + \frac{1}{4}\right)(\sigma_1 + \sigma_2\varepsilon)$, $y_{ext} = \zeta^{1/3}\left(r_D + \frac{1}{4\zeta}\right)$, P_1, P_2, P_3 and P_4 are coefficients to be determined. As $B_i(r_D)$ diverges when $r_D \to \infty$, P_4 has to be zero.

Substituting Eq. (S78) into Eq. (S73b), one has:

$$\left[\left(s\beta_{ext,D} + \frac{1}{2}\right) g_1 - \frac{\partial g_1}{\partial r_D}\right]\Big|_{r_D=r_{wD}} = 0, \tag{S79}$$

which leads to

$$P_1 = -P_2 W. \tag{S80}$$

where $W = \frac{\left(s\beta_{ext,D}+\frac{1}{2}\right)B_i(y_{ext,w}) - \zeta^{1/3}B_i'(y_{ext,w})}{\left(s\beta_{ext,D}+\frac{1}{2}\right)A_i(y_{ext,w}) - \zeta^{1/3}A_i'(y_{ext,w})}$, $y_{ext,w} = \zeta^{1/3}\left(r_{wD} + \frac{1}{4\zeta}\right)$.

According to the properties of Green's function , one has:

$$P_1 A_i\left(y_{ext}|_{r_D=\varepsilon^+}\right) + P_2 B_i\left(y_{ext}|_{r_D=\varepsilon^+}\right) = P_3 A_i\left(y_{ext}|_{r_D=\varepsilon^-}\right). \tag{S81}$$

$$\left[P_3\zeta^{1/3}A_i'(y_{ext})\right]_{r_D=\varepsilon^-} - \left[P_1\zeta^{\frac{1}{3}}A_i'(y_{ext}) + P_2\zeta^{\frac{1}{3}}B_i'(y_{ext})\right]_{r_D=\varepsilon^+} = -1. \tag{S82}$$

The values of P_1, P_2 and P_3 could be determined by Eqs. (S69) - (S71), namely:

$$P_1 = -\frac{\pi A_i\left(y_{ext}|_{r_D=\varepsilon^+}\right)}{\zeta^{1/3}} W \ , \ P_2 = \frac{\pi A_i\left(y_{ext}|_{r_D=\varepsilon^+}\right)}{\zeta^{1/3}},$$

$$P_3 = \frac{\pi A_i\left(y_{ext}|_{r_D=\varepsilon^+}\right)}{\zeta^{1/3}}\left[\frac{B_i\left(y_{ext}|_{r_D=\varepsilon^+}\right)}{A_i\left(y_{ext}|_{r_D=\varepsilon^+}\right)} - W\right].$$

References

[1] Chen, C. S., and G. D. Woodside (1988), Analytical solution for aquifer decontamination by pumping, Water Resources Research, 24(8), 1329-1338.

S2. Numerical simulations

To test the assumptions used in the analytical solution of this study, a 3D finite-element method with the help of COMSOL Multiphysics will be used to solve the three-dimensional model. The grid mesh of the aquifer-aquitard system in the numerical modeling could be seen in

Figure S1. The initial drawdown and the initial concentration are 0 for aquifer and aquitards. The hydraulic parameters are: K_a=0.1 m/day, S_a= S_u= S_l=10^{-4} m^{-1}, and the other parameters are $R_m = R_{im} = R_{um} = R_{uim} = R_{lm} = R_{lim}$=1, $\theta_{um} = \theta_{lm} = 0.1$, $\alpha_r = 2.5$m, $\alpha_u = \alpha_l = 0.5$m, $\mu_m = \mu_{im} = \mu_{um} = \mu_{uim} = \mu_{lm} = \mu_{lim}$=$10^{-7}s^{-1}$, r_w =0.5m, Q_{inj}=Q_{cha} =50 m^3/d, Q_{res}=0 m^3/d, Q_{ext}=-50 m^3/d, t_{inj}=250day, t_{cha}=50day, t_{res}=50day, B=10m, θ_m=0.25, θ_{im}=0.05, and ω=0.01d^{-1}. In this modeling, the finite thickness of the aquitard is used to approximate the infinite thickness of the aquitard, and the finite radial length of the aquifer is used to approximate the infinite radial length of the aquifer. Such treatment works well when the tracer has not approach the boundary.

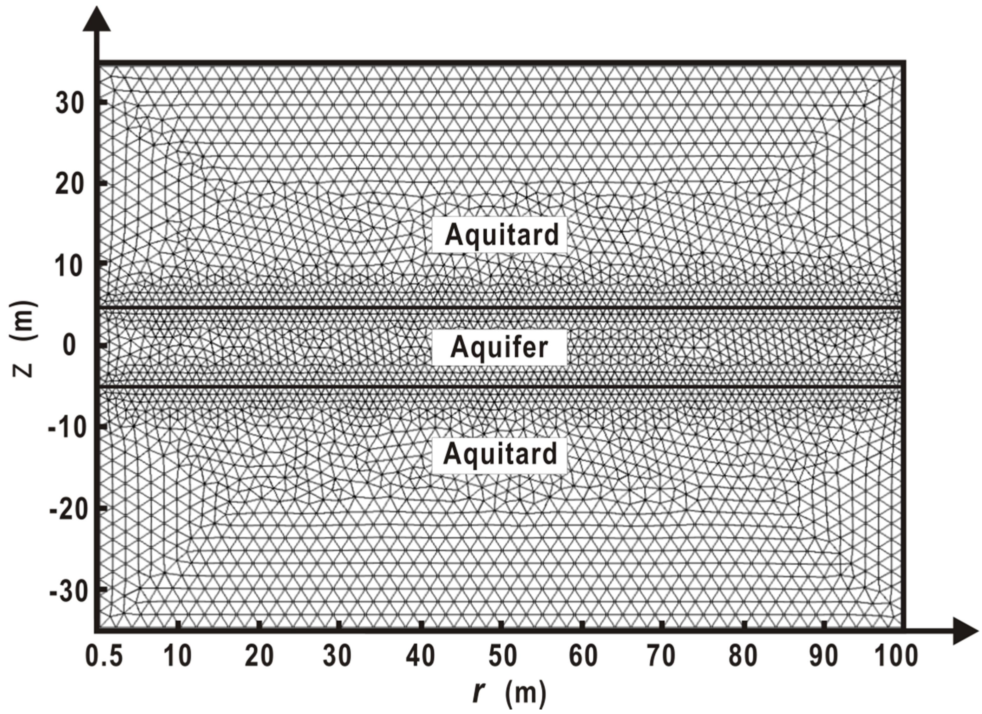

Figure S1. The grid mesh of the aquifer-aquitard system used in the Galerkin finite element program using COMSOL Multiphysics.

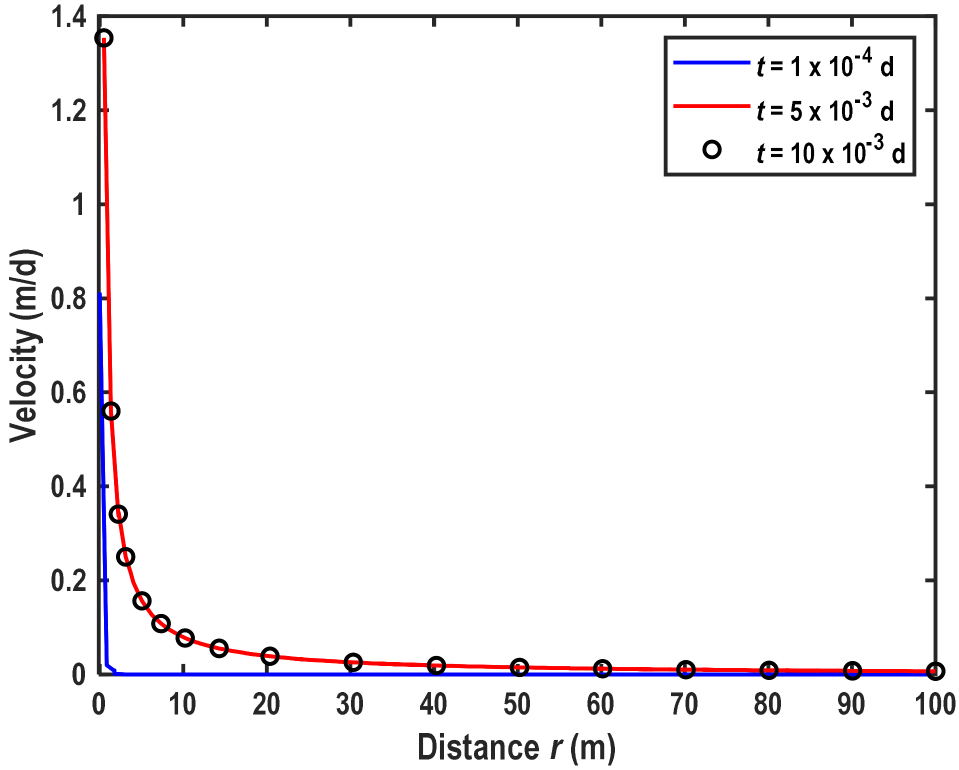

Figure S2. Spatial distribution of the flow velocity for different time. The parameters are the same with ones in Figures 2 and 3.

S3. References for Table 4

[a]. Alvarez, P. J. J., Anid, P. J., and Vogel, T. M.: Kinetics of aerobic biodegradation of benzene and toluene in sandy aquifer material, Biodegradation, 2, 43-51, 1991.

[b]. Bouwer, E. J., and McCarty, P. L.: Utilization rates of trace halogenated organic compounds in acetate-grown biofilms, Biotechnology & Bioengineering, 27, 1564-1571, 1985.

[c]. Brusseau, M. L., Jessup, R. E., and Rao, P. S. C.: Nonequilibrium sorption of organic chemicals: elucidation of rate-limiting processes, Environmental Science & Technology, 1991.

[d]. Chun, J. A., Cooke, R. A., Eheart, J. W., and Kang, M. S.: Estimation of flow and transport

parameters for woodchip-based bioreactors: I. laboratory-scale bioreactor, Biosystems Engineering, 104, 384-395, 2009.

[e]. Davis, B. M., Istok, J. D., and Semprini, L.: Static and push‐pull methods using radon‐222 to characterize dense non‐aqueous phase liquid saturations, Ground water, 41, 470-481, 10.1111/j.1745-6584.2003.tb02381.x, 2003.

[f]. Haggerty, R., Schroth, M. H., and Istok, J. D.: Simplified method of “push‐pull” test data analysis for determining in situ reaction rate coefficients, Ground water, 36, 314-324, 10.1111/j.1745-6584, 1998.

[g]. Javadi, S., Ghavami, M., Zhao, Q., and Bate, B.: Advection and retardation of non-polar contaminants in compacted clay barrier material with organoclay amendment, Applied Clay Science, S0169131716304628, 2017.

[h]. Kookana, R. S., AYLMORE, L. A. G., and GERRITSE, R. G.: Time-dependent sorption of pesticides during transport in soils, Soil Science, 154, 214-225, 1992.

[i]. Liang, X., Zhan, H., Liu, J., Dong, G., and Zhang, Y.: A simple method of transport parameter estimation for slug injecting tracer tests in porous media, Science of The Total Environment, 644, 1536-1546, 2018.

[j]. Pickens, R., Jackson, K., and Meritt, W.: Measurement of distribution coeffcients using a radial injection dual-tracer test, in, 17, Water Resources Research, 529-544, 1981.

[k]. Swami, D., Sharma, P. K., and Ojha, C. S. P.: Behavioral Study of the Mass Transfer Coefficient of Nonreactive Solute with Velocity, Distance, and Dispersion, Journal of Environmental Engineering, 04016076, 2016.

S4. Parameter range used in sensitivity analysis

Table S1: parameter range used in sensitivity analysis

Parameter	Unit	Range
α_u	m	0.05-0.50
α_r	m	0.50-1.00
v_{um}	m/d	0-0.01
θ_{um}	-	0-0.2
ω	1/s	0.0001-0.001
θ_m	-	0.20-0.40
V_w	m^3	0.10-500

"-" represents dimensionless unit.